AFRL-VS-TR-2002-1677

PRISM 1.7e ALGORITHM DESCRIPTION

Robert E. Daniell, Jr.

Computational Physics, Inc.
207 Fulton Street
Norwood, Ma 02062

19 June 2002

Scientific Report No. 1

AIR FORCE RESEARCH LABORATORY
Space Vehicles Directorate
29 Randolph Rd
AIR FORCE MATERIEL COMMAND
HANSCOM AFB, MA 01731-3010

This technical report has been reviewed and is approved for publication.

/Signed/
Contract Manager

/Signed/
Branch Chief

This document has been reviewed by the ESC Public Affairs Office and has been approved for release to the National Technical Information Service.

Qualified requestors may obtain additional copies form the Defense Technical Information Center (DTIC). All others should apply to the National Technical Information Service.

If your address has changed, if you wish to be removed from the mailing list, or if the addressee is no longer employed by your organization, please notify AFRL/VSIM, 29 Randolph Rd., Hanscom AFB, MA 01731-3010. This will assist us in maintaining a current mailing list.

Do not return copies of this report unless contractual obligations or notices on a specific document require that it be returned.

REPORT DOCUMENTATION PAGE

Form Approved
OMB No. 0704-0188

1. AGENCY USE ONLY (*Leave blank*)	2. REPORT DATE	3. REPORT TYPE AND DATES COVERED
	19 June 2002	Scientific Report No. 1 (12 Jul 99 - 9 Jan 02)

4. TITLE AND SUBTITLE
PRISM 1.7e Algorithm Description

5. FUNDING NUMBERS
PE
PR DTRA
TA BB
WU SS
Contract F19628-99-C-0068

6. AUTHOR(S)
Robert E. Daniell, Jr.

7. PERFORMING ORGANIZATION NAME(S) AND ADDRESS(ES)
Computational Physics, Inc.
207 Fulton Street
Norwood, MA 02062

8. PERFORMING ORGANIZATION REPORT NUMBER
AFRL-VS-TR-2002-1677

9. SPONSORING / MONITORING AGENCY NAME(S) AND ADDRESS(ES)
Air Force Research Laboratory
29 Randolph Street
Hanscom AFB, MA 01731-3010
Contract Manager: William Borer/VSBP

10. SPONSORING / MONITORING AGENCY REPORT NUMBER

11. SUPPLEMENTARY NOTES

12A. DISTRIBUTION / AVAILABILITY STATEMENT
Distribution unlimited

12b. DISTRIBUTION CODE

13. ABSTRACT (*Maximum 200 words*)

This report describes the PRISM 1.7e algorithm for data assimilation and near real time global ionospheric specification. It also describes the basis for PRISM climatology, including descriptions of the three physical models which were parameterized to produce it, the parameterization method itself, as well as the semi-analytic representation used to produce a compact representation of the climatology. It includes appendices containing the I/O specification for PRISM and internal memoranda describing the changes for each version from 1.5 through 1.7e.

14. SUBJECT TERMS
Ionosphere, Data assimilation, Ionospheric specification, Space weather, Nowcasting

15. NUMBER OF PAGES
101

16. PRICE CODE

17. SECURITY CLASSIFICATION OF REPORT	18. SECURITY CLASSIFICATION OF THIS PAGE	19. SECURITY CLASSIFICATION OF ABSTRACT	20. LIMITATION OF ABSTRACT
Unclassified	Unclassified	Unclassified	SAR

Contents

List of Figures

List of Tables

Executive Summary

This document provides a description of Version 1.7 (revision e) of the *P*arameterized *R*eal-time *I*onospheric *S*pecification *M*odel (PRISM 1.7e), a global data assimilation model intended to provide near real-time ionospheric specifications for space weather applications. PRISM consists of a semi-analytic representation of a parameterization of three separate physically based computational models of the ionosphere. PRISM uses both ground based and space based data to modify or update the climatological ion density profiles to produce a data driven specification of the state of the ionosphere. Currently, PRISM 1.7e is operational at the Air Force Weather Agency (AFWA) at Offut AFB in Nebraska, and is also a component of OpSEND, an operational space weather software suite developed by the Air Force Research Laboratory (AFRL) for use at the same site. In operational use PRISM typically provides either hourly or quarter hourly ionospheric specifications in near real time. PRISM is capable of ingesting and using electron density profile (EDP) parameters (f_oF_2, h_mF_2, f_oE, and h_mE) produced from automated true height analysis of digital ionograms, TEC measurements from GPS receivers, satellite based *in situ* plasma measurements (electron density, ion composition, electron and ion temperature, and ion drift velocity), satellite based *in situ* observations of precipitating electrons and ions in the high latitude regions, as well as ionospheric parameters derived from observations of airglow and auroral optical emissions.

1. INTRODUCTION

We have modified and updated the Parameterized Real-time Ionospheric Specification Model (PRISM) for the Air Force Research Laboratory (AFRL) for use at the 55th Space Weather Squadron (55 SWXS) and by the Air Force Weather Agency (AFWA). The model is capable of assimilating both ground based and space based data available in near real time to modify theoretical climatology provided by a parameterization of several regional, first principles ionospheric models, thus providing a near real-time specification of the ionosphere. The theoretical climatology is provided by a composite of diurnally reproducible runs of several physical ionospheric models: (1) the Time Dependent Ionospheric Model (TDIM) of Utah State University (USU) [*Schunk*, 1988], (2) the low latitude F-region model (LOWLAT) developed by *Anderson* [1973], (3) the midlatitude version of LOWLAT (called MIDLAT) developed by D. N. Anderson and modified by D. T. Decker, and (4) an E-region local chemistry code developed by D. T. Decker and incorporating photoelectrons using the continuous slowing down method [*Jasperse*, 1982].

PRISM can produce either regional or global output. The output grid of latitude and longitude (which may be either geographic or geomagnetic) is user selectable. (At 55 SWXS the standard PRISM output is a global grid with 1° latitude spacing and 5° longitude spacing.) Profile parameters (f_oF_2, h_mF_2, TEC, etc.), or complete electron density profiles, or both may be output to the specified grid. The user also has the option of specifying output at a list of sites. Although intended for validation purposes – for which the list would be a set of "ground truth" sites – it can used for other purposes, such as approximating the ground track of a satellite.

The last documentation for PRISM described Version 1.5. The current version, 1.7e, corrects a number of bugs that were detected during testing at AFRL and at PRISM has been delivered to the AFWA and is presently undergoing transition to operational code. The present documents incorporates some of the material in the previous documentation for completeness, but in abbreviated form, and concentrates on new information regarding changes to the algorithms.

1.1 *Objectives*

The primary goal of PRISM development was an algorithm for assimilating ionospheric data in near real time in order to produce a near real time specification of the global ionosphere. The data to be assimilated include

(1) bottomside digital soundings from the Digital Ionospheric Sounding System (DISS),
(2) Total Electron Content (TEC) data from the Ionospheric Monitoring System (IMS) and other sources,
(3) in situ plasma data (densities, temperatures, and drift velocities) from the SSIES instrument on DMSP satellites,
(4) auroral electron and ion fluxes from the SSJ/4 instrument on DMSP satellites, and
(5) electron density profile information deduced from observations of airglow and auroral optical emissions by instruments (SSUSI and SSULI) expected to be flown on future DMSP satellites.

Because the SSUSI and SSULI instruments were hardly even on the drawing board when PRISM development began, no explicit input specification was written for this data. Rather it was envisioned that these instruments would provide derived electron density profile (EDP) parameters that would be input to PRISM as if they came from DISS or SSIES or even SSJ/4.

The need for a global specification of the state of the ionosphere is twofold. First, there are operational systems that need to correct for ionospheric effects in real time, or that have operational parameters that are affected by the ionosphere and must be adjusted in near real time. Second, the operation of many systems could be optimized if accurate forecasts of ionospheric conditions were available because this allows the operational parameters to be chosen ahead of time. Any ionospheric forecast algorithm will require an accurate specification of the current state of the ionosphere as an initial condition, which PRISM provides.

In addition to real time needs, many system operators need post-event analysis to determine whether operational problems or outages were caused by system problems or by environmental conditions. PRISM will be used for this purpose at AFWA as well.

1.2 *Approach*

Ideally, the specification of the current state of the ionosphere would be obtained directly from real time observations from a dense network of satellite and ground based instruments. Unfortunately, the complexity and spatial extent of the ionosphere precludes the deployment of a sufficiently dense network of observing instruments. Therefore, any practical ionospheric specification algorithm must be based on an ionospheric model with parameters that can be adjusted on the basis of near real time data. Two approaches are possible: (1) statistical or empirical climatological models or (2) numerical simulations based on physical models. (In this paper "physical model" is synonymous with "first principles numerical model.") For reasons described below, we have chosen the second approach (physical models). However, practical considerations (primarily computational speed) dictate that the algorithms implemented at the AFWA be based on *parameterized* versions of the physical models ("theoretical climatology"). Although the computational requirements are less stringent than when PRISM development first began, state-of-the-art physical models still require high speed supercomputers (especially multi-processor systems) to operate faster than real time.

We feel strongly that a comprehensive physical model of the coupled thermosphere and ionosphere can produce more accurate specifications and forecasts than can statistical or climatological models. The causal relationship between easily monitored solar and geophysical parameters (e.g., K_p, $F_{10.7}$, etc.) and a particular ionospheric configuration is very complex. Any organization of historical ionospheric data inevitably averages over a variety of ionospheric configurations corresponding to similar values of the chosen set of solar-geophysical parameters (usually only one or two). The result is that spatial structure tends to be smeared out or smoothed over, and the resulting model is unrepresentative of the *instantaneous* ionosphere. If a physical model contains all of the relevant physics, and if the inputs are realistic, then it will produce more realistic representations of instantaneous ionospheric structure. However, there is a difference between a *realistic* representation and an *accurate* one.

In order to accurately simulate a time dependent phenomenon like the thermosphere and ionosphere, a physical model needs an accurate specification of the initial conditions and an accurate representation of the energy and momentum flux at the boundaries. For the purposes of providing a specification model, it is the energy and momentum input that is crucial. If the model is run long enough, the effects of the initial conditions are lost and the present state of the model depends only on the recent history of the energy and momentum input. These include the solar EUV (the primary source of ionization outside the auroral zone), high latitude heating of the thermosphere (which affects the global circulation of the thermosphere), high latitude convection, and low latitude dynamo electric fields. While the temporal and spatial resolution of the observations of these quantities are expected to improve in the future, they will probably never be sufficient to allow accurate simulation of the ionosphere without additional data in the form of direct measurements of ionospheric parameters. As a practical matter, ionospheric simulations must be, and will remain, iterative in nature: The energy and momentum input parameters are adjusted until the simulation agrees with observations of ionospheric parameters to some level of accuracy.

There is a superficial similarity between our approach and a climatological approach. The difference, however, is that we begin with a more realistic representation of the spatial structure of the ionosphere than climatological models can provide. The parameter adjustment process should not compromise this advantage. In the future, as more powerful computers and more efficient model algorithms become available, the parameterized models can be replaced by actual physical models to produce more accurate specifications.

2. THE PHYSICAL MODELS

During the original development of PRISM, four separate physical models were used as the basis of PRISM: (1) a low latitude F layer model (LOWLAT), (2) a midlatitude F layer model (MIDLAT), (3) a combined low and middle latitude E layer model (ECSD), and (4) a high latitude E and F layer model (TDIM). In the current version of PRISM, MIDLAT has been replaced by LOWLAT, which is used (separately) for both the low latitude and midlatitude ionospheric representations. All of the models are based on a tilted dipole representation of the geomagnetic field and a corresponding magnetic coordinate system. (Hereafter, "latitude" means "magnetic latitude" unless otherwise noted.) All four models use the MSIS-86 neutral atmosphere model [*Hedin*, 1987]. Chemical reaction rates, collision frequencies, and similar data are consistent among all the models.

2.1 *The Low and Mid-Latitude F Layer Model*

The low latitude *F* region model (LOWLAT) was originally developed by *Anderson*, [1973]. (See also *Moffett*, [1979]). It solves the diffusion equation for O^+ along a magnetic flux tube. Normally, the entire flux tube is calculated with chemical equilibrium boundary conditions at both feet of the flux tube. A large number of flux tubes must be calculated in order to build up an altitude profile.

Since heat transport is not included in this model, ion and electron temperature models must be used. For the PRISM development effort we chose the temperature model of *Brace and Theis* [1981]. The Horizontal Wind Model (HWM) of *Hedin* [1988] was used to describe thermospheric winds. We used production, loss, and diffusion rates as specified by *Decker et al.* [1994].

The critical feature incorporated in the low latitude model is the dynamo electric field. The horizontal component of this field drives upward convection through $\mathbf{E}\times\mathbf{B}$ drift, and this can significantly modify profile shapes and densities. This phenomenon is responsible for the equatorial anomaly, crests in ionization on either side of the magnetic equator at $\pm 15-20°$ magnetic latitude. In the current version of PRISM (Version 1.7e) the $\mathbf{E}\times\mathbf{B}$ driven vertical drift used for these calculations was based on the empirical models derived from data from the Atmospheric Explorer-E (AE-E) satellite [*Fejer et al.*, 1995], which are consistent with the drifts measured at Jicamarca [*Fejer*, 1981; *Fejer et al.*, 1989] but include longitudinal variations as well. We used the *Fejer et al.* [1995] empirical drifts for moderate and high solar activity. Following the their discussion, we modified these drifts by reducing or eliminating the pre-reversal enhancement for low solar activity. Horizontal drifts were neglected in the PRISM runs. Of course, for the midlatitude runs, the drift is irrelevant (as long as the drift vanishes at high altitudes corresponding the flux tubes whose feet are in middle latitudes).

Since its original development this model has undergone extensive validation by comparison with data. The most recent such comparison is *Preble et al.* [1994] using electron density profiles measured by the incoherent scatter radar facility at Jicamarca, Peru.

2.2 *The Low and Midlatitude E Layer Model*

The low and mid- latitude *E* region model (ECSD) was developed by Dwight T. Decker and John R. Jasperse and incorporates photoelectrons calculated using the continuous slowing down (CSD) approximation [*Jasperse*, 1982]. Ion concentrations are calculated assuming local chemical equilibrium. A small nighttime source is included to ensure that an E layer is maintained throughout the night.

2.3 *The High Latitude Model*

The high latitude model (incorporating both *E* and *F* layers) is the Utah State University (USU) Time Dependent Ionospheric Model (TDIM). (See *Schunk* [1988] for a review.) This model is similar to the low and middle latitude models except that the flux tubes are truncated and a flux boundary condition is applied at the top. In addition, the flux tubes move under the influence of the high latitude convection electric field. In the low latitudes, because the magnetic field is mainly horizontal, the effect of the electric field is primarily to move the ionization in altitude. In contrast, the high latitude magnetic field is mainly vertical, and the electric field driven convection is horizontal. Like LOWLAT, this model has a long history and has been validated by numerous comparisons with data.

TDIM includes an *E*-layer model that incorporates the effects of ionization by precipitating auroral particles. The ion production rates used were calculated using the B3C electron transport code [*Strickland*, 1976; *Strickland et al.*, 1994] and incident electron spectra representative of DMSP SSJ/5 data. The characteristics of the electron spectra were taken from the *Hardy et al.* [1987] electron precipitation model. The high latitude convection patterns were those developed by *Heppner and Maynard* [1987] for southward directed B_z.

3. PARAMETERIZATION OF THE PHYSICAL MODELS

Parameterization of the physical models proceeded in two steps. First, the models were used to generate a number of output "databases" for a discrete set of geophysical conditions. Each database consists of ion density profiles on a discrete grid of latitudes and longitudes for a 24 hour period in UT. Second, to reduce storage requirements, the databases were approximated with semi-analytic functions. These two processes are described in the following subsections.

3.1 *Geophysical Parameters*

All the physical models were parameterized in terms of season and solar activity. The middle and high latitude models were also parameterized in terms of magnetic activity, while the high latitude model was additionally parameterized in terms of the sign of the interplanetary magnetic field component B_y. (The high latitude model was only run using B_z southward. Northward B_z conditions are modeled using the low magnetic activity databases.) For the middle and low latitudes, the F layer (O^+) and the E layer ($NO^+$and O_2^+) were computed and parameterized separately. The high latitude model (TDIM) produced all three ions at once.

Due to time and computer resource limitations, only a few values of each parameter were used. The season "values" are the June and December solstices and the March equinox (which also "stands in" for the September equinox). We hope to change from seasonal to monthly values in a future version of PRISM. The values of the other parameters are summarized for each latitude region in Table 1. Note that the USU TDIM and LOWLAT produce output in magnetic local time (MLT), while MIDLAT and ECSD produce output in magnetic longitude. Since the two coordinates are readily interconvertible, we will ignore the distinction and refer only to magnetic longitude in the description that follows.

Table 1: Geophysical Parameter Values

	Solar Activity ($F_{10.7}$)	Magnetic Activity (K_p)	IMF B_y direction	Number of databases
Low Latitude F layer	70, 130, 210	N/A	N/A	36[a]
Midlatitude F layer	70, 130, 210	1, 3.5, 6	N/A	54[b]
Low & Midlatitude E layer	70, 130, 210	1, 3.5, 6	N/A	54[c]
High Latitude E & F layer	70, 130, 210	1, 3.5, 6	+, -	324[d]

[a] 3 seasons × 3 solar activities × 4 longitude sectors

[b] 3 seasons × 3 solar activities × 3 magnetic activities × 2 hemispheres

[c] 3 seasons × 3 solar activities × 3 magnetic activities × 2 species

[d] 3 seasons × 3 solar activities × 3 magnetic activities × 2 By's × 3 species × 2 hemispheres

3.2 *Representation of the Databases*

When the models are run for any one set of geophysical parameters (e.g., June, $F_{10.7}$ = 130, K_p = 1), they produce ion densities (O^+, NO^+, and O_2^+) on a four dimensional grid. MIDLAT and ECSD use a grid of magnetic latitude (λ), magnetic longitude (φ), altitude(z), and Universal Time (τ). TDIM uses magnetic local time (MLT or ψ) instead of magnetic longitude, while LOWLAT uses MLT instead of UT. In order to make this mass of numbers more manageable, we produced a semi-analytical representation of each database. The space and time grid parameters are summarized for each latitude region in Table 2.

Due to the computer resource requirements of the low latitude F layer code, it was used to generate databases at four discrete longitudes (corresponding to longitude sectors for which **E**×**B** drift measurements were available). Each longitude sector was parameterized separately, and the necessary longitude interpolation is carried out in PIM and PRISM during execution, as described below.)

Because we were trying to represent discrete data (rather than continuous functions), and because we were working with regional rather than global data sets, we felt that the usual spherical harmonic expansion techniques were not appropriate. Instead we concentrated on the use of orthogonal functions of discrete variables.

Table 2: Horizontal Grid Parameters

Latitude Region	Magnetic Latitude	Magnetic Longitude	UT	Number of altitude profiles per database
Low Latitude F layer	–44° to 44° in 2° steps	30°, 149°, 250°, and 329°	MLT: 0.0 to 23.5 in 0.5 hr steps	2,160
Midlatitude F layer	34° to 74° and –34° to –74° in 4° steps	0° to 345° in 15° steps	0100 to 2300 in 2 hr steps	3,168
Low and Midlatitude E layer	–76° to 76° in 4° steps	0° to 345° in 15° steps	0100 to 2300 in 2 hr steps	11,232
High Latitude E & F layer	51° to 89° and –51° to –89° in 2° steps	MLT: 0.5 to 23.5 in 1 hour steps	0100 to 2300 in 2 hr steps	5,760

We considered the use of modified Chapman functions for representing altitude profiles of ion densities. These functions have the advantage that peak height and peak density are explicit parameters, but the extremely non-linear nature of these functions necessitates the use of non-linear least squares fitting methods. While such methods produced excellent representations of individual profiles, the variation of the fitted parameters with latitude, longitude (or MLT), and UT was unacceptably noisy. Consequently, we chose to use Empirical Orthornormal Functions for the altitude representation.

Empirical Orthonormal Functions (EOFs) have been used extensively to represent meteorological and climatological data [*Lorenz*, 1956; *Kutzbach*, 1967; *Davis*, 1976; and *Peixota and Oort*, 1991]. They have also been used for empirical ionospheric modeling [*Secan and Tascione*, 1984]. EOFs are described in Appendix A. They have the advantage of providing a representation in terms of linear combinations of orthogonal functions, which allows for straightforward determination of coefficients. However, because peak density and peak height are not explicit parameters of the representation, these parameters can be determined only by reconstructing the entire profile and invoking a peak finding algorithm. At the time of the initial PRISM development effort (1989-1991), limitations on computer recourses and other considerations dictated that we use separate sets of EOFs for each ionospheric database. Since that time we have realized that we could have accumulated the covariance matrix across all of the databases (as long as we used the same altitude grid for every model run) and thus generate a single set of EOFs for the entire model. We have since done this (under separate funding) for a prototype low and midlatitude model and found that it works quite well with only a small increase in the number of EOFs required to represent the ionospheric profiles to high accuracy. We hope to be able to reparameterize the physical model runs using a single set of EOFs for a future version of PRISM. This would permit the interpolation on EOF coefficients rather than on reconstructed EDPs as is required by the current version of PRISM.

For longitude (or local time) variations (and for the low latitude F layer UT variation), the obvious choice is a Fourier series, since trigonometric functions retain their orthogonality properties on uniform discrete grids and because the data is periodic in the independent variable. These worked quite well for the high latitude models under all conditions and for the low and midlatitude models under low to moderate solar activity conditions. However, they did not work well for the low and midlatitude models under high solar activity conditions, apparently because the EOF coefficients exhibited exceptionally large gradients at dawn and dusk. Therefore, we decided to tabulate the coefficients in longitude for all the low and midlatitude databases. We have experimented with using EOFs for the longitude variations in our prototype low and midlatitude model, and may use this approach in a future version of PRISM.

For the latitude variations, we chose to generate grid-specific orthogonal polynomials using the algorithm derived in *Beckmann* [1973] and described in Appendix B. To help keep the notation straight, we summarize it in Table 3.

Table 3. Notation Summary

grid	variable	index	orthogonal function	index
altitude	z_i	$1 \le i \le I$	EOF: $g_m(z_i)$	$1 \le m \le M$
latitude	λ_j	$1 \le j \le J$	polynomial: $u_n(\lambda)$	$0 \le n \le N$
longitude	φ_k	$1 \le k \le K$	trigonometric[a]: $\cos(p\varphi)$ and $\sin(p\varphi)$	$0 \le p \le P$
local time	ψ_k	$1 \le k \le K$	trigonometric[b]: $\cos(p\psi)$ and $\sin(p\psi)$	$0 \le p \le P$
UT	τ_l	$1 \le l \le L$	trigonometric[a]: $\cos(q\tau)$ and $\sin(q\tau)$	$0 \le q \le Q$

[a]Not used for any database in PRISM 1.5, but may be used in future versions.
[b]Used only for high latitude databases.

The semianalytic representation of each database was generated in several steps. For all ionospheric regions, the first step was the determination of the EOFs from the ion densities in the database and a set of coefficients $c_{lm}(\lambda_j, \varphi_k)$ for representing each ion density profile on the latitude, longitude, UT grid (See Appendix A).

$$n_s(z_i, \lambda_j, \psi_k, \tau_l) \approx \sum_{m=1}^{M} c_m^{(s)}(\lambda_j, \psi_k, \tau_l) g_m^{(s)}(z_i) \qquad \text{[TDIM]} \qquad (1a)$$

$$n_s(z_i, \lambda_j, \varphi_k, \tau_l) \approx \sum_{m=1}^{M} c_m^{(s)}(\lambda_j, \varphi_k, \tau_l) g_m^{(s)}(z_i) \qquad \text{[midlatitude LOWLAT, ECSD]} \qquad (1b)$$

$$n_s(z_i, \lambda_j, \varphi_k, \psi_l) \approx \sum_{m=1}^{M} c_m^{(s)}(\lambda_j, \varphi_k, \psi_l) g_m^{(s)}(z_i) \qquad \text{[low latitude LOWLAT]} \qquad (1c)$$

where z_i, λ_j, φ_k, ψ_k, τ_j, and ψ_l are all points on the model output grid, and $g_m^{(s)}(z_i)$ is the m^{th} EOF evaluated at z_i. (Note, however, that a different set of $g_m^{(s)}(z_i)$ functions are used for each ion, for each set of geophysical conditions, and for each model.)

For the high latitude model (TDIM, both *E*- and *F*-layers), the second step was the generation of Fourier coefficients in MLT, $a_{mp}^{(s)}(\lambda_j, \tau_l)$ and $b_{mp}^{(s)}(\lambda_j, \tau_l)$, for each point on the latitude, UT grid.

$$n_s(z_i, \lambda_j, \psi, \tau_l) \approx \sum_{m=1}^{M} \sum_{p=0}^{P} \left\{ a_{mp}^{(s)}(\lambda_j, \tau_l) \cos(p\psi) + b_{mp}^{(s)}(\lambda_j, \tau_l) \sin(p\psi) \right\} g_m^{(s)}(z_i) \qquad \text{[TDIM]} \qquad (2)$$

For the low and midlatitude models, we found that a truncated Fourier series often introduced spurious longitudinal dependences, apparently driven by the steep gradients at dawn and dusk. The effect was particularly pronounced at high solar activity when the day/night contrast is the greatest. Consequently, for these models, the EOF coefficients remain tabulated in longitude.

For all models, the next step was the generation of orthogonal polynomials from the latitude grid (Appendix B). For the high latitude model (TDIM) the coefficients are $\alpha_{mnp}^{(s)}(\tau_l)$ and $\beta_{mnp}^{(s)}(\tau_l)$, and the ion density is approximated by

$$n_s(z_i, \lambda, \psi, \tau_l) \approx \sum_{m=1}^{M} \sum_{n=0}^{N} \sum_{p=0}^{P} \left\{ \alpha_{mnp}^{(s)}(\tau_l) \cos(p\psi) + \beta_{mnp}^{(s)}(\tau_l) \sin(p\psi) \right\} g_m(z_i) u_n(\lambda) \qquad \text{[TDIM]} \qquad (3a)$$

For MIDLAT and ECSD the coefficients are $\gamma_{mn}^{(s)}(\lambda_k, \tau_l)$ and the ion density is approximated by

$$n_s(z_i, \lambda, \varphi_k, \tau_l) \approx \sum_{m=1}^{M} \sum_{n=0}^{N} \gamma_{mn}^{(s)}(\varphi_k, \tau_l) g_m(z_i) u_n(\lambda) \qquad \text{[midlatitude LOWLAT, ECSD]} \qquad (3b)$$

For LOWLAT the coefficients are $\eta_{mn}^{(s)}(\varphi_k, \psi_l)$ and the ion density is approximated by

$$n_s(z_i,\lambda,\varphi_k,\psi_l) \approx \sum_{m=1}^{M}\sum_{n=0}^{N} \eta_{mn}^{(s)}(\varphi_k,\psi_l) g_m(z_i) u_n(\lambda) \qquad \text{[low latitude LOWLAT]} \qquad (3c)$$

The number of terms in each series are listed in Table 4 for each region.

Table 4: Altitude Grids and EOF's

Database	number of altitude points	minimum altitude	maximum altitude	number of EOF's
low latitude O^+	55	160	1600	9
midlatitude O^+	49	125	1600	8
low & midlatitude NO^+ & O_2^+	28	90	400	7
high latitudeO^+, NO^+, & O_2^+	37	100	800	6

Note that in none of these cases was the altitude spacing uniform.

Because of the extensive use of tabulated coefficients, the ion density at an arbitrary point must be obtained by interpolation. In PIM and PRISM, altitude interpolation is quadratic, while UT interpolation is linear. For the MIDLAT databases, the longitude interpolation is also linear, as is the local time interpolation in the LOWLAT databases. However, the longitude interpolation in the LOWLAT databases is more complicated. First, the O^+ profile for the desired magnetic latitude and local time is reconstructed for each of the four longitude sectors. Then the peak height and peak density is determined for each profile. The peak height for the desired longitude is determined by Fourier interpolation, and all four profiles are shifted to match the interpolated peak height. Then Fourier interpolation is used at each altitude to obtain the interpolated ion density profile. This is probably not ideal, but we hope to replace the four longitude sectors with 12 or even 24 in a future version of PRISM.

3.3 *Merging the Regional Models*

Because we used four different regional models in the development of PRISM, the models must be merged at region boundaries. Specifically, the low latitude and midlatitude O^+ models have to be merged across the boundary between low and middle latitudes, while all three ions (O^+, NO^+, and O_2^+) must be merged across the boundary between midlatitudes and high latitudes.

The transition from low latitude O^+ profiles to midlatitude O^+ profiles takes place between 34° and 44° in both hemispheres. The transition is accomplished by taking a weighted average of the h_mF_2 values from the two models in which the weight shifts linearly from 100% low latitude at 34° to 100% midlatitude at 44°. The profiles are shifted to match the averaged h_mF_2 values and then a similar weighted average of the shifted profiles is taken to produce the final merged profile. Because we now use the same model for middle and low latitudes, the transition is smoother than in earlier versions. No transition for NO^+ and O_2^+ is necessary since a single model was used for these ions.

The transition from midlatitude to high latitude takes place over an 8° wide zone whose poleward boundary is the equatorward boundary of the trough. The transition process is similar to the low to midlatitude transition, except that the high latitude profiles are shifted to match the h_mF_2 and h_mE values given by the midlatitude models. The final profile is produced by a weighted average of midlatitude and (shifted) high latitude profiles.

Although PRISM uses geomagnetic coordinates internally, it can produce output in either geomagnetic or geographic coordinates. A contour map of N_mF_2 in geographic coordinates (cylindrical projection) for 1200 UT on 21 June 2001 with solar activity and geomagnetic activity indices set to their actual values is displayed in Figure 1. The equatorial anomaly is clearly visible between East longitudes 30° and 180°, corresponding to local times of 1400 and 2400.

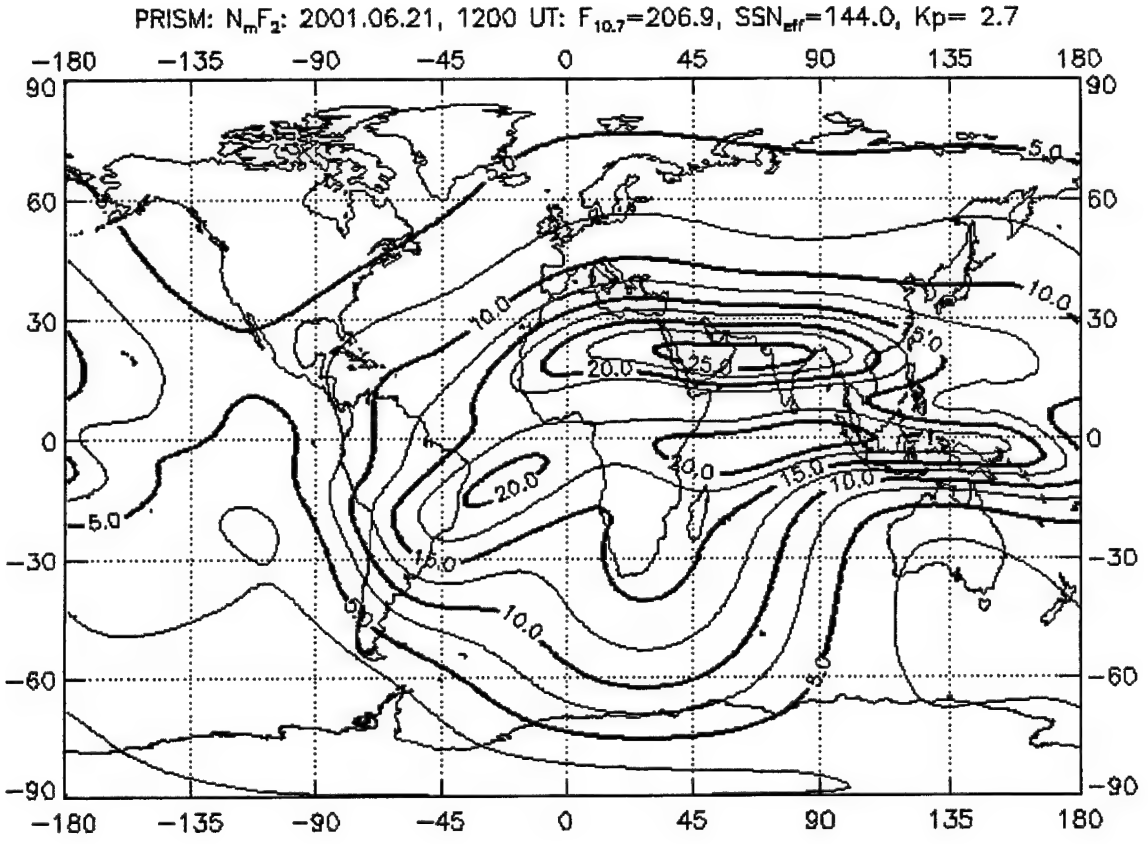

Figure 1. Contours of N_mF_2 (in units of 10^5 cm^{-3}) in cylindrical equidistant projection from PRISM for 1200 UT on 21 June 2001. The equatorial anomaly is clearly evident from about 1400 to 2400 local time.

The high latitude region is more clearly seen in a polar projections such as is displayed in Figures 2 and 3, again in geographic coordinates. Figure 2 shows the Northern (Summer) Hemisphere and the Southern (Winter) Hemisphere for the same date and conditions as Figure 1.

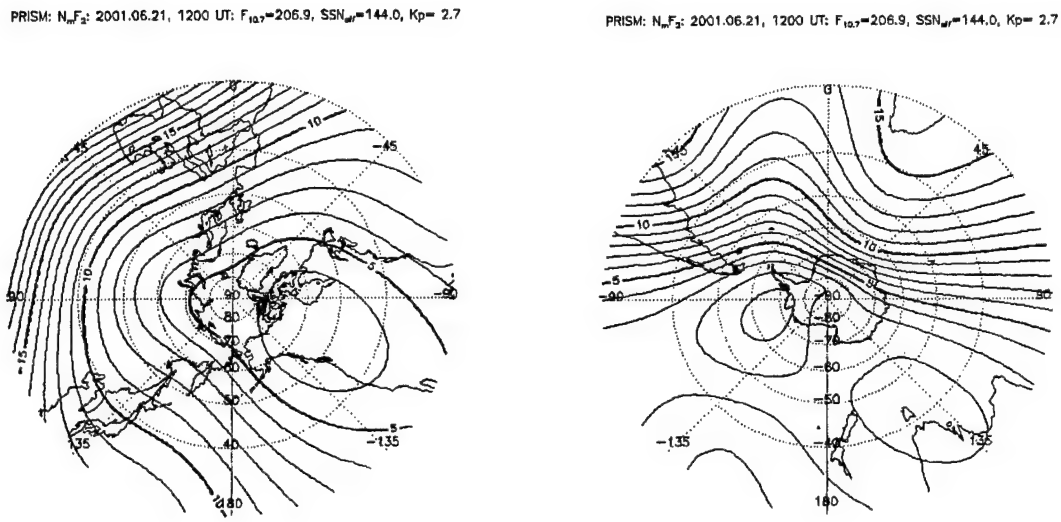

Figure 2. Contours of $N_m F_2$ (in units of 10^5 cm^{-3}) in polar projection for the Northern (Summer) Hemisphere (left) and for the Southern (Winter) Hemisphere (right) for the same date and conditions as Figure 1. Note that noon is at the top and dawn is at the right in both diagrams.in both

4. REAL TIME ADJUSTMENT ALGORITHM

The Real Time Adjustment (RTA) algorithm for the low and middle latitude regions is different from the algorithm used in the high latitude region. This is partly due to the relatively complex morphology of the high latitude ionosphere and partly due to an evolution in our ideas about the real time adjustment process during the development of PRISM.

The basic philosophy of the low and midlatitude RTA is to reproduce the input data nearly exactly and to interpolate correction factors smoothly between measurement points. Thus the first step is to compare PRISM climatology with the measurements and derive corrections that will bring PRISM into agreement with the measurements at the points of measurement. Then the next step is to calculate an "global" correction field (or an interpolation field) that spreads the corrections across the entire low and midlatitude region. The final step is to apply the correction field to PRISM climatology and write the resulting ionospheric specification to the output file. (In practice, the correction field is calculated "on the fly" and applied to each output point as it is needed.)

The high latitude RTA has a somewhat different philosophy. Because of the large amount of horizontal structure that is present in the high latitude region and the relative paucity of data available in near real time, the RTA involves a region-by-region least squares approach. The RTA distinguishes between "indirect" parameters (such as an effective $F_{10.7}$ or Kp) and "direct" measurements (such as a measurement of electron density at a point). It treats the indirect parameters as adjustable, and varies them until the difference between PRISM and the direct measurements is minimized in a least squares sense. In practice, the RTA uses certain measurements (e.g., energy flux of particle precipitation and horizontal ion drift) to set.

It should be noted that PRISM was originally envisioned as assimilating data that was nominally obtained at the instant of the run time. That is, if PRISM is run for 1200 UT, then only data taken within a few minutes of 1200 UT would be assimilated. However, it quickly became apparent that much data is not immediately available and that PRISM, which was already anticipated to be data starved, would have very little data to assimilate if operated in that fashion. Therefore, we adopted a data window that would allow PRISM to assimilate all data taken within a four hour window centered on the nominal run time. For real time (or near real time) operation, this effectively means that PRISM will accept data that is up to two hours old, while for post event analysis, PRISM will also accept data that was taken up to two hours after the nominal run time.

4.1 Available Data

The near real time data available for use in the adjustment process comes from the Digital Ionospheric Sounding System (DISS), the Ionospheric Monitoring System (IMS), and a suite of Special Sensors on the DMSP satellites. The DISS network consists of a more than a dozen digital ionosondes measuring critical frequencies, critical heights, and bottomside profiles. The DISS ionosondes are derived from the Digisonde 256 (D256) developed by the University of Massachusetts at Lowell (UML). The Ionospheric Monitoring System consists of a separate

network of dual frequency GPS receivers measuring TEC. In addition AFWA receives GPS TEC data in near real time from a network of approximately 24 GPS receivers that are part of the International GPS System (IGS) used to monitor plate tectonics and other geophysical data. The DMSP Special Sensors include the in situ plasma properties measured by the SSIES instrument and the precipitating particle measurements of the SSJ/4 instrument. In the near future, the SSJ/4 instrument will be replaced by the SSJ/5 instrument and a new set of ionospheric remote sensing instruments, SSUSI and SSULI will be added. SSUSI (a multispectral UV imager) and SSULI (a multispectral limb imager) will make measurements of dayglow, nightglow, and auroral optical emissions (mostly ultraviolet). The observed intensities will be processed on the ground to deduce ionospheric properties in the form of PRISM profile parameters [e.g., *Fox et al.*, 1994].

Because TEC is an integral quantity, it is not easy to incorporate it into the PRISM real time scheme. In PRISM 1.7, we have chosen to convert TEC into an equivalent point datum. Our method for doing so is described in Appendix C.

4.2 *Low and Midlatitude Adjustment Parameters*

The PRISM real time adjustment algorithm operates on six parameters that prescribe how an electron density profile is to be modified or "corrected":

1. $\Delta f_o F_2$, the correction to the model $f_o F_2$,
2. $\Delta f_o E$, the correction to the model $f_o E$,
3. $\Delta h_m F_2$, the correction to the model $h_m F_2$,
4. $\Delta h_m E$, the correction to the model $h_m E$,
5. ΔN_{top}, the correction to the O^+ density at a specific altitude (i.e., the DMSP altitude)
6. ΔH_{top}, the correction to the O^+ scale height at a specific altitude (i.e., the DMSP altitude)

The nominal value for each of these parameters is zero. A positive (negative) value means that the model value must be increased (decreased). Using the available near real time data, the real time adjustment process will assign non-zero values at each location where data is available (the driver sites).

Parameters 1-4 are based on direct measurements by DISS digital ionosondes. Parameter 5 is based on the direct measurement of the O^+ density by the SSIES instrument on board the DMSP satellite. In contrast, Parameter 6 must be inferred from the electron and ion temperatures (T_e, T_i) measured by the SSIES instrument. At midlatitudes, PRISM assumes that the topside ionosphere is in diffusive equilibrium and calculates the topside scale height from

$$H_{top} = \frac{k(T_e + T_i)}{m_{O^+} g} \tag{4}$$

The corresponding model value is obtained from the model O^+ densities (n_2, n_1) at the grid altitudes (z_2, z_1) immediately above and below the DMSP altitude:

$$H_m = \frac{z_2 - z_1}{\ln(n_1/n_2)} \tag{5}$$

At low latitudes, the topside scale height is determined by diffusive processes alone, so the scale height cannot be inferred from the SSIES temperature data.

After PRISM reads all of the input data files and writes them into a single scratch file, the data ingestion process proceeds with five passes through the combined input data file. The first pass searches for layer height data (Parameters 3 and 4) and calculates the height correction for each such datum. On the second pass, PRISM searches for peak density data (Parameters 1 and 2) applying the height corrections as it goes along. On the third pass, the code searches for TEC data that is *farther* than the parameter DCL (decorrelation length, currently set to 1000 km at compile time) from the nearest ionosonde station and calculates peak density corrections as described in Section 4.5 below. On the fourth pass, the code searches for SSIES in situ plasma data and calculates topside corrections (Parameters 5 and 6). On the fifth and final pass, the code searches for TEC data that is *closer* than DCL to the nearest ionosonde but *farther* than DCL from the nearest SSIES datum. Any TEC data that meet this criteria are used to calculate topside corrections as described in Section 4.5 below. (Any TEC data not meeting the criteria of the third or fifth pass are ignored.)

4.3 *Real Time Adjustment of the Low and Midlatitude Profile Parameters*

In PRISM 1.7, after the values of the profile adjustment parameters have been determined at each driver site, the global correction field is determined using a weighted average method.

1. Given N driver locations and the associated geomagnetic coordinates (λ_n, ϕ_n), let the unadjusted PRISM value at the n^{th} point be u_n and the measured value be v_n.
2. The correction to be applied to the unadjusted PRISM (i.e., PIM) value at the n^{th} point is $c_n = v_n - u_n$.
3. At any other point, (λ, ϕ), the correction to be applied to the PIM value is

$$c(\lambda,\phi) = \frac{\sum_{n=1}^{N} w_n(\lambda,\phi) c_n}{\sum_{n=1}^{N} w_n(\lambda,\phi)} \tag{6}$$

where the $w_n(\lambda,\phi)$ are weight functions that depend on the *distance measure* $d_n(\lambda,\phi)$ between the point (λ,ϕ) and the n^{th} point(λ_n,ϕ_n).

$$w_n(\lambda,\phi) = \frac{\prod_{k=1}^{N} d_k(\lambda,\phi)}{d_n(\lambda,\phi)} = \prod_{k\neq n}^{N} d_k(\lambda,\phi) \tag{7}$$

In PRISM 1.7 we have used the following distance measure.

$$d_n(\lambda,\phi) = \tfrac{1}{2}\left[1 - \cos\gamma_n(\lambda,\phi)\right] \tag{8}$$

where $\gamma_n(\lambda,\phi)$ is the great circle distance between (λ,ϕ) and (λ_n,ϕ_n):

$$\cos\gamma_n(\lambda,\phi) = \sin\lambda\sin\lambda_n + \cos\lambda\cos\lambda_n\cos(\phi-\phi_n) \tag{9}$$

As a practical matter, the actual weighting function used in PRISM is $w_n(\lambda,\varphi) = 1/d_n(\lambda,\varphi)$ unless $d_m(\lambda,\varphi) < \delta$ for some driver station m. In that case, $w_m = 1$ and $w_n = 0$ for $n \neq m$. In PRISM 1.7, δ is set to 10^{-6}. It should be noted that in the case where a station has supplied several measurements during PRISM's four hour data window, the above algorithm effectively averages the corrections for that station. Consequently, the RTA may not precisely reproduce a measurement taken at the nominal time of the run.

Because the decorrelation length of the ionosphere is of the order of 1000 km or less, no interpolation scheme can hope to accurately reproduce ionospheric parameters where there is no data. Clearly, the denser the data net, the better the model will do. Unfortunately, the data sets available so far are rather sparse, particularly over the oceans. PRISM provides the option of introducing "phantom stations" in regions with no data in order to force PRISM to relax to climatology in those regions. We recommend that under normal circumstances PRISM be run without PHANTOM stations. (The option is a compile time option, requiring that PRISM – or at least the main program – be recompiled in order to exercise this option.) For completeness, we describe the procedure the PRISM follows for placing phantom stations.

The low and midlatitude region is divided into 32 rectangular subregions with boundaries defined by the following parallels of latitude and meridians of longitude:

parallels of latitude: 60°S, 30°S, 0°, 30°N, and 60°N

meridians of longitude: 30°E, 75°E, 120°E, 165°E, 210°E, 255°E, 300°E, and 345°E

There is a phantom station located at the center of each rectangle. During the data ingestion process, PRISM keeps track of how many stations are located in each rectangular subregion, and how many have f_oF_2 data. As long as at least one station in a subregion reports a value for f_oF_2, then the phantom station for that subregion is ignored. If, however, no station in the subregion reports a value for f_oF_2, then the phantom station is assigned a value provided by PRISM climatology at that point. A similar procedure is followed for h_mF_2, F_oE, and h_mE data. These phantom stations force the correction field to relax to values near zero in regions where there is no data.

4.4 *Modifying the Low and Midlatitude Model Profiles*

The interpolation method described above provides a global correction field that can be used to calculate the profile correction parameters at any location. In this section, we describe the way in which the profiles are adjusted using the profile correction parameters. First the layer heights are adjusted, then the layer peak densities, and finally the topside correction is applied.

The layer height correction, using parameters 3 and 4 is a simple shifting of the profiles. If the F layer correction is Δh_mF_2, then the O^+ profile is shifted so that

$$n_{O^+}{}^{new}(z) = n_{O^+}{}^{old}(z - \Delta h_mF_2) \tag{10}$$

A similar shift is applied to the molecular ion profiles, except that the altitude shift is Δh_mE.

Once the altitude corrections have been applied, parameters 1 and 2, the critical frequencies, will be used to scale the ion density profiles. First, the peak densities of the *E*- and *F*-layers are first converted to critical frequencies. The additive correction is applied to each critical frequency, which is then converted back to a density. The ratios of the critical corrected to climatological peak densities are use to scale the molecular and atomic ion density profiles.

$$R_F = \frac{N_m F_2^{(corrected)}}{N_m F_2^{(climo)}}$$
$$R_E = \frac{N_m E^{(corrected)}}{N_m E^{(climo)}} \tag{11}$$

The ratio, R_F, is used to scale the ion density profiles (molecular and atomic) above the *F*-layer peak. The ratio, R_E, is used to scale ion density profiles (molecular and atomic) below the *E*-layer peak. Between the two layer peaks, the scaling process is more complicated. First we define a transition altitude h_bF_2 which is the larger of the (a) altitude at which the O^+ density has fallen to $e^{-2}N_mF_2$ and (b) $h_{2/3} = h_mF_2 - \frac{2}{3}(h_mF_2 - h_mE) = h_mE + \frac{1}{3}(h_mF_2 - h_mE)$. Then we define a scale factor that smoothly varies between R_E at h_mE and R_F at h_bF_2. Explicitly, the density scale factor (applied to both molecular and atomic ions) is

$$S(z) = \begin{cases} R_F, & z \geq h_bF_2 \\ R_E + \frac{1}{2}(R_F - R_E)\left[1 - \cos\left(\frac{\pi(z - h_mE)}{h_bF_2 - h_mE}\right)\right], & h_mE < z < h_bF_2 \\ R_E, & z \leq h_mE \end{cases} \tag{12}$$

At the altitude boundaries h_mE and h_bF_2, $S(z)$ has the desired properties

$$S(h_mE) = R_E$$
$$\left.\frac{dS}{dz}\right|_{h_mE} = 0 \tag{13a}$$

and

$$S(h_bF_2) = R_F$$
$$\left.\frac{dS}{dz}\right|_{h_mF_2} = 0 \tag{13b}$$

so that it varies smoothly across the altitude boundaries.

Parameters 5 and 6 are used to correct the topside profile based on n_e, n_i, T_e, and T_i measurements from SSIES on DMSP (nominally 840 km). Let $N_m(z)$ be the model O^+ profile (*after* f_oF_2 and h_mF_2 corrections have been applied). Further, let $z_p = h_mF_2$, and let z_{top}= the

altitude at which ΔN_{top} and ΔH_{top} were measured (usually the DMSP altitude). Let $N_c(z)$ be the corrected profile based on ΔN_{top} and ΔH_{top}. $N_c(z)$ must satisfy the following conditions:

$$N_c\left(z_{top}\right) = N_{top} \equiv N_m\left(z_{top}\right) + \Delta N_{top} \tag{14a}$$

and

$$\frac{1}{H_c\left(z_{top}\right)} \equiv -\left(\frac{1}{N_c}\frac{\partial N_c}{\partial z}\right)_{z=z_{top}} = \frac{1}{H_{top}} \equiv \frac{1}{H_m\left(z_{top}\right) + \Delta H_{top}} \tag{14b}$$

In PRISM the corrected profile is obtained from the model profile by scaling the altitude so that

$$N_c(z) = N_m(\zeta) \tag{15a}$$

where

$$\zeta(z) = \begin{cases} z, & z \le z_p \\ z_p + \left[2x_1 - R_H\right]\left(z - z_p\right) + \left[R_H - x_1\right]\dfrac{\left(z - z_p\right)^2}{z_{top} - z_p}, & z_p < z < z_{top} \\ z_1 + R_H\left(z - z_{top}\right), & z \ge z_{top} \end{cases} \tag{15b}$$

where

$$N_m(z_1) = N_{top} \tag{16a}$$

$$x_1 = \frac{z_1 - z_p}{z_{top} - z_p} \tag{16b}$$

$$R_H = \frac{H_m(z_1)}{H_{top}} \tag{16c}$$

and

$$\frac{1}{H_m(z_1)} = -\left(\frac{1}{N_m}\frac{\partial N_m}{\partial z}\right)_{z=z_1} \tag{16d}$$

Direct substitution of $z = z_{top}$ in Equation (15) verifies that $\zeta\left(z_{top}\right) = z_1$ so that Equation (14a) is satisfied. That Equation (14b) is satisfied may be seen from

$$\begin{aligned} \frac{1}{H_c\left(z_{top}\right)} &= -\left(\frac{1}{N_c}\frac{\partial N_c}{\partial z}\right)_{z_{top}} \\ &= -\left(\frac{1}{N_m(\zeta)}\frac{\partial N_m}{\partial \zeta}\frac{\partial \zeta}{\partial z}\right)_{z_{top}} = \frac{1}{H_m(z_1)}\left\{2x_1 - R_H + 2\left[R_H - x_1\right]\right\} \\ &= \frac{1}{H_{top}} \end{aligned} \tag{17}$$

This form ensures that the correction and its first derivative vanish at the peak and that the O^+ concentration and its slope are as specified at z_{top}.

When there is no topside scale height data (as at low latitudes), PRISM sets H_{top} to the value

$$H_{top} = \frac{1}{x_1} H_m(z_1) \qquad \text{(when } H_{top} \text{ is not determined from data)} \tag{18}$$

so that the altitude scaling becomes linear

$$\zeta(z) = z_p + x_1(z - z_p) \qquad \text{(when } H_{top} \text{ is not determined from data)} \tag{19}$$

Now let us examine the behavior of $\zeta(z)$. When H_{top} is not determined from the data, ζ is clearly well behaved: $\zeta(z_2) > \zeta(z_1)$ if $z_2 > z_1$ or in other words,

$$\frac{d\zeta}{dz} > 0 \tag{20}$$

as long as $z_1 > z_p$, which it should always be. On the other hand, in the quadratic case,

$$\frac{d\zeta}{dz} = \begin{cases} 1, & z \le z_p \\ (2x_1 - R_H) + 2(R_H - x_1)\dfrac{z - z_p}{z_{top} - z_p}, & z_p < z < z_{top} \\ R_H, & z \ge z_{top} \end{cases} \tag{21}$$

We require $d\zeta/dz > 0$ for $z_p < z < z_{top}$. This means that z_{ex}, the altitude at which $d\zeta/dz = 0$, must either be below z_p or above z_{top}. If it is below z_p, then we require that it represent a minimum, i.e. that $d^2\zeta/dz^2 > 0$. On the other hand, if it is above z_{top}, then we require that it represent a maximum, i.e., that $d^2\zeta/dz^2 < 0$.

$$z_{ex} = z_p + \frac{1}{2}(z_{top} - z_p)\frac{2x_1 - R_H}{x_1 - R_H} \tag{22}$$

$$\frac{d^2\zeta}{dz^2} = \frac{2(R_H - x_1)}{z_{top} - z_p}, \quad z > z_p \tag{23}$$

Since $z_{top} > z_p$ is almost always true, $z_{ex} < z_p$ only if

$$\frac{2x_1 - R_H}{x_1 - R_H} < 0 \tag{24}$$

which implies that $\frac{1}{2}R_H < x_1 < R_H$, since $R_H > 0$ by definition. On the other hand, $z_{ex} > z_{top}$ implies that

$$\frac{2x_1 - R_H}{x_1 - R_H} > 2 \tag{25}$$

or

$$\frac{x_1}{x_1 - R_H} > 1 \tag{26}$$

which is always true as long as $x_1 > R_H > 0$.

As an example, let us consider the following case:

$$N_m(z) = N_m(z_p)\exp\left\{\tfrac{1}{2}\left[1 - \frac{z - z_p}{H_0} - \exp\left(-\frac{z - z_p}{H_0}\right)\right]\right\} \tag{27}$$

where z_p and N_m have already been adjusted to fit the data. Suppose that we have measurements of N_{top} and H_{top} at $z_{top} = z_p + 8H_0$. Then z_1 is determined from

$$N_{top} = N_m(z_1) = N_m(z_p)\exp\left\{\tfrac{1}{2}\left[1 - \frac{z_1 - z_p}{H_0} - \exp\left(-\frac{z_1 - z_p}{H_0}\right)\right]\right\} \tag{28}$$

or

$$z_1 = z_p + H_0\left\{1 - 2\ln\left[\frac{N_{top}}{N_m(z_p)}\right] - \exp\left(-\frac{z_1 - z_p}{H_0}\right)\right\} \tag{29}$$

Solving iteratively, we have the "zeroth" approximation

$$z_1^{(0)} = z_p + H_0\left\{1 - 2\ln\left[\frac{N_{top}}{N_m(z_p)}\right]\right\} \tag{30}$$

and the first approximation

$$z_1^{(1)} = z_p + H_0\left\{1 - 2\ln\left[\frac{N_{top}}{N_m(z_p)}\right] - \exp\left[-1 + 2\ln\left(\frac{N_{top}}{N_m(z_p)}\right)\right]\right\} \tag{31a}$$

or

$$z_1^{(1)} = z_p + H_0\left\{1 - 2\ln\left[\frac{N_{top}}{N_m(z_p)}\right] - e^{-1}\left(\frac{N_{top}}{N_m(z_p)}\right)^2\right\} \tag{31b}$$

and

$$x_1 = \frac{z_1 - z_p}{z_{top} - z_p} \approx \frac{H_0}{z_{top} - z_p}\left\{1 - 2\ln\left[\frac{N_{top}}{N_m(z_p)}\right] - e^{-1}\left(\frac{N_{top}}{N_m(z_p)}\right)^{-2}\right\} \tag{32}$$

Suppose $N_{top} = e^{-2}N_m(z_p)$, then $z_1^{(1)} = z_p + H_0\left\{1 + 4 - e^{-1}e^{-4}\right\} \approx z_p + 4.99H_0$ and $x_1 \approx \frac{4.99H_0}{z_{top} - z_p}$.

With $z_{top} = z_p + 8H_0$, $x_1 \approx 0.624$.

Now

$$\frac{1}{H_m(z_1)} = -\frac{1}{N_m(z_1)}\left.\frac{\partial N_m}{\partial z}\right|_{z_1} = \frac{1}{2H_0}\left[1 - \exp\left(-\frac{z_1 - z_p}{H_0}\right)\right] \tag{33}$$

so

$$R_H = \frac{H_m(z_1)}{H_{top}} = \frac{2H_0}{H_{top}}\frac{1}{1 - \exp\left(-\frac{z_1 - z_p}{H_0}\right)} \approx \frac{2H_0}{H_{top}}\frac{1}{1 - e^{-4.99}} \approx \frac{2.02H_0}{H_{top}} \tag{34}$$

$$\zeta(z) = \begin{cases} z, & z \le z_p \\ z_p + \left[1.248 - \frac{2.02H_0}{H_{top}}\right](z - z_p) + \left[\frac{2.02H_0}{H_{top}} - 0.624\right]\frac{(z - z_p)^2}{8H_0}, & z_p < z < z_{top} \\ z_p + 0.624(z - z_p), & z \ge z_{top} \end{cases} \tag{35}$$

$$\frac{d\zeta}{dz} = \begin{cases} 1, & z \le z_p \\ \left(1.248 - \frac{2.02H_0}{H_{top}}\right) + 2\left(\frac{2.02H_0}{H_{top}} - 0.624\right)\frac{z - z_p}{8H_0}, & z_p < z < z_{top} \\ 0.624, & z \ge z_{top} \end{cases} \tag{36}$$

An example of the midlatitude profile correction algorithm applied to a single profile is shown in Figure 3, for which we have used Incoherent Scatter Radar (ISR) data from Arecibo to simulate simultaneous Digisonde and SSIES data. In this case, the data is from 1800 UT on 4 October 1989. In Figure 3a, the ISR data is compared with PRISM climatology. A profile from the Ionospheric Conductivity and Electron Density (ICED) model [*Tascione et al.*, 1988] is shown for comparison. The actual N_mF_2 is a factor of two higher, and the actual h_mF_2 is about 40 km higher, than the climatological values. In Figure 3b, the PRISM profile has been adjusted only to match the actual N_mF_2. In Figure 3c, both N_mF_2 and h_mF_2 have been adjusted to match the actual data. Finally, in Figure 3d, both the peak and topside adjustments have been made. If we define an RMS density error as

$$\text{RMS density error} = \sqrt{\frac{1}{13}\sum_{k=1}^{13}\left[\frac{N_{PRISM}(z_k) - N_{data}(z_k)}{N_{data}(z_k)}\right]^2} \tag{37}$$

then PRISM's RMS density error declines from 46% with no profile adjustment to 25% with an N_mF_2 adjustment only, to 18% with both N_mF_2 and h_mF_2 adjusted, and to 16% with both peak and topside adjustments.

Note that in operational use there are normally many data sites, and the topside and bottomside data are seldom co-located. Operationally, PRISM uses all available h_mF_2 and h_mE data to establish global layer height correction fields, then it uses the available N_mF_2 and N_mE data to calculate global profile scaling fields, and finally it uses the topside data to calculate global topside correction fields. These correction fields are then applied to each profile on the output grid as described above.

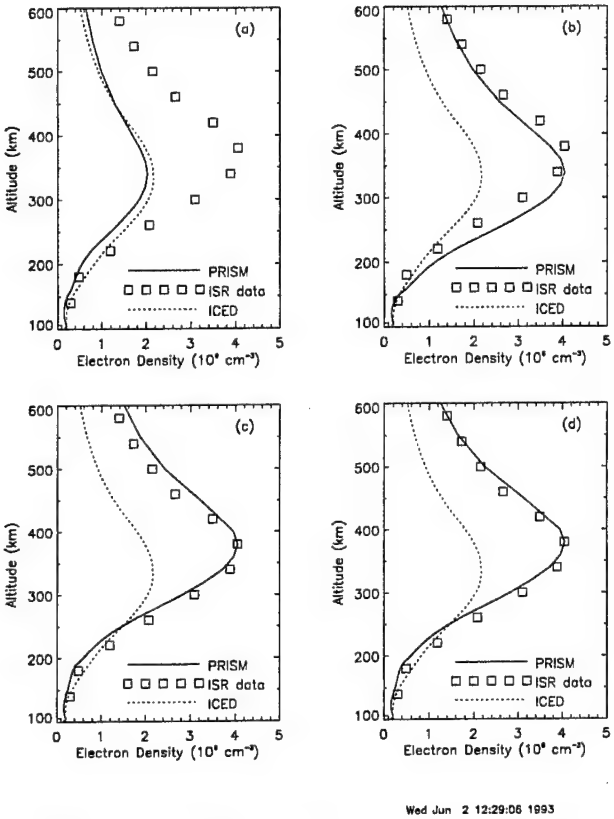

Figure 3. The PRISM profile adjustment procedure illustrated using Incoherent Scatter Radar (ISR) data from Arecibo. (a) No adjustment: The RMS density error is 46%. (b) N_mF_2 adjustment only: The RMS density error is 25%. (c) N_mF_2 and h_mF_2 adjustment: The RMS density error is 18%. (d) N_mF_2, h_mF_2, and topside adjustments: The RMS density error is 16%.

4.5 The use of TEC data in the low and midlatitude RTA

In order to use TEC data, PRISM must convert the TEC measurement into an equivalent point measurement. TEC data is ingested as vertical equivalent TEC at the Ionospheric Intersection Point (IIP). If the IIP is farther than DCL (currently 1000 km) from the nearest DISS site, then the TEC is converted into equivalent values of N_mF_2 and N_mE by scaling the entire electron density profile:

$$R_{TEC} = \frac{TEC^{(observed)}}{TEC^{(PRISM)}}$$
$$N_m F_2^{(corrected)} = R_{TEC} N_m F_2^{(climo)} \tag{38}$$
$$N_m E^{(corrected)} = R_{TEC} N_m E^{(climo)}$$

The corrected peak densities are converted into critical frequency parameters and critical frequency corrections are calculated as if the data were obtained from ionosondes:

$$\Delta f_o F_2 = f_o F_2^{(climo)} \left[\sqrt{R_{TEC}} - 1 \right]$$
$$\Delta f_o E = f_o E^{(climo)} \left[\sqrt{R_{TEC}} - 1 \right] \tag{39}$$

From this point, PRISM treats TEC data as if it were ionosonde data with $h_m F_2$ missing.

If the IIP is within DCL of a DISS site but further than DCL from the nearest SSIES datum, then the TEC measurement is converted into an equivalent SSIES density measurement. First, the $\Delta f_o F_2$ and $\Delta h_m F_2$ corrections determined from the nearest DISS site is applied to the PRISM profile at the IIP. Then the topside portion of the profile is corrected to force agreement with the TEC measurement:

$$n_{O^+}^{(new)}(z) = n_{O^+}^{(old)}(\zeta) \tag{40}$$

$$\zeta(z) = \begin{cases} z, & z \le h_m F_2 \\ h_m F_2 + a(z - h_m F_2), & z > h_m F_2 \end{cases} \tag{41}$$

where a is a scale factor to be determined from TEC.

The difference in TEC is

$$\Delta\text{TEC} = \int_{h_m F_2}^{\infty} n_{O^+}^{(new)} dz - \int_{h_m F_2}^{\infty} n_{O^+}^{(old)} dz \tag{42}$$

or

$$\Delta\text{TEC} = \frac{1-a}{a} \int_{h_m F_2}^{\infty} n_{O^+}^{(old)} dz \tag{43}$$

resulting in

$$a = \frac{\int_{h_m F_2}^{\infty} n_{O^+}^{(old)} dz}{\Delta\text{TEC} + \int_{h_m F_2}^{\infty} n_{O^+}^{(old)} dz} \tag{44}$$

If we identify the scale factor a with the ratio $(z_1 - h_m F_2)/(z_d - h_m F_2)$, then

$$z_1 = h_m F_2 + (z_d - h_m F_2)a \tag{45a}$$

$$N_{top} = n_{O^+}^{(old)}(z_1) \tag{45b}$$

and

$$H_{top} = aH_m \tag{45c}$$

If the IIP is within 1000 km of both a DISS station and a DMSP orbital track, the TEC measurement is ignored. In a future version of PRISM, in which the plasmasphere is included, TEC measurements in such situations will be used to constrain the H^+ density.

4.6 *The High Latitude Adjustment Algorithm*

Due to the complexity of the high latitude ionosphere, the real time adjustment algorithm differs appreciably from the low and midlatitude algorithm. Until SSUSI data becomes available, there will be insufficient data to adjust the parameterized USU model in the way that the parameterized low and midlatitude models can be adjusted. Even with SSUSI data, it is not clear that the midlatitude algorithm is appropriate for the high latitude regions.

In PRISM 1.2, the first step in the high latitude real time adjustment process is the establishment of boundary locations. Three boundaries are required: (1) the equatorward edge of the trough, (2) the equatorward edge of the auroral oval, and (3) the poleward edge of the auroral oval.

The equatorward edge of the trough is determined from SSIES drift meter data as the point where the measured ion drift speed departs from the corotation value. The trough boundary as a function of magnetic longitude is given by the formula

$$\theta_t(\varphi) = \theta_0(I_t) + a \exp\left[-\left(\frac{\varphi - b}{c}\right)^p\right] \tag{46}$$

where φ is the magnetic local time (MLT, hours), and I_t is a "trough index" correlated with K_p. $\theta_0(I_t)$ is the radius of the trough boundary at magnetic local midnight and is given by

$$\theta_0(I_t) = 24.4^\circ + 2.12^\circ I_t \tag{47}$$

The second term represents the dayside distortion of the boundary, which would otherwise be a circle centered on the magnetic pole. The parameter values are

a = -10.5°
b = 11.5 hr
c = 3.88 hr
p = 2.73

This model is an approximation to the convection boundaries shown in *Heppner and Maynard* [1987].

The trough index, I_t, is determined according to the following algorithm.

1. If there is no ion drift data, or if a boundary cannot be identified in the data, then $I_t = K_p$.
2. If a single boundary crossing is identified at colatitude θ_b and local time φ_b, then

$$\theta_0 = \theta_b - a \exp\left[-\left(\frac{\varphi_b - b}{c}\right)^2\right] \tag{48}$$

and

$$I_t = \frac{\theta_0 - 24.4°}{2.12°} \tag{49}$$

3. If two or more crossings are identified, then the value of I_t used is the average of the values determined for each crossing.

The boundaries of the auroral oval are determined from electron and ion precipitation data from the SSJ/4 instrument. Separate boundaries are determined for electron and ion precipitation. The algorithm for determining the electron and ion precipitation boundaries from the SSJ/4 data is described in Appendix D.

The next step in the high latitude adjustment process depends on the amount and kind of data available. The decision of how to proceed is made separately for the E layer (NO^+ and O_2^+) and the F layer (O^+). In each case, two choices are available:

F layer:

1. Perform a simple least squares adjustment of the USU O^+ model.
2. Use a semi-empirical f_oF_2 model (FMODEL) to adjust the USU O^+ profiles.

E layer:

1. Perform a simple least squares adjustment of the USU NO^+ and O_2^+ models.
2. Use a fast, first principles, E layer local chemistry model (HLE).

The decision matrix used in PRISM is shown in Table 5.

Table 5. PRISM High Latitude Decision Matrix

Data Available?			Model Used by PRISM	
DISS	SSIES	SSJ/4	*F* layer	*E* layer
Yes	Yes	Yes	FMODEL	HLE
Yes	Yes	No	FMODEL	USU
Yes	No	Yes	FMODEL	HLE
Yes	No	No	USU	USU
No	Yes	Yes	USU	USU
No	Yes	No	USU	USU
No	No	Yes	USU	USU
No	No	No	USU	USU

In experimenting with high latitude data, we found that extrapolating SSJ/4 data taken along the DMSP orbital track to points well away from the orbital track was very risky. We found no suitable model of the *instantaneous* auroral precipitation for this extrapolation.

When SSUSI auroral image data becomes available, this limitation will be removed because much less extrapolation will be required. It should be possible to use HLE whenever timely SSUSI images are available.

FMODEL is a semi-empirical model of f_oF_2 based on a combination of theory and data. It is divided into three regions: the subauroral trough, the auroral oval, and the polar cap. The f_oF_2 determined by least squares adjustment of the model parameters is used to scale the USU O^+ profiles. No further adjustment of the profiles is performed.

The subauroral trough is divided into two local time regimes: evening (from 1200 to 0000 MLT) and morning (from 0000 to 1200 MLT). Each trough (morning and evening) has a depth parameter that specifies the difference between the midlatitude value of f_oF_2 at the equatorward edge and the trough minimum. The local time variation of the trough depth is fixed (not part of the least squares adjustment process). If the width of the trough is less than 3°, the depth is reduced in proportion to the width so that when the width vanishes so does the depth. The thickness of the (equatorward) trough wall is always 60% of the total width of the trough. The poleward edge of the trough is the equatorward edge of the auroral F-layer, so the poleward "wall" is considered to be part of the auroral region.

At fixed magnetic local time, the auroral F layer f_oF_2 is simply a cubic polynomial in magnetic latitude:

$$f_oF_2(\lambda) = f_{max} + A(\lambda - \lambda_{max})^2 + B(\lambda - \lambda_{max})^3 \tag{50}$$

where $f_{max} = f_oF_2(\lambda_{max})$ is an extremum, and A and B are chosen so that f_oF_2 is continuous across the boundaries with the trough and polar cap.

The background polar cap f_oF_2 is obtained from the URSI coefficients using an internally derived effective sunspot number, the value of which is determined as part of the least squares adjustment process based on ionosonde data. It should be noted that this part of the model describes only the background polar cap ionosphere, not "polar cap patches" or "polar cap arcs."

5. VALIDATION

AFRL is conducting an extensive effort to validate PRISM using some of the many new data sources that have become available in recent years. The role of CPI in this effort will be documented in a future report.

6. DISCUSSION

Although PRISM represents the first ionospheric model to attempt near real time assimilation of a wide variety of ionospheric data, it's development began a decade and a half ago. Many of the design decisions were made with the limitations on disk storage, computer memory, and CPU processing speeds that were prevalent at the time. All of these limitations have been lifted and those design decisions should be reexamined. For example, there is no longer any reason not to increase the longitude resolution of the low latitude region to match that of the midlatitude region. Nor is there any reason not to replace PRISM's seasonal coefficient sets with monthly coefficient sets. And PRISM's operation could be streamlined by using a single set of EOFs for all latitudes, seasons, and solar/geomagnetic conditions. This would make it possible to interpolate on these variables in coefficient space rather than configuration space.

Beyond bringing PRISM up to date with modern computer capabilities, there are a number of other design decisions that ought to be revisited. One of these is the design of the Real Time Adjustment (RTA) algorithm. While it has the virtue of reproducing the input data (which virtue depends on the integrity and accuracy of such data), it is not capable of handling vertical TEC data very well, and slant TEC not at all. The use of a Kalman filter or Discrete Inverse Theory approach ought to be investigated to see if either or both could more effectively facilitate the assimilation of slant TEC data.

Another design feature that needs to be reexamined is the entire High Latitude RTA. This was the first part of PRISM to be developed and has not been either adequately validated or reexamined since that time. Kevin Scro of AFSMC, who is responsible for transitioning software to AFWA, has expressed legitimate concerns over the fact that the algorithm changes discontinuously depending on the kind of data available to PRISM. The entire high latitude algorithm needs to be reexamined and reformulated to take into account the capability of mapping the auroral oval boundaries over much of the high latitude region from SSUSI images that will soon be forthcoming from DMSP. Other enhancements that should be considered are (a) the addition of a good plasmasphere model, whether empirical or theoretical and (b) the inclusion of low latitude vertical drift (especially the pre-reversal enhancement) among the geophysical parameters.

Appendix A. Empirical Orthonormal Functions

This treatment of empirical orthogonal functions (EOF's) is based on the Appendix of *Secan and Tascione* [1984], which was based on *Lorenz* [1956], *Kutzbach* [1967], and *Davis* [1976]. See also *Peixota and Oort* [1991]. The reader is referred to these references for mathematical proofs of the assertions made below. In the following discussion, we use the notation given in Table 3 of the main text.

A database consists of altitude profiles at certain longitudes, certain latitudes, and certain Universal Times. (See Tables 1-4 of the main text.) Let S be the number of altitude profiles in a database, and let I be the number of points in each altitude profile. We would like to represent each altitude profile of the quantity Ψ (e.g., O^+concentration) as an expansion in orthogonal functions, $g_m(z_i)$:

$$\Psi_s(z_i) = \sum_{m=1}^{M} \alpha_{sm} g_m(z_i) + r_s(z_i), \qquad s = 1...S,\ i = 1...I \tag{A1}$$

where $r_s(z_i)$ is the residual, and the coefficients α_{sm} are calculated from

$$\alpha_{sm} = \sum_{i=1}^{I} \Psi_s(z_i) g_m(z_i) \tag{A2}$$

In principle, any orthogonal set of functions may be used. However, the references cited above provide an algorithm for finding the set which minimizes the RMS error for a given number of terms, $M \le I$. We summarize the algorithm here.

First define the $I \times I$ covariance matrix $\boldsymbol{C}$ with elements

$$C_{ij} = \frac{1}{S} \sum_{s=1}^{S} \Psi_s(z_i) \Psi_s(z_j), \qquad i, j = 1,2,...I \tag{A3}$$

Now consider the eigenvalue/eigenvector problem $\mathbf{C}\varphi = \varphi\mathbf{L}$ or

$$\sum_{j=1}^{I} C_{ij} \varphi_{jk} = \sum_{j=1}^{I} \varphi_{ij} \delta_{jk} \lambda_k = \varphi_{ik} \lambda_k \tag{A4}$$

where $\varphi = \{\varphi_{ij}\}$ is the matrix of eigenvectors of $\mathbf{C} = \{C_{ij}\}$, and $\mathbf{L} = \{\delta_{ij}\lambda_j\}$ is a diagonal matrix whose elements are the corresponding eigenvalues. (The k^{th} column of φ is the eigenvector corresponding to the k^{th} eigenvalue, λ_k.) By convention, the eigenvectors and eigenvalues are ordered so that $\lambda_1 > \lambda_2 > ... > \lambda_I$. Because $\mathbf{C}$ is a real symmetric matrix, eigenvectors corresponding to unique eigenvalues are guaranteed to be orthogonal [See, e.g., *Hildebrand*, 1965]. Because of the origin of the matrix $\mathbf{C}$, it is unlikely that any of its eigenvalues will be degenerate, so we may assume that φ is an orthogonal set. According to *Secan and Tascione* [1984] and references therein, the set of orthogonal functions that minimizes the RMS error for M terms is just the first M eigenvectors:

$$g_m(z_i) = \varphi_{im}, \qquad i = 1,2,...I;\ m = 1,2,...M \tag{A5}$$

These are the Empirical Orthonormal Functions (EOFs).

As a practical matter, we have found that the number of EOFs needed to provide a reasonably good representation for all the profiles is about $I/6$, as illustrated in Table 4 in the

main text. The only exception is the low and midlatitude E layer (NO^+ and O_2^+), probably because these databases covered both hemispheres simultaneously. We have also found that substantial improvement in representation does not occur until the number of EOF's is about *I*/2. Furthermore, the EOF's derived for one database were inadequate for any other database, and the EOF's simultaneously derived from several databases produce noticeably poorer representations than those derived for each database individually. Consequently, we have derived separate EOF sets for each database.

The first nine EOF's derived from the low latitude F region (O^+) database for the US longitude sector, the December solstice, and moderate solar activity, are shown in Figure A1. The first EOF always has the least structure, and successive EOF's become progressively more structured. Although differing in detail, the EOF's for the other databases are qualitatively similar.

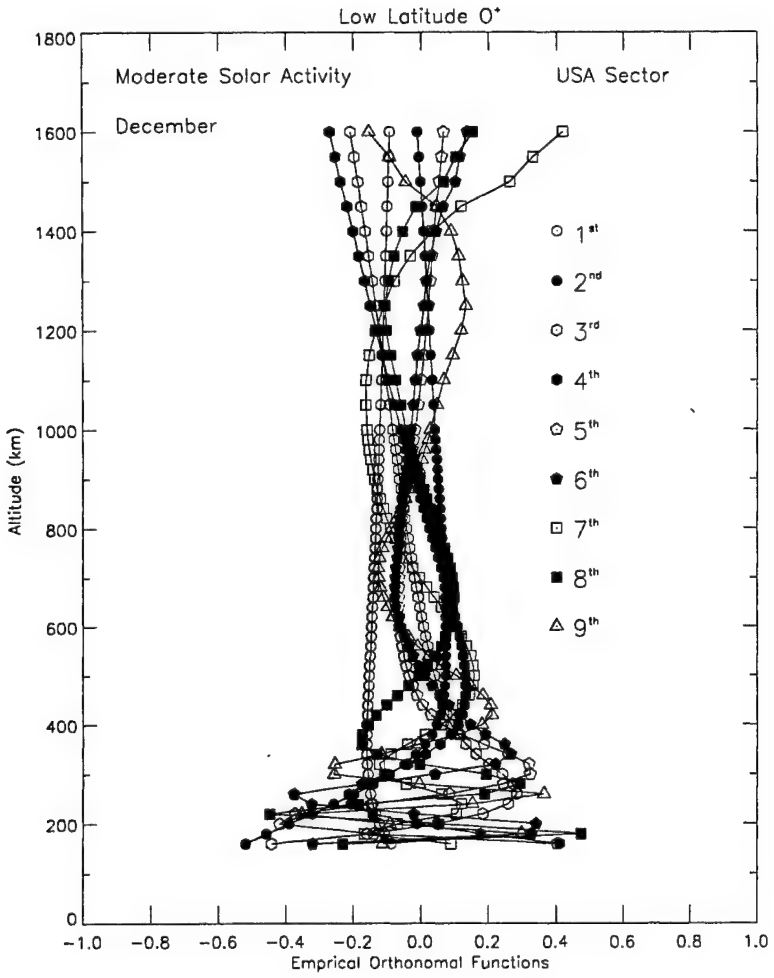

Figure A1. The Empirical Orthonormal Functions (EOF's) for low latitude O^+ derived from the LOWLAT output databases for the USA longitude sector, December solstice, moderate magnetic activity, and moderate solar activity. Only the first nine EOF's are plotted because these are the ones used in PRISM.

Appendix B. Orthogonal Polynomials of Discrete Variables

Because the databases to which we desire analytic approximations have discrete latitude grids, we preferred to use polynomials whose orthogonality is defined in terms of that grid, rather than in terms of integrals over the interval. The algorithm for generating orthogonal polynomials on a specified grid is given by *Beckmann* [1973]. Let us denote the desired polynomials by $u_n(\lambda)$ and define $u_{-1}(\lambda) \equiv 0$ and $u_0(\lambda) \equiv 1$. Note that the polynomials are continuous functions of the continuous variable λ even though their orthogonality is defined in terms of the discrete grid $\{\lambda_j, j = 1,2,...J\}$. The recursion relation for the polynomials is

$$u_{n+1}(\lambda) = (\lambda - B_n)u_n(\lambda) - \frac{h_n^2}{h_{n-1}^2}u_{n-1}(\lambda) \tag{B1}$$

where the norms h_n are given by

$$h_n = \sum_{j=1}^{J} u_n^2(\lambda_j) \tag{B2}$$

and the recursion constants B_n are given by

$$B_n = \frac{1}{h_n^2}\sum_{j=1}^{J} \lambda_j u_n(\lambda_j) \tag{B3}$$

The polynomials generated by this algorithm may be used to represent the latitude variations of the Fourier coefficients a_{mp} and b_{mp} (see main text):

$$a_{mp}(\lambda_j, \tau_l) = \sum_{n=1}^{N} \alpha_{mnp}(\tau_l)u_n(\lambda_j) \tag{B4}$$

$$b_{mp}(\lambda_j, \tau_l) = \sum_{n=1}^{N} \beta_{mnp}(\tau_l)u_n(\lambda_j) \tag{B5}$$

where

$$\beta_{mnp}(\tau_l) = \frac{1}{h_n^2}\sum_{j=1}^{J} a_{mp}(\lambda_j, \tau_l)u_n(\lambda_j) \tag{B6}$$

$$\beta_{mnp}(\tau_l) = \frac{1}{h_n^2}\sum_{j=1}^{J} b_{mp}(\lambda_j, \tau_l)u_n(\lambda_j) \tag{B7}$$

Appendix C. Auroral boundary determination

There are four auroral precipitation boundaries in each hemisphere: The equatorward and poleward electron boundaries and the equatorward and poleward ion boundaries. Since there are always two DMSP satellites in orbit, there are potentially four crossings of each boundary. The specification of a given boundary depends on the number of crossings detected in the data. The boundary detection is performed as follows.

1. If SSJ/4 data are available, then divide each orbit's worth of data into four segments, each segment extending from the most equatorward point to the most poleward point.
2. Each segment is searched from equator toward the pole until the electron energy flux exceeds 0.25 erg cm^{-2} s^{-1} (for the equatorward electron boundary) and the ion energy flux exceeds 0.1 erg cm^{-2} s^{-1} (for the equatorward ion boundary).
3. Search each segment from pole toward the equator until the same thresholds are exceeded to establish the poleward boundaries.

The boundaries are always assumed to be circular. The specification of each boundary circle (in terms of its center and radius) depends on the number of crossings detected.

1. If four crossings are found, there are four possible combinations of three points. Each of the four possible combinations defines a circle, which may be described by its center and radius. The center coordinates and radii of the four circles are averaged to determine the boundary used in PRISM.
5. If only three crossings are found, the boundary is uniquely defined by the circle passing through the three points.
6. If only two crossings are found, the boundary is taken to be the circle that passes through both points and has a radius equal to the mean of the colatitudes of the two points.

If only one crossing of a boundary is found, or if no crossings are found (or SSJ/4 data is missing), the boundaries are determined as follows. Equatorward boundaries are based on an analytic representation of the *Gussenhoven et al.* [1983] boundary. The boundary itself is a circle whose center is displaced from the magnetic pole. The radius (in degrees) of the circle is

$$\theta_1(P_1) = 20.9° + 1.7° P_1 \tag{C1}$$

where P_1 is a "precipitation index". The center of the circle is located at

$$\lambda_{c1}(P_1) = 87.3°–0.267° P_1 \tag{C2}$$

$$\varphi_{c1}(P_1) = 39.5°–1.25° P_1 + 0.076° P_1^2 \tag{C3}$$

where λ_{c1} is magnetic latitude and φ_{c1} is magnetic local time (in degrees).

Poleward boundaries have almost the same form, except that they are parameterized in terms of a separate "precipitation index" P_2.

$$\theta_2(P_2) = 13.4° + 1.7° P_2 \tag{C4}$$

$$\lambda_{c2}(P_2) = \begin{cases} 89.2° + 0.267° P_2, & P_2 < 3 \\ 90.8° - 0.267° P_2, & P_2 \geq 3 \end{cases} \tag{C5}$$

$$\varphi_{c2}(P_2) = \begin{cases} \varphi_{c1} + 180°, & P_2 < 3 \\ \varphi_{c1}, & P_2 \geq 3 \end{cases} \tag{C6}$$

If there is no data, or if no boundaries are detected in the data, then $P_1 = P_2 = K_p$. However, if a single crossing is detected, then the precipitation index is chosen so that the above boundary matches the crossing.

Appendix D. PRISM Input/Output File Specifications

PRISM 1.7e External Input/Output File Specifications

(for files created by or under the control of the User)

CONTENTS

Input Files

Output Files

PRISM 1.7e
9 January 2002

Input Stream Specification for PRISM 1.7e
9 January 2002

Record #	Element Name	Data Type	ASCII Format	Units	Description	Repetition Rate	Notes
1	INTER	Character	"Y" or "N"	N/A	"Y" indicates this is an interactive run; "N" indicates this is a batch run	1 per file	
2	YEAR	Integer	XXXX	years	4 digit year (e.g., 1989)	1 per file	
3	DAY	Integer	XXX	days	day of year (1 Jan = 001, etc.)	1 per file	
4	UT	Integer	XXXX	hours and minutes	Universal Time of observation in HHMM format	1 per file	
5	ST_OUT	Integer	X	N/A	Type of output for station sites: 0 = profile parameters (critical frequencies and layer heights) only 1 = electron density profiles only 2 = both profile parameters and electron density profiles 3 = no output at station sites	1 per file	
6	GR_OUT	Integer	X	N/A	Type of output for grid points: 0 = profile parameters only 1 = electron density profiles only 2 = both profile parameters and electron density profiles 3 = no gridded output	1 per file	
7	FNORM	Integer	X	N/A	Normalization for f_oF_2 : 0 = normalize to URSI-88 1 = no normalization	1 per file	

Continues on next page

Continued from previous page

Record #	Element Name	Data Type	ASCII Format	Units	Description	Repetition Rate	Notes
8	SSNSRC	Integer	X	N/A	Source indicator for SSN_{eff}: 0 = determine SSN_{eff} from DISS and IMS input, using input value as starting point 1 = use input value of SSN_{eff} (Record 26, SSNEFF)	1 per file	1
9	ST_DIF	Character	"Y" or "N"	N/A	"Y" if output stations are different than input stations.	1 per file	2
10	ST_FIL	Character	see note 3	N/A	name of file containing list of output stations.	1 per file	3
11	GR_FIL	Character	see note 5	N/A	output file name for gridded output, e.g., "TEST1.OUT"	1 per file	4,5
12	USRGRD	Character	"Y" or "N"	N/A	"Y" indicates that a user specified grid will be used; "N" indicates that the default grid will be used	1 per file	4
13	G_OR_M	Character	"G" or "M"	N/A	gridded output coordinate system: "G" = geographic (geocentric) "M" = corrected geomagnetic	1 per file	4
14	LATSW	Real	±XX.XX	degrees	latitude of southwest corner of user specified grid (positive north)	1 per record	6
	LONSW	Real	±XXX.XX	degrees	longitude of southwest corner of user grid (positive east)	1 per record	

Continues on next page

Continued from previous page

Record #	Element Name	Data Type	ASCII Format	Units	Description	Repetition Rate	Notes
15	LATNE	Real	±XX.XX	degrees	latitude of northeast corner of user specified grid (positive north)	1 per record	6
	LONNE	Real	±XXX.XX	degrees	longitude of northeast corner of user grid (positive east)	1 per record	
16	SPACNG	Character	"N" or "G"	N/A	"N" indicates user will specify number of grid points; "G" indicates user will specify size of grid intervals	1 per file	6
17	NUMLAT	Integer	XXX	N/A	number of latitude points in user specified grid	1 per record	7
	NUMLON	Integer	XXX	N/A	number of longitude points in user specified grid	1 per record	
18	DLAT	Real	±XX.XX	degrees	latitude spacing of user specified grid	1 per record	8
	DLON	Real	±XXX.XX	degrees	longitude spacing of user specified grid	1 per record	
19	USRALT	Character	"Y" or "N"	N/A	"Y" indicates that user will specify output altitude grid; "N" indicates that default altitude grid will be used	1 per file	9
20	ALTFIL	Character	see note 9	N/A	name of file containing user specified altitude grid	1 per file	10

Continues on next page

Continued from previous page							
Record #	Element Name	Data Type	ASCII Format	Units	Description	Repetition Rate	Notes
21	RKP	Real	X.X	N/A	K_p value for UT of run	1 per file	
22	BZ	Real	±XX.X	nT	z-component of Interplanetary Magnetic Field (IMF).	1 per record	11
	BY	Real	±XX.X	nT	y-component of IMF	1 per record	
23	F10P7A	Real	XXX.X	solar flux units	90 day mean $F_{10.7}$ value (as used by MSIS model)	1 per file	
24	F10SSN	Integer	X	N/A	specifies relationship between $F_{10.7}$ and effective SSN: 0 = SSN and $F_{10.7}$ are unrelated 1 = SSN is computed from $F_{10.7}$ 2 = $F_{10.7}$ is computed from SSN	1 per file	12
25	F10P7	Real	XXX.X	solar flux units	the daily $F_{10.7}$ value (most recent measurement)	1 per file	13
26	SSNEFF	Real	XXX.X	N/A	effective sunspot number	1 per file	14
27	GO	N/A	N/A	N/A	1 carriage return	1 per file	

General Notes:

The Data Element Names do not necessarily correspond to the FORTRAN variable names in the source code. This is because the FORTRAN names are not always descriptive of the actual contents of the data element (for historical reasons).

Shaded records indicate that the record's presence is contingent on the contents of one or more preceding records.

Because PRISM uses FORTRAN list directed input for all numeric input, the numeric format is flexible. The formats indicated in the table are suggested formats only. Plus (+) signs are always optional. The variables may be separated by (a) one or more spaces, (b) a comma (,), or (c) a comma and one or more spaces.

Numbered Notes:

1. This record is present only if FNORM (record 7) is 0.
2. This record is present only if ST_OUT (record 5) is 0, 1, or 2.

3. This record is present only if ST_DIF (record 9) is "Y". It should contain a valid file name of or more than 32 characters, and the file must be located in the directory specified in record 3 of the file PATH_NAME.TXT. (See *Data Control Input Specification for PRISM.*)
4. This record is present only if GR_OUT (record 6) is 0, 1, or 2.
5. If present, record 11 must contain a valid file name of no more than 32 characters. The file will be written to the default directory (the one containing PRISM.EXE).
6. This record is present only if USRGRD (record 12) is present and contains "Y".
7. This record is present only if SPACNG (record 16) is present and contains "N".
8. This record is present only if SPACNG (record 16) is present and contains "G".
9. This record is present only if one or both of ST_OUT (record 5) or GR_OUT (record 6) has the value 1 or 2.
10. This record is present only if USRALT (record 19) contains "Y". If present, it must contain a valid file name of no more than 32 characters, and the file must be located in the default directory.
11. nT = nanoTesla. PRISM uses only the sign of B_z and B_y to select coefficients corresponding to Heppner-Maynard convection patterns, so the units are not crucial, and even a crude estimate is useful.
12. F10SSN = 0 is strongly recommended.
13. This record is present only if F10SSN (record 24) is 0 or 1.
14. This record is present only if F10SSN (record 24) is 0 or 2.

38

Original Document:	2 September 1994	
Revision 1:	16 September 1994	(record 19 and note 9)
Revision 2:	3 November 1994	(record 15)
Revision 3:	28 June 1995	(records 25-29 and notes 13 and 14)

Data Control Input File Specification for PRISM 1.7e
9 January 2002

File Name: PATH_NAM.TXT

Record #	Element Name	Data Type	ASCII Format	Units	Description	Repetition Rate	Notes
1	DACCES	Integer	X	N/A	indicates how direct access files are opened. Should always be 2 for VAX VMS systems. See note 1.	1 per file	1
2	CGPATH	Character	see note 2	N/A	specifies the directory that contains the file that contains the coefficients for converting from geocentric to corrected geomagnetic coordinates.	1 per file	2,3
3	RTPATH	Character	see note 2	N/A	specifies the directory containing the real time data (DISS, TISS, SSIES, SSJ/4, etc.)	1 per file	2
4	USUPATH	Character	see note 2	N/A	specifies the directory containing the USU model coefficient databases.	1 per file	2
5	MFPATH	Character	see note 2	N/A	specifies the directory containing the midlatitude F layer coefficient databases	1 per file	2
6	LFPATH	Character	see note 2	N/A	specifies the directory containing the low latitude F layer coefficient databases	1 per file	2
7	LMEPATH	Character	see note 2	N/A	specifies the directory containing the low and midlatitude E layer coefficient databases	1 per file	2

Continues on next page

Continued from previous page							
Record #	Element Name	Data Type	ASCII Format	Units	Description	Repetition Rate	Notes
8	HLEPATH	Character	see note 2	N/A	specifies directory containing files needed by HLE (High Latitude E-layer model).	1 per file	2
9	URSIPATH	Character	see note 2	N/A	specifies directory containing the URSI-88 coefficients	1 per file	2
10	DISS	Character	see note 4	N/A	identifies file(s) containing DISS data.	5 per record	4
11	DMSP	Character	see note 4	N/A	identifies file(s) containing DMSP (SSIES & SSJ/4) data.	8 per record	4
12	TISS	Character	see note 4	N/A	identifies file(s) containing TISS data.	5 per record	4

40

General Notes:

The Data Element Names do not necessarily correspond to the FORTRAN variable names in the source code. This is because the FORTRAN names are not always descriptive of the actual contents of the data element (for historical reasons).

Numbered Notes:

1. VAX VMS FORTRAN opens direct access files with record lengths specified in longwords (4 byte words). DOS and UNIX FORTRAN usually open direct access files with record lengths specified in bytes. For the latter case, the value should be specified as 1.
2. Directory (or path) names must be valid directory names of no more than 80 characters in length.
3. The coefficient file is named CGLALO.DAT.
4. This record may contain up to five fields for DISS and TISS data and up to eight fields for DMSP data. Each field is exactly 11 characters in length. Each field may contain one file name, left justified, of no more than 10 characters. The 11th character is used for improved readability and is ignored by PRISM. The file names actually represent prefixes to the full file names of the form "xxxxxxxxxx.DAT".

The user is free to choose any unique character string (of 10 characters or less), but blank fields are ignored. (That is, PRISM does not attempt to open files named ".DAT".) If there is no data of this type, the record should be empty or blank.

Original Document:	2 September 1994	
Revision 1:	9 January 1995	(Note 4 clarified, Note 5 eliminated)
Revision 2:	28 June 1995	(Added "2" under Notes column for all path names except CGPATH)
Revision 3:	12 August 1995	(Amended Note 4 to give correct maximum allowed number of fields for DMSP data)

41

Ionosonde (DISS) Input Files for PRISM 1.7e
9 January 2002

File Name: As specified in the Data Control Input File ("PATH_NAM.TXT")

Record #	Element Name	Data Type	ASCII Format	Units	Description	Repetition Rate	Notes
1...N	YEAR	Integer	XXXX	years	4 digit year of observation	1 per record	1,2,3
	DAY	Integer	XXX	days	day of year of observation	1 per record	3
	UT	Integer	XXXX	hours and minutes	Universal Time of observation in HHMM format	1 per record	3
	GLAT	Real	±XX.XX	degrees	geographic latitude of ionosonde	1 per record	4
	GLON	Real	±XXX.XX	degrees	geographic longitude of ionosonde	1 per record	4
	FOF2	Real	XX.XX	MHz	observed critical frequency of the F_2 layer	1 per record	5,6
	HMF2	Real	XXX.X	km	observed height of the F_2 layer	1 per record	5,7
	FOF1	Real	XX.XX	MHz	observed critical frequency of the F_1 layer	1 per record	8
	HMF1	Real	XXX.X	km	observed height of the F_1 layer	1 per record	8
	FOE	Real	XX.XX	MHz	observed critical frequency of the E layer	1 per record	5,9
	HME	Real	XXX.X	km	observed height of the E layer	1 per record	5,10
	OPTIONAL	Character	N/A	N/A	Optional information (e.g., WMO number): ignored by PRISM, may be left blank	1 per record	

General Notes:

The Data Element Names do not necessarily correspond to the FORTRAN variable names in the source code. This is because the FORTRAN names are not always descriptive of the actual contents of the data element (for historical reasons).

Because PRISM uses FORTRAN list directed input for all numeric input, the numeric format is flexible. The formats indicated in the table are suggested formats only. Plus (+) signs are always optional. The variables may be separated by (1) one or more spaces, (2) a comma (,), or (3) a comma and one or more spaces.

Numbered Notes:

1. All records have the same format. PRISM recognizes the end-of-file (eof) mark as an "end-of-data" indicator. Thus the number of records, N, does not have to be specified.
2. PRISM can accept a maximum of 850 records from all DISS input files combined, not including those records ignored (see Notes 3-10). PRISM ignores any remaining records and DISS input files if it reaches its limit of 850 accepted records. The limit of 850 accepted records is based on 50 DISS stations and a time resolution of 15 minutes in a +/- 2 hour time window centered on the date and UT of the run (see Records 2-4 in the *PRISM Input Stream Specification*).
3. The record is ignored if the date and UT in the record is outside a +/- 2 hour time window centered on the date and UT of the run (see Records 2-4 in the *PRISM Input Stream Specification*).
4. If the run is producing gridded output (see Record 6 in the *PRISM Input Stream Specification*), then the record is ignored if the geographic location in the record is outside the bounds of the output grid (see records 12-15 in the *PRISM Input Stream Specification*). If the run is not producing gridded output, then all records are accepted based on geographic location.
5. The record is ignored if none of the E and F_2 layer parameters in the record are accepted (see Notes 6, 7, 9, and 10).
6. The accepted range of the observed critical frequency of the F_2 layer (f_oF_2) in the record is $0 < f_oF_2 \leq 28.4$ MHz. The range maximum corresponds to a peak F_2 layer density of 10^7 cm^{-3} using the approximation $n_mF_2(\text{cm}^{-3})=1.24\times10^4 \cdot f_oF_2(\text{MHz})^2$, where n_mF_2 is the peak F_2 layer density. If the f_oF_2 parameter in the record is outside this range, then the f_oF_2 parameter in the record is ignored.
7. The accepted range of the observed height of the F_2 layer (h_mF_2) in the record is $200 \leq h_mF_2 \leq 1000$ km. If the h_mF_2 parameter in the record is outside this range, then the h_mF_2 parameter in the record is ignored.
8. PRISM versions through the above ignore F_1 layer parameters. However, future versions *may* make use of these parameters so space is reserved in the input file for them.
9. The accepted range of the observed critical frequency of the E layer (f_oE) in the record is $0 < f_oE \leq 28.4$ MHz. The range maximum corresponds to a peak E layer density of 10^7 cm^{-3} using the approximation $n_mE(\text{cm}^{-3})=1.24\times10^4 \cdot f_oE(\text{MHz})^2$, where n_mE is the peak E layer density. If the f_oE parameter in the record is outside this range, then the f_oE parameter in the record is ignored.
10. The accepted range of the observed height of the E layer (h_mE) in the record is $90 \leq h_mE \leq 150$ km. If the h_mE parameter in the record is outside this range, then the h_mE parameter in the record is ignored.

Original Document: 2 September 1994
Revision 1: 28 June 1995
Revision 2: 12 August 1995 (Changed Note 2 to remove the PRISM version number)

Revision 3:	29 September 1995	(Changed Note 2 to Note 8; Added Notes 2-7, 9, and 10)
Revision 4:	7 November 1996	(Changed maximum allowed number of accepted records in Note 2; added explanation for that number to Note 2)

TEC (IMS) Input Files for PRISM 1.7e
9 January 2002

File Name: As specified in the Data Control Input File ("PATH_NAM.TXT")

Record #	Element Name	Data Type	ASCII Format	Units	Description	Repetition Rate	Notes
1...N	YEAR	Integer	XXXX	years	4 digit year of observation	1 per record	1,2,3
	DAY	Integer	XXX	days	day of year of observation	1 per record	3
	UT	Integer	XXXX	hours and minutes	Universal Time of observation in HHMM format	1 per record	3
	GLAT	Real	±XX.XX	degrees	geographic latitude of ionospheric penetration point (IPP)	1 per record	4
	GLON	Real	±XXX.XX	degrees	geographic longitude of ionospheric penetration point (IPP)	1 per record	4
	TEC	Real	XXX.X	TEC Units	vertical equivalent TEC obtained from slant TEC and assigned to IIP	1 per record	5,6,7
	OPTIONAL	Character	N/A	N/A	Option descriptive information (e.g., TISS site ID). Ignored by PRISM, may be left blank	1 per record	

45

General Notes:

The Data Element Names do not necessarily correspond to the FORTRAN variable names in the source code. This is because the FORTRAN names are not always descriptive of the actual contents of the data element (for historical reasons).

Because PRISM uses FORTRAN list directed input for all numeric input, the numeric format is flexible. The formats indicated in the table are suggested formats only. Plus (+) signs are always optional. The variables may be separated by (1) one or more spaces, (2) a comma (,), or (3) a comma and one or more spaces.

Numbered Notes:

1. All records have the same format. PRISM recognizes the end-of-file (eof) mark as an "end-of-data" indicator.

2. PRISM can accept a maximum of 40800 records from all IMS input files combined, not including those records ignored (see Notes 3-5). PRISM ignores any remaining records and IMS input files if it reaches its limit of 40800 accepted records. The limit of 40800 accepted records is based on 200 IMS stations reporting 12 simultaneous measurements and a time resolution of 15 minutes in a +/- 2 hour time window centered on the date and UT of the run (see Records 2-4 in the *PRISM Input Stream Specification*).
3. The record is ignored if the date and UT in the record is outside a +/- 2 hour time window centered on the date and UT of the run (see Records 2-4 in the *PRISM Input Stream Specification*).
4. If the run is producing gridded output (see Record 6 in the *PRISM Input Stream Specification*), then the record is ignored if the geographic location in the record is outside the bounds of the output grid (see records 12-15 in the *PRISM Input Stream Specification*). If the run is not producing gridded output, then all records are accepted based on geographic location.
5. The accepted range of the vertical equivalent TEC in the record is $0 < \text{TEC} \leq 250$ TEC Units. If the vertical equivalent TEC in the record is outside this range, then the record is ignored.
6. The precise definition of the IIP used to calculate the vertical equivalent TEC is not critical as long as it is used consistently.
7. 1 TEC Unit = 10^{12} cm^{-2} = 10^{16} m^{-2}.

Original Document:	2 September 1994	
Revision 1:	28 June 1995	
Revision 2:	29 September 1995	(Changed Note 2 to Note 6; Added Notes 2-5 and 7)
Revision 3:	7 November 1996	(Changed maximum allowed number of accepted records in Note 2; added explanation for that number to Note 2)
Revision 4:	14 February 1997	(Corrected maximum allowed number of accepted records in Note 2)

DMSP Input Files for PRISM 1.7e
9 January 2002

File Name: As specified in the Data Control Input File ("PATH_NAM.TXT")

Record #	Element Name	Data Type	ASCII Format	Units	Description	Repetition Rate	Notes
1	HEADER	Character	50 character string	N/A	data identification header: one of 1. "SSIES ION DRIFT" 2. "SSIES IN SITU PLASMA" 3. "SSJ/4 DATA"	0-24 per data type	1
2 ("SSIES ION DRIFT")	YEAR	Integer	XXXX	years	4 digit year of observation	1 per record	2,3,4, 5
	DAY	Integer	XXX	days	day of year of observation	1 per record	5
	UT	Integer	XXXXX	seconds	Universal Time of observation	1 per record	5
	GLAT	Real	±XX.XX	degrees	geographic latitude of observation	1 per record	
	GLON	Real	±XXX.XX	degrees	geographic longitude of observation	1 per record	
	VV	Real	±X.XXE±XX	$m\ s^{-1}$	vertical ion drift velocity in instrument coordinates	1 per record	
	VH	Real	±X.XXE±XX	$m\ s^{-1}$	horizontal ion drift velocity in instrument coordinates	1 per record	
	EDEN	Real	±X.XXE±XX	cm^{-3}	in situ electron density	1 per record	

Continues on next page

Continued from previous page							
Record #	Element Name	Data Type	ASCII Format	Units	Description	Repetition Rate	Notes
2 ("SSIES IN SITU PLASMA")	YEAR	Integer	XXXX	years	4 digit year of observation	1 per record	2,3,6, 7
	DAY	Integer	XXX	days	day of year of observation	1 per record	7
	UT	Integer	XXXXX	seconds	Universal Time of observation	1 per record	7
	GLAT	Real	±XX.XX	degrees	geographic latitude of observation	1 per record	
	GLON	Real	±XXX.XX	degrees	geographic longitude of observation	1 per record	
	ALTN	Real	XXXXX.X	km	altitude of spacecraft	1 per record	
	NE	Real	±X.XXE±XX	cm^{-3}	in situ electron density	1 per record	8
	TE	Real	±X.XXE±XX	°K	in situ electron temperature	1 per record	9
	FOP	Real	±X.XXE±XX	N/A	fraction of ions that are O^+	1 per record	
	FHEP	Real	±X.XXE±XX	N/A	fraction of ions that are He^+	1 per record	
	FHP	Real	±X.XXE±XX	N/A	fraction of ions that are H^+	1 per record	
	TI	Real	±X.XXE±XX	°K	in situ ion temperature	1 per record	9
2 ("SSJ/4 DATA")	YEAR	Integer	XXXX	years	4 digit year of observation	1 per record	2,3, 10,11
	DAY	Integer	XXX	days	day of year of observation	1 per record	11
	UT	Integer	XXXXX	seconds	Universal Time of observation	1 per record	11
	GLAT	Real	±XX.XX	degrees	geographic latitude of spacecraft field line at 110 km	1 per record	12
	GLON	Real	±XXX.XX	degrees	geographic longitude of spacecraft filed line at 110 km	1 per record	12
	EBARE	Real	XXXX.XXX	keV	mean electron energy	1 per record	
	EFLUXE	Real	XXXX.XXX	erg cm^{-2} s^{-1}	energy flux of electrons	1 per record	
	EBARI	Real	XXXX.XXX	keV	mean ion energy	1 per record	
	EFLUXI	Real	XXXX.XXX	erg cm^{-2} s^{-1}	energy flux of protons	1 per record	
	SIGE	Real	XXXX.XXX	erg cm^{-2} s^{-1}	1 sigma uncertainty in EFLUXE	1 per record	
	SIGI	Real	XXXX.XXX	erg cm^{-2} s^{-1}	1 sigma uncertainty in EFLUXI	1 per record	

General Notes:

The Data Element Names do not necessarily correspond to the FORTRAN variable names in the source code. This is because the FORTRAN names are not always descriptive of the actual contents of the data element (for historical reasons).

Because PRISM uses FORTRAN list directed input for all numeric input, the numeric format is flexible. The formats indicated in the table are suggested formats only. Plus (+) signs are always optional. The variables may be separated by (1) one or more spaces, (2) a comma (,), or (3) a comma and one or more spaces.

Numbered Notes:

1. A DMSP input file for PRISM may contain three kinds of data, each identified by a unique header string:
   "SSIES ION DRIFT" identifies Drift Meter (DM) data
   "SSIES IN SITU PLASMA" identifies data from the Scintillation Meter (SM), Langmuir Probe (EP), and Retarding Potential Analyzer (RPA)
   "SSJ/4 DATA" identifies electron and ion precipitation data
   PRISM can accept a maximum of 24 orbits, or sets, of each kind of DMSP data from all DMSP input files combined. PRISM ignores any remaining sets in the DMSP input files if it reaches its limit of 24 sets. The limit of 24 sets of each kind of DMSP data is based on 8 satellites, an orbital period of 6060 seconds, and a +/- 2 hour time window centered on the date and UT of the run (see Records 2-4 in the *PRISM Input Stream Specification*); the number of orbits per satellite in the +/- 2 hour time window has been rounded up to 3.
2. The contents of Record 2 depend on the contents of Record 1.
3. This record is repeated until the data of this kind is exhausted. PRISM detects the end of the data by recognizing (1) the EOF mark, or (2) encountering a new header string.
4. PRISM can accept a maximum of 1451 records per set for SSIES ION DRIFT data, not including those records ignored (see Note 5). PRISM ignores any remaining records in the set if it reaches its limit of 1451 accepted records. The limit of 1451 accepted records is based on a 5 second time resolution in a -2 to 0 hour time window relative to the date and UT of the run (see Records 2-4 in the *PRISM Input Stream Specification*), with 10 extra records allowed for orbital overlap.
5. The record is ignored if the date and UT in the record is outside a -2 to 0 hour time window relative to the date and UT of the run (see Records 2-4 in the *PRISM Input Stream Specification*).
6. PRISM can accept a maximum of 3848 records of SSIES IN SITU PLASMA data from all sets combined, not including those records ignored (see Notes 7-9). PRISM ignores any remaining records and SSIES IN SITU PLASMA sets if it reaches its limit of 3848 accepted

records. The limit of 3848 accepted records is based on 8 satellites and a time resolution of 30 seconds in a +/- 2 hour time window centered on the date and UT of the run (see Records 2-4 in the *PRISM Input Stream Specification*).

7. The record is ignored if the date and UT in the record is outside a +/- 2 hour time window centered on the date and UT of the run (see Records 2-4 in the *PRISM Input Stream Specification*).
8. The accepted range of the in situ electron density (n_e) in the record is $10^3 \leq n_e \leq 10^7$ cm^{-3}. If the n_e parameter in the record is outside this range, then the record is ignored.
9. The accepted range of the in situ electron temperature (T_e) in the record is $0 < T_e \leq 6000$ °K. The accepted range of the in situ ion temperature (T_i) in the record is $0 < T_i \leq 6000$ °K. If either of the in situ temperatures is outside its range, then both in situ temperatures are ignored.
10. PRISM can accept a maximum of 7211 records per set for SSJ/4 data, not including those records ignored (see Note 11). PRISM ignores any remaining records in the set if it reaches its limit of 7211 accepted records. The limit of 7211 accepted records is based on a time resolution of 1 second in a -2 to 0 hour time window relative to the date and UT of the run (see Records 2-4 in the *PRISM Input Stream Specification*), with 10 extra records allowed for orbital overlap.
11. The record is ignored if the date and UT in the record is outside a -2 to 0 hour time window relative to the date and UT of the run (see Records 2-4 in the *PRISM Input Stream Specification*).
12. Because precipitating electrons and ions are constrained to move along magnetic field lines, and because PRISM is trying to determine the effects in the auroral E-layer near 110 km altitude, the desired coordinates are the geographic location of the geomagnetic field line that passes through the spacecraft at 110 km instead of the actual location of the spacecraft.

50

Original Document:	27 September 1994	
Revision 1:	5 October 1994	(record 1; record 2, "SSJ/4 DATA"; and note 4)
Revision 2:	28 June 1995	
Revision 3:	12 August 1995	(Changed Record 1 for new data set limit; Changed Note 1 to remove the PRISM version number and to correct description of data set limit)
Revision 4:	29 September 1995	(Changed "in situ ion density" to "in situ ion temperature" in Record 2 of SSIES IN SITU PLASMA data type; Changed Note 4 to Note 12; Added Notes 4-11)
Revision 5:	7 November 1996	(Added explanation of maximum allowed number of sets to Note 1; Added explanation of maximum allowed number of accepted SSIES ION DRIFT records to Note 4; Changed maximum allowed number of accepted SSIES IN SITU PLASMA records in Note 6; added explanation for that number to Note 6; Added explanation of maximum allowed number of accepted SSJ/4 records to Note 10)

Output Station List Input File for PRISM 1.7e
9 January 2002

File Name: As specified in the PRISM Input Stream

Record #	Element Name	Data Type	ASCII Format	Units	Description	Repetition Rate	Notes
1...N	GLAT	Real	±XX.XX	degrees	geographic latitude of ionosonde	1 per record	1
	GLON	Real	±XXX.XX	degrees	geographic longitude of ionosonde	1 per record	
	OPTIONAL	Character	N/A	N/A	Optional information (e.g., WMO number): ignored by PRISM, may be left blank	1 per record	

General Notes:

The Data Element Names do not necessarily correspond to the FORTRAN variable names in the source code. This is because the FORTRAN names are not always descriptive of the actual contents of the data element (for historical reasons).

Because PRISM uses FORTRAN list directed input for all numeric input, the numeric format is flexible. The formats indicated in the table are suggested formats only. Plus (+) signs are always optional. The variables may be separated by (1) one or more spaces, (2) a comma (,), or (3) a comma and one or more spaces.

Numbered Notes:

1. All records have the same format. PRISM recognizes the end-of-file (eof) mark as an "end-of-data" indicator. Thus the number of records, N, does not have to be specified.

Original Document: 2 September 1994
Revision 1: 28 June 1995

Altitude Grid Input File for PRISM 1.7e
9 January 2002

File Name: As specified in the PRISM Input Stream

Record #	Element Name	Data Type	ASCII Format	Units	Description	Repetition Rate	Notes
1...N	ALT	Real	XXXX.XX	km	Altitude	1 per record	1

General Notes:

The Data Element Names do not necessarily correspond to the FORTRAN variable names in the source code. This is because the FORTRAN names are not always descriptive of the actual contents of the data element (for historical reasons).

Because PRISM uses FORTRAN list directed input for all numeric input, the numeric format is flexible. The formats indicated in the table are suggested formats only. Plus (+) signs are always optional. The variables may be separated by (1) one or more spaces, (2) a comma (,), or (3) a comma and one or more spaces.

Numbered Notes:

1. All records have the same format. PRISM recognizes the end-of-file (eof) mark as an "end-of-data" indicator. Thus the number of records, N, does not have to be specified.

Original Document: 28 June 1995

Station Output File Specification for PRISM 1.7e
9 January 2002

File Name: TMPA.DAT

Record #	Element Name	Data Type	ASCII Format	Units	Description	Repetition Rate	Notes
1	Header	Character	" YEAR DAY ..."	N/A	column labels for numeric data in record 2	1 per file	
2	Separator	Character	"-------..."	N/A	separator (row of hyphens)	1 per file	
3	YEAR	Integer	XXXX	N/A	4 digit year (e.g., 1989)	1 per file	
	DAY	Integer	XXX	N/A	day of year (1 Jan = 001, etc.)	1 per file	
	UT	Real	XXXXX.X	seconds	Universal Time	1 per file	
	F10P7	Real	XXX.X	solar flux units	Solar radio flux at 10.7 cm (2800 MHz) (daily value)	1 per file	
	RKP	Real	XX.X	N/A	K_p geomagnetic activity index	1 per file	
	SSN	Real	XXXX.X	N/A	Solar Sunspot Number	1 per file	
4	DTYPE	Character	" IONOSONDE "	N/A	identifies data type	1 per record	
	text	Character	" data "	N/A		1 per record	
	NRECL	Integer	XXX	N/A	number of output station sites	1 per record	
	text	Character	" records"	N/A		1 per record	
5	IOUTS	Integer	X	N/A	indicator for type of output at each station: 0 = profile parameters only 1 = electron density profiles only 2 = both profile parameters and electron density profiles 3 = no output at station sites	1 per file	1

Continues on next page

Continued from previous page

Record #	Element Name	Data Type	ASCII Format	Units	Description	Repetition Rate	Notes
6 (IOUTS=0)	Header	Character	" NUM UT..."	N/A	column labels	1 per record	2
7 (IOUTS=0)	NUM	Integer	XXX	N/A	site number	1 per record	2
	UT	Real	XX.XX	hours	UT (decimal hours)	1 per record	
	LAT	Real	±XX.XX	degrees	geographic latitude	1 per record	
	LON	Real	±XXX.XX	degrees	geographic longitude	1 per record	
	MLAT	Real	±XX.XX	degrees	geomagnetic latitude	1 per record	
	MLON	Real	±XXX.X	degrees	geomagnetic longitude	1 per record	
	MLT	Real	XX.XX	hours	geomagnetic local time	1 per record	
	FOF2	Real	XX.XX	MHz	critical frequency of F_2 layer	1 per record	
	HMF2	Real	XXX.XX	km	height of F_2 layer	1 per record	
	FOF1	Real	XX.XX	MHz	critical frequency of F_1 layer	1 per record	3
	HMF1	Real	XXX.XX	km	height of F_1 layer	1 per record	3
	FOE	Real	XX.XX	MHz	critical frequency of E layer	1 per record	
	HME	Real	XXX.XX	km	height of E layer	1 per record	
	TEC	Real	XXX.X	TEC Units	vertical TEC	1 per record	7

Continues on next page

Continued from previous page

Record #	Element Name	Data Type	ASCII Format	Units	Description	Repetition Rate	Notes
6 (IOUTS=1)	label	Character	"Number of altitude points = "	N/A	label for numeric element NALT	1 per file	
	NALT	Integer	XXXXXX	N/A	number of altitudes on altitude grid	1 per file	
7 (IOUTS=1)	Header	Character	"Altitudes"	N/A	header for list of altitude grid	1 per file	
8 (IOUTS=1)	ALT	Real	XXXX.XX	km	altitude of a point on the altitude grid	5 per record	4
9 (IOUTS=1)	blank line	N/A	N/A	N/A	blank line	1 per record	5
10 (IOUTS=1)	NUM	Real	XXX	N/A	site number		5
	UT	Real	XX.XX	hours	Universal Time (decimal hours)		
	LAT	Real	±XXX.XX	degrees	geographic latitude		
	LON	Real	±XXX.XX	degrees	geographic longitude		
	MLAT	Real	±XXX.XX	degrees	geomagnetic latitude		
	MLON	Real	±XXX.XX	degrees	geomagnetic longitude		
	MLT	Real	XXXX.XX	decimal hours	geomagnetic local time		
11 (IOUTS=1)	Header	Character	" Densities"	N/A	header for electron densities	1 per record	5
12 (IOUTS=1)	EDEN	Real	±X.XXE±XX	cm^{-3}	electron density corresponding to altitude grid in record 8	5 per record	4,5

Continues on next page

Continued from previous page							
Record #	Element Name	Data Type	ASCII Format	Units	Description	Repetition Rate	Notes
6 (IOUTS=2)	Label	Character	"Number of altitude points = '	N/A	label for numeric element NALT	1 per file	
	NALT	Integer	XXXXXX	N/A	number of altitudes on grid	1 per file	
7 (IOUTS=2)	Header	Character	"Altitudes"	N/A	header for list of altitude grid	1 per file	
8 (IOUTS=2)	ALT	Real	XXXX.XX	km	altitude of a point on the altitude grid	5 per record	4
9 (IOUTS=2)	blank line	N/A	N/A	N/A	blank line	1 per record	6
10 (IOUTS=2)	NUM	Integer	XXX	N/A	site number	1 per record	6
	UT	Real	XX.XX	hours	UT (decimal hours)	1 per record	
	LAT	Real	±XX.XX	degrees	geographic latitude	1 per record	
	LON	Real	±XXX.XX	degrees	geographic longitude	1 per record	
	MLAT	Real	±XX.XX	degrees	geomagnetic latitude	1 per record	
	MLON	Real	±XXX.X	degrees	geomagnetic longitude	1 per record	
	MLT	Real	XX.XX	hours	geomagnetic local time	1 per record	
	FOF2	Real	XX.XX	MHz	critical frequency of F_2 layer	1 per record	
	HMF2	Real	XXX.XX	km	height of F_2 layer	1 per record	
	FOF1	Real	XX.XX	MHz	critical frequency of F_1 layer	1 per record	3
	HMF1	Real	XXX.XX	km	height of F_1 layer	1 per record	3
	FOE	Real	XX.XX	MHz	critical frequency of E layer	1 per record	
	HME	Real	XXX.XX	km	height of E layer	1 per record	
	TEC	Real	XXX.X	TEC Units	vertical TEC	1 per record	6,7
11 (IOUTS=2)	Header	Character	" Densities"	N/A	header for electron densities	1 per record	
12 (IOUTS=2)	EDEN	Real	±X.XXE±XX	cm^{-3}	electron density corresponding to altitude in record 8	5 per record	4,6

General Notes:

The Data Element Names do not necessarily correspond to the FORTRAN variable names in the source code. This is because the FORTRAN names are not always descriptive of the actual contents of the data element (for historical reasons).

Numbered Notes:

1. The structure of the PRISM station output file after Record 5 depends on the content of Record 5.
2. For IOUTS=0, Records 6 and 7 are repeated NRECL times.
3. PRISM versions through the above do not actually compute F_1 layer parameters, but future versions may do so.
4. This record is repeated until the contents of the data element have been exhausted.
5. For IOUTS=1, Records 9-12 are repeated NRECL times.
6. For IOUTS=2, Records 9-12 are repeated NRECL times.
7. 1 TEC Unit = 10^{12} cm^{-2} = 10^{16} m^{-2}.

Original Document:	2 September 1994	
Revision 1:	26 September 1994	(records 2, and 3-11; notes 4-7)
Revision 2:	3 November	(File Name, on first page)
Revision 3:	28 June 1995	(Addition of header records 1-3)
Revision 4:	12 August 1995	(Put "2" in Notes column of Record 6 (IOUTS=0); Changed Note 2 to include Record 6; Changed Note 3 to remove the PRISM version number)
Revision 5:	29 September 1995	(Added *General Notes* section)

Gridded Output File Specification for PRISM 1.7e
9 January 2002

File Name: As specified in the PRISM Input Stream

Record #	Element Name	Data Type	ASCII Format	Units	Description	Repetition Rate	Notes
1	Header	Character	" YEAR DAY ..."	N/A	column labels for numeric data in record 2	1 per file	
2	Separator	Character	"--------..."	N/A	separator (row of hyphens)	1 per file	
3	YEAR	Integer	XXXX	N/A	4 digit year (e.g., 1989)	1 per file	
	DAY	Integer	XXX	N/A	day of year (1 Jan = 001, etc.)	1 per file	
	UT	Real	XXXXX.X	seconds	Universal Time	1 per file	
	F10P7	Real	XXX.X	solar flux units	Solar radio flux at 10.7 cm (2800 MHz) (daily value)	1 per file	
	RKP	Real	XX.X	N/A	K_p geomagnetic activity index	1 per file	
	SSN	Real	XXXX.X	N/A	Solar Sunspot Number	1 per file	
4	blank line	N/A	N/A	N/A	blank line	1 per file	
5	blank line	N/A	N/A	N/A	blank line	1 per file	
6	IGM	Integer	X	N/A	flag indicating coordinate system: 0 = geographic, 1 = geomagnetic	1 per file	
7	Header	Character	" Latitude Longitude ..."	N/A	header for grid information	1 per file	
8	Header	Character	" Starting Ending ..."	N/A	subheader for grid information	1 per file	

Continues on next page

Continued from previous page

Record #	Element Name	Data Type	ASCII Format	Units	Description	Repetition Rate	Notes
9	LAT0	Real	XXXX.XX	degrees	starting latitude of grid (southwest corner)	1 per file	
	LATF	Real	XXXX.XX	degrees	ending latitude of grid (northeast corner)	1 per file	
	LON0	Real	XXXX.XX	degrees	starting longitude of grid (southwest corner)	1 per file	
	LONF	Real	XXXX.XX	degrees	ending longitude of grid (northeast corner)	1 per file	
	NUMLAT	Integer	XXXXXX	N/A	number of latitude points in grid	1 per file	
	NUMLON	Integer	XXXXXX	N/A	number of longitude points in grid	1 per file	
	DLAT	Real	XXXX.XX	degrees	latitude spacing	1 per file	
	DLON	Real	XXXX.XX	degrees	longitude spacing	1 per file	
10	IOUT	Integer	XX	N/A	indicator for type of output at each grid point: 0 = profile parameters (critical frequencies and heights) only 1 = electron density profiles only 2 = both electron density profiles and profile parameters	1 per file	1

Continues on next page

Continued from previous page

Record #	Element Name	Data Type	ASCII Format	Units	Description	Repetition Rate	Notes
11 (IOUT=0)	blank line	N/A	N/A	N/A	blank line	1 per record	2
12 (IOUT=0)	GGLAT	Real	XXXX.XX	degrees	geographic latitude of grid point	1 per record	2
	GGLON	Real	XXXX.XX	degrees	geographic longitude of grid point	1 per record	
	MLAT	Real	XXXX.XX	degrees	geomagnetic latitude of grid point	1 per record	
	MLON	Real	XXXX.XX	degrees	geomagnetic longitude of grid point	1 per record	
	MLT	Real	XX.XX	hours	geomagnetic local time	1 per record	
13 (IOUT=0)	Header	Character	" foF2 hmF2 ..."	N/A	header for profile parameters	1 per record	2
14 (IOUT=0)	FOF2	Real	XXXX.XX	MHz	critical frequency of F_2 layer	1 per record	2
	HMF2	Real	XXXX.XX	km	height of F_2 layer	1 per record	
	FOF1	Real	XXXX.XX	MHz	critical frequency of F_1 layer	1 per record	8
	HMF1	Real	XXXX.XX	km	height of F_1 layer	1 per record	8
	FOE	Real	XXXX.XX	MHz	critical frequency of E layer	1 per record	
	HME	Real	XXXX.XX	km	height of E layer	1 per record	
	TEC	Real	XXX.X	TEC Units	Total Electron Content	1 per record	7

Continues on next page

Continued from previous page

Record #	Element Name	Data Type	ASCII Format	Units	Description	Repetition Rate	Notes
11 (IOUT=1)	label	Character	"Number of altitude points = '	N/A	label for numeric element NALT	1 per file	3
	NALT	Integer	XXXXXX	N/A	number of altitudes on grid	1 per file	
12 (IOUT=1)	Header	Character	"Altitudes"	N/A	header for list of altitude grid	1 per file	3
13 (IOUT=1)	ALT	Real	XXXX.XX	km	altitude of a point on the altitude grid	5 per record	4
14 (IOUT=1)	blank line	N/A	N/A	N/A	blank line	1 per record	5
15 (IOUT=1)	GGLAT	Real	XXXX.XX	degrees	geographic latitude of grid point	1 per record	5
	GGLON	Real	XXXX.XX	degrees	geographic longitude of grid point	1 per record	
	MLAT	Real	XXXX.XX	degrees	geomagnetic latitude of grid point	1 per record	
	MLON	Real	XXXX.XX	degrees	geomagnetic longitude of grid point	1 per record	
	MLT	Real	XX.XX	hours	geomagnetic local time	1 per record	
16 (IOUT=1)	Header	Character	" Densities"	N/A	header for electron densities	1 per record	5
17 (IOUT=1)	EDEN	Real	±X.XXE±XX	cm^{-3}	electron density corresponding to altitude in record 13	5 per record	4,5

Continues on next page

Continued from previous page							
Record #	Element Name	Data Type	ASCII Format	Units	Description	Repetition Rate	Notes
11 (IOUT=2)	Label	Character	"Number of altitude points = '	N/A	label for numeric element NALT	1 per file	3
	NALT	Integer	XXXXXX	N/A	number of altitudes on grid	1 per file	3
12 (IOUT=2)	Header	Character	"Altitudes"	N/A	header for list of altitude grid	1 per file	3
13 (IOUT=2)	ALT	Real	XXXX.XX	km	altitude of a point on the altitude grid	5 per record	4
14 (IOUT=2)	blank line	N/A	N/A	N/A	blank line	1 per record	6
15 (IOUT=2)	GGLAT	Real	XXXX.XX	degrees	geographic latitude of grid point	1 per record	6
	GGLON	Real	XXXX.XX	degrees	geographic longitude of grid point	1 per record	
	MLAT	Real	XXXX.XX	degrees	geomagnetic latitude of grid point	1 per record	
	MLON	Real	XXXX.XX	degrees	geomagnetic longitude of grid point	1 per record	
	MLT	Real	XX.XX	hours	geomagnetic local time	1 per record	
16 (IOUT=2)	Header	Character	" Densities"	N/A	header for electron densities	1 per record	6
17 (IOUT=2)	EDEN	Real	±X.XXE±XX	cm^{-3}	electron density corresponding to altitude in record 13	5 per record	4,6
18 (IOUT=2)	Header	Character	" foF2 hmF2 ..."	N/A	header for profile parameters	1 per record	6
19 (IOUT=2)	FOF2	Real	XXXX.XX	MHz	critical frequency of F_2 layer	1 per record	6
	HMF2	Real	XXXX.XX	km	height of F_2 layer	1 per record	
	FOF1	Real	XXXX.XX	MHz	critical frequency of F_1 layer	1 per record	8
	HMF1	Real	XXXX.XX	km	height of F_1 layer	1 per record	8
	FOE	Real	XXXX.XX	MHz	critical frequency of E layer	1 per record	
	HME	Real	XXXX.XX	km	height of E layer	1 per record	
	TEC	Real	XXX.X	TEC Units	Total Electron Content	1 per record	7

General Notes:

The Data Element Names do not necessarily correspond to the FORTRAN variable names in the source code. This is because the FORTRAN names are not always descriptive of the actual contents of the data element (for historical reasons).

Numbered Notes:

1. The structure of the PRISM gridded output file after Record 10 depends on the content of Record 10.
2. For IOUT=0, Records 11-14 are repeated until the data for every grid point has been written.
3. For IOUT=1 or 2, Records 11 and 12 are written only once.
4. This Record is repeated until the contents of the Data Element have been exhausted.
5. For IOUT=1, Records 14-17 are repeated until the data for every grid point has been written.
6. For IOUT=2, Records 14-19 are repeated until the data for every grid point has been written.
7. 1 TEC Unit = 10^{12} cm^{-2} = 10^{16} m^{-2}.
8. PRISM versions through the above do not calculate F_1 layer parameters, but future versions may do so.

63

Original Document:	2 September 1994	
Revision 1:	6 September 1994	(record 13, IOUT=0; record 19, IOUT=2)
Revision 2:	26 September 1994	(record 13, IOUT=0; record 13, IOUT=1 & 2; record 19, IOUT=2; Notes 6 & 8)
Revision 3:	10 November 1994	(record 12, IOUT=0, record 15, IOUT=1 & 2)
Revision 4:	28 June 1995	(insertion of record 13, IOUT=0;record 17,IOUT=1 & 2;Note 2)
Revision 5:	12 August 1995	(Changed Note 8 to remove the PRISM version number)
Revision 6:	29 September 1995	(Added *General Notes* section)
Revision 7:	12 February 1996	(Corrected definition of IGM in record 6)

Appendix F. Changes Memos for Versions 1.6 through 1.7e

The following memoranda provide detailed descriptions of the changes made to each version of PRISM to produce the next version.

M·E·M·O·R·A·N·D·U·M

DATE: *12-August-1995*

TO: *Rob Daniell*

FROM: *Lincoln Brown*

RE: *Changes to PRISM 1.5 for PRISM 1.5a*

The changes to PRISM 1.5 for PRISM 1.5a focus on a change to the Station Output File Specification requested by Hughes STX, the correction of reported problems regarding ingestion and use of DMSP and TISS data, and miscellaneous bug fixes. The changes are summarized as follows:

I. The third header line at the beginning of the station output file has been removed and a header line added above each critical parameters data record for station output type IOUTS=0. This was requested by Hughes STX and requires a change to the Station Output File Specification.

II. The ingestion of DMSP data has been corrected and strengthened based on problems reported by Hughes STX. PRISM can now handle up to 24 sets of each kind of DMSP data in a DMSP data file, and it can handle up to 8 DMSP data files.

III. The ingestion of TEC data has been corrected based on problems reported by George Born's group.

IV. Under certain conditions, several uninitialized variables in common block INDIRECT were referenced. They are now initialized in BLOCK DATA ITR4.

V. The internal option of producing O^+ density instead of electron density on output has been removed because it was not correctly implemented.

VI. Several subroutines that are no longer used have been removed.

The table below describes the changes that I made to PRISM 1.5 to produce PRISM 1.5a.

Module	Program Unit	Description of Changes (*Begins*)
CGM_UTIL.FOR	Subroutine BOUNDS	Removed since it is no longer used.
GETDAT.FOR	Subroutine DO_DIR	Increased the first dimension of matrix NDUMDAT from 5 to 8 to allow for 8 DMSP data files. Removed an unnecessary initialization of matrix NDUMDAT from the TEC data ingestion section. Increased the upper loop limit from 5 to 8 in the initialization of matrix NDUMDAT in the DMSP data ingestion section to allow for 8 DMSP data files.
	Subroutine DO_DMSP	Decreased PARAMETER MAXIES from 7000 to 1451 based on expected time resolutions and time windows of DMSP Ion Drift and In Situ Plasma data. Increased PARAMETER MAXJ4 from 7000 to 7211 based on the expected time resolution and time window of DMSP SSJ/4 data. Moved dummy assignment "DEN1=DEN1" from DMSP Ion Drift data ingestion section to end of routine. Changed line "GOTO 150" to "IF(NSSIES .LE. MAXIES) GOTO 150" to avoid an array-out-of-bounds error when reading a DMSP Ion Drift data set larger than the size allocated by PARAMETER MAXIES. Changed line "GOTO 214" to "IF(NSSIES .LE. MAXIES) GOTO 214" to avoid an array-out-of-bounds error when reading a DMSP In Situ Plasma data set larger than the size allocated by PARAMETER MAXIES. Changed line "goto 250" to "IF(NSSJ4 .LE. MAXJ4) GOTO 250" to avoid an array-out-of-bounds error when reading a DMSP SSJ/4 data set larger than the size allocated by PARAMETER MAXJ4. Changed line "GOTO 100" to "IF(IORB .LT. MAXORB) GOTO 100" to avoid an array-out-of-bounds error when more than MAXORB DMSP Ion Drift data sets are present in a DMSP data file. Added line "IORB=0" before line "221 CONTINUE" and line "IORB=IORB+1" after line "221 CONTINUE" to count the number of DMSP In Situ Plasma data sets in the DMSP data file. Added line "IF(IORB .LT. MAXORB) GOTO 221" before line "330 CONTINUE" to allow up to MAXORB DMSP In Situ Plasma data sets in a DMSP data file. Changed line "GOTO 300" to "IF(IORB .LT. MAXORB) GOTO 300" to avoid an array-out-of-bounds error when more than MAXORB DMSP SSJ/4 data sets are present in a DMSP data file. Changed loop upper bounds corresponding to the last dimension of common block PRECP1 arrays MLATR, MLTR, and VALTR from 2 to MAXORB because of the change in size of those arrays. Changed loop upper bounds corresponding to the last dimension of common block PRECP1 arrays LAT, MLT, and ERG from 2 to MAXORB because of the change in size of those arrays. Removed a commented-out call to subroutine GET_OVAL.
	Subroutine CONFIX	Changed PARAMETER MLATMID from 40. to 35. Changed the loop logic in the calculation of the mean midlatitude horizontal ion velocity and mean midlatitude corotation velocity to avoid an array-out-of-bounds error when no midlatitude data points are present. In the calculation of the mean midlatitude horizontal ion velocity and mean midlatitude corotation velocity, midlatitude data points are now detected by checking their calculated magnetic latitude instead of their geographic latitude. If three midlatitude data points are not available for the calculation of the mean midlatitude horizontal on velocity and mean midlatitude corotation velocity, then the data set is now ignored.
HLIM.FOR	Subroutine REGMOD	References to common block INDIRECT variable ONLYOP have been removed.
INDIRECT.INC	n/a	References to variable ONLYOP have been removed.
INIT.FOR	Subroutine INIT	Added assignments of logical flags ITR, USUE, and USUF to .TRUE. for ITY=1 when either no DISS or no high-latitude DISS data is present but high-latitude TEC data is present. This allows iteration on high-latitude TEC data in the absence of high-latitude DISS data.
	Subroutine INITPR	Removed commented-out calls to routine GET_CIRCL. Added local arrays VALTRA, MLATRA, and MLTRA. Changed the argument list in calls to routine GET_TR_KP to allow for more DMSP Ion Drift data. Added local matrices ERGA and LATA. Added local variable I. Changed the argument list in the call to routine GET_CIRCL to allow for more DMSP SSJ/4 data. Removed local variable IC since it is no longer used.
	Subroutine GET_CIRCL	Complete rewrite to allow for more DMSP SSJ/4 data.
	Subroutine GET_TR_KP	Complete rewrite to allow for more DMSP Ion Drift data.
	Subroutine CENTER	Removed since it is no longer used.
	Subroutine GET_ST_NUM	The logical flag TEC is now set to .TRUE. only if at least one TEC direct data point lies in the latitude region determined by the logical flag ITY. Previously the logical flag TEC was set to .TRUE. if any TEC direct data was present.
	Subroutine SET	Removed since it is no longer used.
	Subroutine FULL_CIRCLE	Removed since it is no longer used.
NEWFIT.INC	n/a	Changed the value of PARAMETER NMAX from 700 to 2000 to support more DMSP In Situ Plasma data. Changed the value of PARAMETER NNMAX from 2000 to 5000 to support more DMSP In Situ Plasma data.

Continues

Module	Program Unit	Description of Changes (*Continued*)
OUTPUT.FOR	Subroutine WR_ST_DATA	Removed the third header line at the beginning of the station output file for station output type IOUTS=0. Added a header line above the critical parameters data record line in the station output file for station output type IOUTS=0.
PRECIP.INC	n/a	Added PARAMETER MAXORB. Changed the last dimension of common block PRECP1 arrays LAT, MLT, and ERG from 2 to MAXORB to support more DMSP SSJ/4 data. Changed the last dimension of common block PRECP1 arrays MLATR, MLTR, and VALTR from 2 to MAXORB to support more DMSP Ion Drift data.
PRISM.FOR	Block Data ITR4	Added initialization of common block INDIRECT variables HDFE, HDHE, HDF2, and HDHF2.
	Block Data PREC	Complete rewrite for more flexible initialization of arrays in common block PRECP1.
	Program PRISM	Updated the version number and version date.
Ends		

M·E·M·O·R·A·N·D·U·M

DATE: *29-September-1995*

TO: *Rob Daniell*

FROM: *Lincoln Brown*

RE: *Changes to PRISM 1.5a for PRISM 1.6*

The changes to PRISM 1.5a for PRISM 1.6 focus on the resolution of problem report PRF-PRISM19 from Bob Prochaska at Hughes STX and final enhancements for the last planned delivery of PRISM 1. The changes are summarized as follows:

I. Problem report PRF-PRISM19 has been resolved. PRISM uses the plasma temperature to calculate a topside scale height for the midlatitude electron density, where the plasma temperature is the sum of the electron and ion temperatures from a DMSP SSIES In Situ Plasma data record. The topside scale height varies linearly with the plasma temperature. Missing electron and ion temperature data in the DMSP SSIES In Situ Plasma data record is flagged by zero values. Previously, however, if one of the temperatures was zero but the other temperature was nonzero, PRISM continued to calculate and use a plasma temperature, resulting in a topside scale height roughly half as large as it should have been. The erroneously small scale height drove the topside midlatitude electron density to fall off rapidly, resulting in very a small electron density at the top of the altitude grid. Now, PRISM ignores the temperature data in a DMSP SSIES In Situ Plasma data record and does not calculate a topside scale height for the data record if either the electron or ion temperature is zero.

II. PRISM now checks Ionosonde (DISS) data for nonphysical values. The following tests have been added to the Ionosonde data ingestion:

A. The observed critical frequency of the F_2 layer (f_oF_2) in the Ionosonde data record must be in the range $0 < f_oF_2 \leq 28.4$ MHz. The range maximum corresponds to a peak F_2 layer density (n_mF_2) of 10^7 cm^{-3} using the approximation $n_mF_2(\text{cm}^{-3})=1.24\times10^4 \cdot f_oF_2(\text{MHz})^2$. If the f_oF_2 parameter in the Ionosonde data record is outside this range, then the f_oF_2 parameter is ignored.

B. The observed height of the F_2 layer (h_mF_2) in the Ionosonde data record must be in the range $200 \leq h_mF_2 \leq 1000$ km. If the h_mF_2 parameter in the Ionosonde data record is outside this range, then the h_mF_2 parameter is ignored.

C. The observed critical frequency of the E layer (f_oE) in the Ionosonde data record must be in the range $0 < f_oE \leq 28.4$ MHz. The range maximum corresponds to a peak E layer density (n_mE) of 10^7 cm^{-3} using the approximation $n_mE(\text{cm}^{-3})=1.24\times10^4 \cdot f_oE(\text{MHz})^2$. If the f_oE parameter in the Ionosonde data record is outside this range, then the f_oE parameter is ignored.

D. The observed height of the E layer (h_mE) in the Ionosonde data record must be in the range $90 \leq h_mE \leq 150$ km. If the h_mE parameter in the Ionosonde data record is outside this range, then the h_mE parameter is ignored.

III. PRISM now checks TEC (IMS) data for nonphysical values. The vertical equivalent *TEC* in the TEC data record must be in the range $0 < TEC \leq 250$ TEC Units (1 TEC Unit=10^{12} cm^{-2}= 10^{16} m^{-2}) . If the vertical equivalent *TEC* in the TEC data record is outside this range, then the TEC data record is ignored.

IV. PRISM now checks DMSP SSIES In Situ Plasma data for nonphysical values. The following tests have been added to the DMSP SSIES In Situ Plasma data ingestion:

A. The in situ electron density (n_e) in the DMSP SSIES In Situ Plasma data record must be in the range $10^3 \le n_e \le 10^7$ cm^{-3}. If the n_e parameter in the DMSP SSIES In Situ Plasma data record is outside this range, then the *entire* data record is ignored.

B. The in situ electron temperature (T_e) in the DMSP SSIES In Situ Plasma data record must be in the range $0 < T_e \le 6000$ °K. The in situ ion temperature (T_i) in the DMSP SSIES In Situ Plasma data record must be in the range $0 < T_i \le 6000$ °K. If either the electron or ion temperature in the DMSP SSIES In Situ Plasma data record is outside its range, then both temperatures are ignored.

V. Phantom Ionosonde data has been added to PRISM. In the absence of any valid real-time Ionosonde and TEC data in 30°×30° corrected geomagnetic latitude/longitude zones between -60° and +60° corrected geomagnetic latitude, PRISM now adds phantom Ionosonde data centered in the zones to reduce the global effect of sparse real-time Ionosonde and TEC data. The phantom Ionosonde data is generated using the parameterized models in PRISM for the UT of the run, and is included in the set of real-time data that PRISM uses for its real-time adjustment of the parameterized models.

VI. Phantom In Situ Plasma data has been added to PRISM. In the absence of any real-time SSIES In Situ Plasma data in 30°×30° corrected geomagnetic latitude/longitude zones between -60° and +60° corrected geomagnetic latitude, PRISM now adds phantom In Situ Plasma data (density only since PRISM does not contain electron and ion temperature models) centered in the zones to reduce the global effect of sparse real-time In Situ Plasma data. The phantom In Situ Plasma density data is generated using the parameterized models in PRISM for the UT of the run and DMSP altitude (840 km), and is included in the set of real-time data that PRISM uses for its real-time adjustment of the parameterized models.

VII. Commented-out coding has been removed.

VIII. Unused routines have been removed.

IX. Unused variables have been removed.

The table below describes the changes that I made to PRISM 1.5a to produce PRISM 1.6.

Module	Program Unit	Description of Changes (*Begins*)
FMODEL.FOR	Subroutine FMODEL	Removed local variables TFOF2, THMF2, CFOF2, POFOF2, CFOE, and CHME since they are not used.
	Subroutine TRO_DEP	Removed local variables FOF2, HMF2, FOF2ML, and HMF2ML since they are not used.
GETDAT.FOR	Subroutine DO_DIR	Removed argument NDUMDAT(I,2) from the first call to routine DO_IONO since it is not used by that routine. Removed argument NDUM1 from the second call to routine DO_IONO since it is not used by that routine. Removed local variable NDUM1 since it is no longer used.
	Subroutine DO_IONO	Expanded the range validation of ingested E and F_2 layer Ionosonde data. Removed commented-out code for defunct BOTTOMSIDE data type. Removed PARAMETER AFPE since it is no longer used. Removed output parameter NBREC since it is no longer used.
	Subroutine DO_TEC	Expanded the range validation of ingested TEC data.
	Subroutine DO_DMSP	Expanded the range validation of ingested DMSP SSIES In Situ Plasma data. This resolves problem report PRF-PRISM19 from Bob Prochaska at Hughes STX. Removed PARAMETER TDIFMAX since it is no longer used.
	Subroutine IES_DATA	Removed since it is not used.
IO_UTIL.FOR	Subroutine CLOSFL	Removed since it is not used.

Continues

Module	Program Unit	Description of Changes (*Continued*)
MATH_UTI.FOR	Subroutine SORT7	Removed since it is not used.
	Subroutine SWPARR	Removed since it is no longer used.
	Subroutine INDEXX	Removed since it is no longer used.
	Subroutine GETGAM	Removed since it is no longer used.
MIDLAT.FOR	Subroutine MIDLAT	Removed commented-out PRINT statements. Removed FORMAT statement 91000 since it is no longer used. Removed local variables AF and FIRST since they are no longer used.
	Subroutine PHIONO	Removed since it is not used.
	Subroutine DST1	Removed since it is no longer used.
	Subroutine PHIES	Removed since it is not used.
	Subroutine INS_TRACK	Removed since it is no longer used.
PHANTOM.FOR	n/a	New module containing routine PHANTM.
PRISM.FOR	Program PRISM	Added calls to routines INIT and PHANTM after the conversion of the nominal UT from hours to seconds. Updated the version number and version date.
READ_DBA.FOR	Subroutine READAWS	Commented out references to local variable KF000 since it is not needed.
RTA.FOR	Subroutine RTA	Removed commented-out code for bottomside fitting.
	Subroutine BOTTOM	Removed since it is not used.
STRINGS.FOR	Subroutine STRDEL	Removed since it is no longer used.
	Subroutine STRFLL	Removed since it is no longer used.
	Subroutine STRINS	Removed since it is no longer used.
	Subroutine STRNPO	Removed since it is no longer used.
	Subroutine STRRPL	Removed since it is no longer used.
	Subroutine STRSHC	Removed since it is no longer used.
	Subroutine STRSHI	Removed since it is no longer used.
	Subroutine STRTRM	Removed since it is no longer used.
	Subroutine STRUCA	Removed since it is no longer used.
	Subroutine CONCAT	Removed since it is not used.
	Subroutine DELETE	Removed since it is not used.
	Subroutine FILL	Removed since it is not used.
	Subroutine INSERT	Removed since it is not used.
	Subroutine LOCASE	Removed since it is not used.
	Subroutine LENGTH	Removed since it is not used.
	Subroutine NTHPOS	Removed since it is not used.
	Subroutine REPLAC	Removed since it is not used.
	Subroutine SHIFTC	Removed since it is not used.
	Subroutine SHIFT	Removed since it is not used.
	Subroutine TRIM	Removed since it is not used.
	Subroutine UPCASE	Removed since it is not used.
TIMELIB.FOR	Subroutine TIMMDT	Removed since it is no longer used.
	Subroutine DELTAT	Removed since it is not used.
	Subroutine GETDOY	Removed since it is not used.
	Subroutine LEAPYR	Removed since it is not used.
	Subroutine GETMDM	Removed since it is not used.
	Subroutine MODATE	Removed since it is not used.
Ends		

M·E·M·O·R·A·N·D·U·M

DATE: *12-February-1996*

TO: *Rob Daniell*

FROM: *Lincoln Brown*

RE: *Changes to PRISM 1.6 for PRISM 1.6a*

The changes to PRISM 1.6 for PRISM 1.6a focus on the replacement of the LLF parameterized model coefficients, the resolution of PRF PRISM-24, and a change to the Gridded Output Specification. The changes are summarized as follows:

I. The LLF parameterized model coefficients have been replaced, resulting in several improvements in the low-latitude O^+ density representation in PRISM:

A. The solar activity dependence is now correctly represented. Previously, due to bugs in the LOWLAT theoretical model used to generate the coefficients, and misuse of one of the LOWLAT input files, no variation in the O^+ density due to solar activity level was present.

B. The peak of the dayside O^+ density is more in line with expected dayside densities. It is believed that the dayside electron temperature model used in LOWLAT resulted in dayside O^+ densities that were too large. The upper limit of the dayside electron temperature has been increased from 2500°K to 3000°K to maintain a smaller dayside O^+ density.

C. The bottomside O^+ density has been improved. Previously, spline interpolation of rapidly decreasing O^+ density on a sparse bottomside altitude grid could result in a false and substantial peak near the bottom of the LLF altitude grid (160 km). The interpolation algorithm has been modified to eliminate this problem.

II. PRF PRISM-24 has been resolved. DMSP SSIES Ion Drift and SSJ/4 data sets are now no longer allowed to overrun allocated space in PRISM. Previously, if the maximum allowed number of data points was accepted by PRISM before the end of the dataset was reached, an array-out-of-bounds error occurred. A slight change in logic has resolved this problem. This problem was reported by Bob Prochaska at Hughes STX.

III. The coordinate system flag IGM in the Gridded Output Specification is now consistent with the PRISM source code. Previously, the convention given in the Gridded Output Specification was opposite that used in PRISM. This problem was reported by Vince Eccles at Space Environment Corp., and its resolution was approved by Bob Prochaska at Hughes STX.

The table below describes the changes that I made to PRISM 1.6 to produce PRISM 1.6a.

Module	Program Unit	Description of Changes
GETDAT.FOR	Subroutine DO_DMSP	Changed the line "IF(NSSIES .LE. MAXIES) GOTO 150" to "IF(NSSIES .LT. MAXIES) GOTO 150" to avoid an array-out-of-bounds error when MAXIES data points in a SSIES Ion Drift data set have been accepted before the end of the data set has been reached. Changed the line "IF(NSSJ4 .LE. MAXJ4) GOTO 250" to "IF(NSSJ4 .LT. MAXJ4) GOTO 250" to avoid an array-out-of-bounds error when MAXJ4 data points in a SSJ/4 data set have been accepted before the end of the data set has been reached.
PRISM.FOR	Program PRISM	Updated the version number and version date.

M·E·M·O·R·A·N·D·U·M

DATE: *19-August-1996*

TO: *Rob Daniell*

FROM: *Lincoln Brown*

RE: *Changes to PRISM 1.6a for PRISM 1.6b*

The changes to PRISM 1.6a for PRISM 1.6b focus on improving the midlatitude real-time adjustment. The changes are summarized as follows:

I. Several improvements have been made to the midlatitude real-time adjustment:

A. Real-time and phantom data that agree exactly with the parameterized models are no longer prevented from influencing the midlatitude real-time adjustment. Previously, data agreeing exactly with the parameterized models was ignored by the midlatitude real-time adjustment. This problem was reported by David Coxwell at Air Force Institute of Technology.

B. The actual magnetic latitude of real-time and phantom data is now used in the distance-weighting for the midlatitude real-time adjustment. Previously, the magnetic latitude of data used in the distance-weighting was normalized to the range [-90,90] degrees based on the magnetic latitude of the equatorward trough boundary. The normalization introduced error into the midlatitude correction field by artificially extending the latitudinal distance between the data and the location of interest, resulting in an elliptical rather than a circular weighting function.

C. The actual magnetic longitude of real-time and phantom data is now used in the distance-weighting for the midlatitude real-time adjustment. Previously, the magnetic local time of the data converted to hour angle was used in the distance-weighting. The use of the magnetic local time instead of magnetic longitude introduced as much as a 30 degree (2 hour) error in magnetic longitude in the midlatitude correction field, depending on the time difference between the data and the nominal UT.

D. The peak density corrections of the midlatitude real-time adjustment have been improved by using total ion densities at h_mE and h_mF_2 instead of the molecular ion density at h_mE and the O^+ density at h_mF_2. This removes the assumptions that O^+ is negligible at h_mE compared to the molecular ions and that molecular ions are negligible at h_mF_2 compared to O^+.

E. The density scaling correction of the midlatitude real-time adjustment has been improved by applying the E-layer and F_2-layer density scalings to both the molecular ion density profile and the O^+ density profile, resulting in a self-consistent correction. This removes the assumptions that O^+ is negligible at h_mE compared to the molecular ions and that molecular ions are negligible at h_mF_2 compared to O^+.

II. Several minor changes have been made for compatibility with Microsoft FORTRAN. They do not impact the results.

III. Commented-out code has been removed from several routines.

IV. Unused FORMAT statements have been removed from several routines.

V. Several typographical errors in comments have been corrected.

The table below describes the changes that I made to PRISM 1.6a to produce PRISM 1.6b.

Module	Program Unit	Description of Changes
MIDLAT.FOR	Subroutine MIDLAT	Removed conditionals so that data agreeing exactly with the model is not ignored in the midlatitude real-time adjustment. Magnetic local time stored in local arrays IMLT and JMLT is no longer converted to hour angle. Added local arrays IMLON and JMLON. Magnetic longitude is now stored in local arrays IMLON and JMLON. Local array JMLON is now passed to routine PER_ARR. Corrected typo in comment by changing ",HME = 8" to ",HME = 6".
	Subroutine PER_ARR	Added array JMLON to argument list. Magnetic local time stored in argument array JMLT is no longer expressed as hour angle. Magnetic latitude stored in argument array JMLAT is no longer normalized to the range [-90,90] degrees by the magnetic latitude of the equatorward trough boundary. Magnetic longitude is now stored in argument array LON instead of magnetic local time.
OUTPUT.FOR	Subroutine WRITE_DATA	Changed "1PE11.4" to ",1PE11.4" in FORMAT statement 8000 to avoid compiler error under Microsoft Fortran PowerStation. Removed commented-out code. Removed unused FORMAT statements.
	Subroutine W_ST_DATA	Removed commented-out code. Removed unused FORMAT statements, including FORMAT statement 8000, which caused a compiler error under Microsoft Fortran PowerStation.
PARAM.FOR	Subroutine PARAM	Magnetic longitude is now passed to routine RTA instead of magnetic local time by changing argument MLT to MLON in the call to routine RTA. Removed commented-out code.
PHANTOM.FOR	Subroutine PHANTM	Corrected typos in comments by changing "to added" to "to be added".
PRISM.FOR	Block Data INTRAT1	Character strings in array LABEL longer than the allocated length have been truncated. The DATA statement defining the LABEL array has been reformatted to eliminate line continuations in the middle of character strings.
	Program PRISM	Removed commented-out code. Removed unused FORMAT statements. Updated the version number and version date.
RTA.FOR	Subroutine RTA	Changed argument MLT to MLON. Variables MLAT and MLON are now passed to routine CORRECT1 instead of variables LATADJ and LTADJ. Removed local variables LATADJ and LTADJ since they are no longer used. Removed commented-out code.
	Subroutine COR_MAX	Replaced variable EE (molecular ion density at height h_mE) with argument EE+FE (total ion density at height h_mE) in the first call to routine GET_ONE_FO so that the correct ratio n_mE_{new}/n_mE_{old} (variable FRE) is returned. Removed variables NME and DNE from the first call to routine GET_ONE_FO. Replaced variable FF (O^+ density at height h_mF_2) with argument EF+FF (total ion density at height h_mF_2) in the second call to routine GET_ONE_FO so that the correct ratio $n_mF_{2,new}/n_mF_{2,old}$ (variable FRF) is returned. Removed variables NMF2 and DNF from the second call to routine GET_ONE_FO. Variables EE, EF, FE, and FF are now passed to routine DO_ADJ instead of variables DNE, DNF, and DNM. Removed local variables NME, NMF2, DNE, DNF, and DNM since they are no longer used. Removed commented-out code.
	Subroutine DO_ADJ	Complete rewrite to change algorithm and to improve coding and internal documentation. E-layer and F_2-layer density adjustments are now done on both the O^+ and molecular ion density profiles.
	Subroutine GET_ONE_FO	Removed variables NMAX and DNMAX from argument list. Removed variables NMAX and DNMAX since they are no longer used. Removed commented-out code. Removed unused FORMAT statements.
TECCALC.FOR	Subroutine LOCATE	Modified logic to eliminate .EQV. logical operator, which caused a run-time access violation error under Microsoft Fortran PowerStation.

M·E·M·O·R·A·N·D·U·M

DATE: *30-September-1996*

TO: *Rob Daniell*

FROM: *Lincoln Brown*

RE: *Changes to PRISM 1.6b for PRISM 1.7*

The changes to PRISM 1.6b for PRISM 1.7 focus on replacing the LLF coefficient set again, on improving the handling of collocated data in the real-time adjustment, and on improving the merging of the parameterized model density profiles. The changes are summarized as follows:

I. **BUG FIX**: The LLF parameterized model coefficient set has been replaced again. Because of a bug in the processing of the LOWLAT output, the magnetic latitude grid in the PRISM 1.6b LLF coefficient files was defined to start at -33°N instead of the correct value of -34°N. This resulted in an erroneous northward 1° magnetic latitude shift in the O^+ densities from the LLF parameterized model. The LLF coefficient files have been regenerated with the correct starting value for the magnetic latitude grid. Note that this fix requires no change to the PRISM source code.

II. **BUG FIX**: The conversion of UT from hours to HHMM in routine PARAM for the URSI f_oF_2 model has been corrected. Previously, the conversion of UT from decimal hours to HHMM resulted in truncation of the minutes to zero, e.g. a UT of 1.5 hours was erroneously converted to 0100. The conversion has been modified so that the minutes are not truncated to zero, e.g. a UT of 1.5 hours is correctly converted to 0130.

III. Based on work done by Pat Doherty, we now recommend that a 27-day running mean of $F_{10.7}$ be used instead of a daily value. Pat found that a mean $F_{10.7}$ correlates much better with the ionosphere than a daily value, either because the solar EUV has less day-to-day variability than $F_{10.7}$ or because the day-to-day variability in solar EUV is uncorrelated with the day-to-day variability in $F_{10.7}$. The same applies to Sunspot Number (use a 27-day running mean instead of a daily value), although we recommend using $F_{10.7}$ instead of Sunspot Number as the solar activity index.

IV. Multiple data points critically close to an output grid point are now handled correctly in the real-time adjustment. Previously, if one or more data points was within the critical distance of an output grid point, then the correction returned by the real-time adjustment was the correction from the last data point within the critical distance. Now, if one or more data points are within the critical distance of an output grid point, then the correction returned from the real-time adjustment is the average of corrections from those data points.

V. The top-level parameterized model routine PARAM has undergone substantial changes. The original motivation was a report from Jim Secan at Northwest Research Associates illustrating a discontinuity in PRISM 1.6b TEC at the latitude transition region between the mid-latitude and high-latitude parameterized models. A closer examination of routine PARAM has yielded the following improvements:

   A. It has been completely rewritten for optimization and readability. The number of routine calls has been reduced.

   B. The transition between the mid-latitude and high-latitude parameterized models is smoother. Previously, in the mid/high-latitude transition region, the mid-latitude peak density and height were used to merge the mid-latitude and high-latitude density profiles, resulting in a discontinuity in density at the boundary between the high-latitude region and the mid/high-latitude transition region. Now, weighted

averages of mid-latitude and high-latitude peak densities and heights are used in the merging, resulting in a smoother transition.

C. The transition between the low-latitude and mid-latitude parameterized models is smoother. Previously, a weighted average of low-latitude and mid-latitude critical frequencies was used to calculate the peak density for the merging of the low-latitude and mid-latitude density profiles. Now, the peak density used in the merging is calculated from a weighted average of low-latitude and mid-latitude peak densities. This is consistent with the profile merging process, and results in a smoother transition between the low-latitude and mid-latitude parameterized models.

VI. The mid-level parameterized model routines LOW_PARAM, MID_PARAM, and USUMODEL have been rewritten to accommodate changes in the top-level parameterized model routine PARAM, to provide small performance gains by reducing routine calls and eliminating unnecessary calculations, and to improve readability.

VII. The low-level parameterized USU model routines RECON, FOUR_COEFF, and FULL_DATA have been modified to accommodate changes to the mid-level parameterized model routine USUMODEL.

VIII. Several routines in module ENVIRON.FOR have been replaced for compatibility with PIM.

IX. Several routines have been modified to accommodate the new version of routine SOLDEC.

X. Several minor changes have been made for compatibility with Microsoft FORTRAN. They do not impact the results.

The table below describes the changes that I made to PRISM 1.6b to produce PRISM 1.7.

Module	Program Unit	Description of Changes
ADJ_FNH.FOR	Subroutine GET_FOS	Removed argument ERR from the call to INFLECTION since it is no longer used by that routine. Removed local variable ERR since it is no longer used.
	Subroutine INFLECTION	Removed input argument ERR since it is not used. Changed declaration of local variable TEST from LOGICAL*1 to LOGICAL.
	Subroutine GET_FOE	Removed since it is no longer used.
ENVIRON.FOR	Subroutine SOLZA	Removed since it has been replaced by routine SOLSZA.
	Subroutine SSOLPT	Removed since it has been replaced by routine SOLSUB.
	Function SOLDEC	Replaced by routine of the same name.
	Function SOLANG	New routine.
	Subroutine SOLSUB	New routine.
	Function SOLSZA	New routine.
FMODEL.FOR	Subroutine FMODEL	Removed argument HBOT from call to PARAM since it is not used by that routine. Removed last argument in call to PARAM since it is no longer used by that routine. Removed local variable HBOT since it is no longer used.
GETDAT.FOR	Subroutine GETDAT	Removed argument ESWITCH from call to MODEL_FLAGS since it is no longer used.
	Subroutine MODEL_FLAGS	Removed assignment of input argument ESW. Removed input argument ESW since it is no longer used.
	Subroutine PREC_DATA	Changed declaration of local variable TEST from LOGICAL*1 to LOGICAL.
	Subroutine J4ARR	Changed declaration of local variable TEST from LOGICAL*1 to LOGICAL.
HLIM.FOR	Subroutine REGMOD	Removed argument HBOT from call to PARAM since it is not used by that routine. Removed last argument in call to PARAM since it is no longer used by that routine. Removed local variable HBOT since it is no longer used. Replaced call to SOLZA with call to SOLSZA.
HLISM.FOR	Subroutine HLISM	Removed local variable MFLAG since it is no longer used.
INDIRECT.INC	n/a	Removed common block INDIRECT variable ESWITCH since it is no longer used.
INIT.FOR	Subroutine LDITER	Changed declaration of output argument LAYFLG from LOGICAL*1 to LOGICAL.
	Subroutine GETFC	Changed declaration of local variable ERROR from LOGICAL*1 to LOGICAL.
	Subroutine LUDCMP	Changed PAUSE statement to STOP statement.
IO_UTIL.FOR	Subroutine UDETID	Added input argument UT. Argument DAY is no longer converted to a real number in call to SOLDEC. Added argument UT to call to SOLDEC.
LAYFLG.INC	n/a	Changed declaration of common block LAYFLG variable LAYFLG from LOGICAL*1 to LOGICAL.

Module	Program Unit	Description of Changes (*continued*)
LOW_PARA.FOR	Subroutine LOW_PARAM	Rewrite for optimization and readability. Removed input argument LAYR since it is no longer used. Changed intrinsic function ALOG to its generic equivalent LOG.
MATH_UTI.FOR	Subroutine INTRP	Modified logic to eliminate arithmetic IF statements.
	Subroutine SVDCMP	Changed PAUSE statement to PRINT statement.
MID_PARA.FOR	Subroutine MID_PARAM	Rewrite for optimization and readability. Removed input argument LAYR since it is no longer used. Changed intrinsic function ALOG to its generic equivalent LOG.
OUTPUT.FOR	Subroutine FINAL	Changed declaration of local variable TEST from LOGICAL*1 to LOGICAL.
PARAM.FOR	Subroutine PARAM	Rewrite for optimization and readability. Fixed a bug in the conversion of UT from hours to HHMM for the call to F2URSI. In the mid/high-latitude transition region, weighted averages of mid-latitude and high-latitude peak densities and heights are now used in the merging of profiles instead of the mid-latitude peak density and height. In the low/mid-latitude transition region, the peak density used to merge profiles is calculated from a weighted average of low-latitude and mid-latitude peak density instead of a weighted average of low-latitude and mid-latitude critical frequency, to be consistent with the profile merging process. Simplified logic since LAYR flag is no longer used. Removed input argument LAYR since it is no longer used. Removed input argument HBOT since it is not used. Removed last argument from calls to USUMODEL since it is no longer used. A single call to USUMODEL is now used instead of two calls. Removed last argument from calls to MID_PARAM since it is no longer used. A single call to MID_PARAM is now used instead of two calls. Removed last argument from calls to LOW_PARAM since it is no longer used. A single call to LOW_PARAM is now used instead of two calls. Removed call to GET_FOE since it is no longer used. Removed logic involving common block INDIRECT variable ESWITCH since it is no longer used. Changed intrinsic function ALOG to its generic equivalent LOG.
PRISM.FOR	Program PRISM	Updated the version number and version date.
READ_DBA.FOR	Subroutine READ_DBASES	Added argument UT to call to RDLOW.
	Subroutine RDLOW	Added input argument UT. Added argument UT to call to LDETID.
	Subroutine LDETID	Added input argument UT. Argument DAY is no longer converted to a real number in call to SOLDEC. Added argument UT to call to SOLDEC.
	Subroutine READ_E	Added argument UT to call to EDETID.
	Subroutine EDETID	Added input argument UT. Argument DAY is no longer converted to a real number in call to SOLDEC. Added argument UT to call to SOLDEC.
	Subroutine READMID	Added argument UT to call to DETID.
	Subroutine DETID	Added input argument UT. Argument DAY is no longer converted to a real number in call to SOLDEC. Added argument UT to call to SOLDEC.
	Subroutine READUSU	Added argument UT to calls to UDETID.
RTA.FOR	Subroutine RTA	Changed declaration of local variable IERR from LOGICAL*1 to LOGICAL.
	Subroutine CORRECT1	Rewrite for optimization and readability. If one or more data points is within the critical distance of the point of interest, then the correction at the point of interest is now calculated as the average of corrections from those data points instead of the correction of the last data point within the critical distance being used.
	Subroutine COR_MAX	Changed declaration of output argument IERR from LOGICAL*1 to LOGICAL.
	Subroutine GET_ONE_FO	Changed declaration of output argument IERR from LOGICAL*1 to LOGICAL.
	Subroutine COR_PRO	Changed declaration of output argument IERR from LOGICAL*1 to LOGICAL.
USER_INP.FOR	Subroutine CHECK_STAT	Changed declaration of input argument TEST from LOGICAL*1 to LOGICAL.
	Subroutine GIVE_DATA	Changed declaration of local variable TEST from LOGICAL*1 to LOGICAL.

Module	Program Unit	Description of Changes (*continued*)
USUMODEL.FOR	Subroutine USUMODEL	Rewrite for optimization and readability. Removed input argument LAYR since it is no longer used. Changed intrinsic function ALOG to its generic equivalent LOG.
	Subroutine RECON	Replaced input argument XNMLAT with input arguments SMLATE and SMLATF. Replaced argument XNMLAT with argument SMLATE and SMLATF in call to FOUR_COEFF. Removed argument LAYR from calls to FOUR_COEFF and FULL_DATA. Removed input argument LAYR since it is no longer used.
	Subroutine FOUR_COEFF	Replaced input argument XNMLAT with input arguments SMLATE and SMLATF. Fourier coefficients are now calculated for all three ions. Removed input argument LAYR since it is no longer used.
	Subroutine FULL_DATA	Altitude profiles are now calculated for all three ions. Removed input argument LAYR since it is no longer used.

The figure below illustrates the improvement in the merging of the regional parameterized models. It shows a profile of f_oF_2 vs. geographic latitude. Note the discontinuity in PRISM 1.6b f_oF_2 in the mid/high-latitude transition region and the smoother transition in the PRISM 1.7 profile. The differences at low latitudes are due to the change in the low/mid-latitude transition method and the corrected LLF parameterized model coefficients.

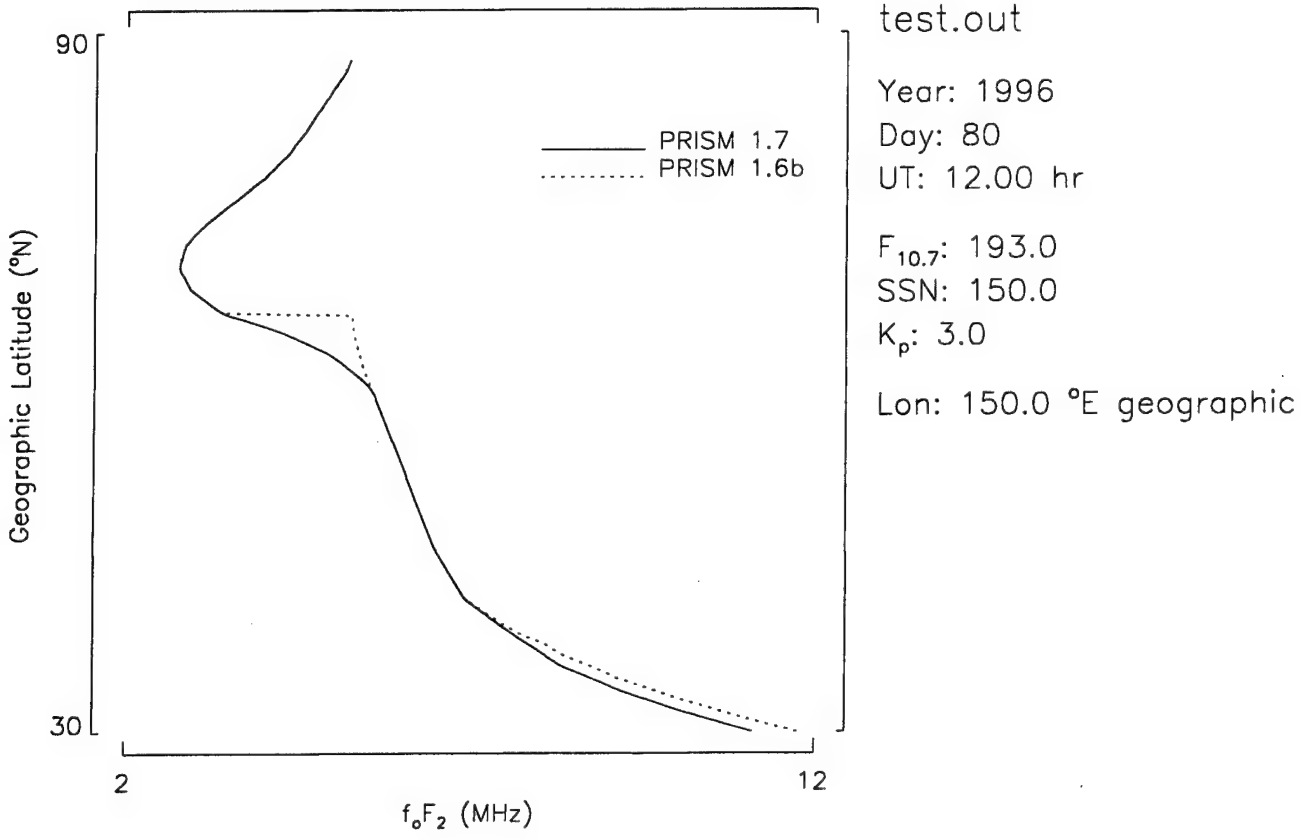

M·E·M·O·R·A·N·D·U·M

DATE: *7-November-1996*

TO: *Rob Daniell*

FROM: *Lincoln Brown*

RE: *Changes to PRISM 1.7 for PRISM 1.7a*

The changes to PRISM 1.7 for PRISM 1.7a focus on improvements to the real-time data ingestion. The changes are summarized as follows:

I. **BUG FIX**: The presence of all five possible DISS real-time data files no longer causes an array-out-of-bounds error in the DISS data ingestion. Previously, if root names for all five DISS data files were given in the PATH_NAM.TXT file, then the DISS data ingestion would attempt to access a nonexistent sixth element of the array that holds the DISS data file root names. This problem has been eliminated due to the rewrite of the DISS data ingestion (see item 5).

II. **BUG FIX**: The presence of all five possible IMS real-time data files no longer causes an array-out-of-bounds error in the IMS data ingestion. Previously, if root names for all five IMS data files were given in the PATH_NAM.TXT file, then the IMS data ingestion would attempt to access a nonexistent sixth element of the array that holds the IMS data file root names. This problem has been eliminated due to the rewrite of the IMS data ingestion (see item 6).

III. **BUG FIX**: The presence of all eight possible DMSP real-time data files no longer causes an array-out-of-bounds error in the DMSP data ingestion. Previously, if root names for all eight DMSP data files were given in the PATH_NAM.TXT file, then the DMSP data ingestion would attempt to access a nonexistent sixth element of the array that holds the DMSP data file root names. This problem has been eliminated due to the rewrite of the DMSP data ingestion (see item 7).

IV. **BUG FIX**: Large amounts of DISS f_oF_2 real-time data and/or large amounts of IMS real-time data no longer cause an array-out-of-bounds error in the midlatitude correction algorithm. Previously, array allocation in the midlatitude correction algorithm for corrections for these kinds of data was inconsistent with limits defined in the real-time data ingestion. This problem was reported by David Coxwell at Air Force Institute of Technology. This problem has been eliminated due to the rewrite of the DISS and IMS data ingestion (see items 5 and 6) and the rewrite of the midlatitude correction algorithm (see item 9).

V. The DISS real-time data ingestion has been rewritten for speed and readability. A single pass through the DISS data is now required instead of two passes. Up to 850 DISS data records can now be accepted (i.e. meet criteria for use in the real-time adjustment) from all DISS data files combined, a reduction from the previous limit of 7000 accepted records per DISS data file. The limit of 850 accepted DISS data records is based on 50 DISS stations and a 15 minute time resolution in a [-2,2] hour time window relative to the time of the run.

VI. The IMS data ingestion has been rewritten for speed and readability. A single pass through the IMS data is now required instead of two passes. Up to 21600 IMS data records can now be accepted (i.e. meet criteria for use in the real-time adjustment) from all IMS data files combined, a reduction from the previous limit of 7000 accepted records per IMS data file. The limit of 21600 accepted IMS data records is based on 200 IMS stations reporting 12 simultaneous measurements and a time resolution of 15 minutes in a [-2,2] hour time window relative to the time of the run.

VII. The DMSP data ingestion has been rewritten for speed and readability. A single pass through the DMSP data is now required instead of three passes. Up to 24 sets of each of the three kinds of DMSP data are now accepted by PRISM from all DMSP data files combined, a reduction from the previous limit of 24 sets per DMSP data file. The limit of 24 sets is based on 8 satellites, an orbital period of 6060 seconds, and a [-2,2] hour time window relative to the time of the run. Up to 1451 SSIES ION DRIFT data records can be accepted (i.e. meet criteria for use in determining equatorward trough boundaries) per set, a limit which has not changed. The limit of 1451 accepted SSIES ION DRIFT data records is based on a 5 second time resolution in a [-2,0] hour time window relative to the time of the run, with 10 extra records allowed for orbital overlap. Up to 3848 SSIES IN SITU PLASMA data records can now be accepted (i.e. meet criteria for use in the real-time adjustment) from all DMSP data files combined, a reduction from the previous limit of 1451 accepted records per DMSP data file. The limit of 3848 accepted SSIES IN SITU PLASMA data records is based on 8 satellites and a time resolution of 30 seconds in a [-2,2] hour time window relative to the time of the run. Up to 7211 SSJ/4 data records can be accepted (i.e. meet criteria for use in determining auroral oval boundaries and for use in the real-time adjustment) per set, a limit which has not changed. The limit of 7211 accepted SSJ/4 data records is based on a time resolution of 1 second in a [-2,0] hour time windows relative to the time of the run, with 10 extra records allowed for orbital overlap.

VIII. The output station list determination has been rewritten for speed and readability. A single pass through the output station list is now required instead of two passes. The number of output stations is now unlimited, a change from the previous limit of 7000 stations.

IX. The midlatitude correction algorithm has been rewritten for the following reasons:

A. To optimize for speed.

B. To prevent extraneous zero corrections from being included in the real-time adjustment. The extraneous corrections were not based on valid data, and, although zero, influenced the correction fields and increased run time.

C. To remove coding for BOTTOMSIDE data since that data type is no longer considered by PRISM.

D. To remove redundant and commented-out coding.

E. To improve readability.

X. Limits on the ingestion of real-time data are now globally defined in new INCLUDE file *rtdlimit.inc*.

XI. The HLE model has been removed since it is no longer used. All components of PRISM upon which HLE solely depends have also been removed, such as the MSIS-86 neutral atmosphere model and a number of INCLUDE files. The HLE data files CHEM.FIL, TIMING.FIL, and SOLAR.FIL are no longer used. The path to the HLE files is still read from the PATH_NAM.TXT file for compatibility, but it is not used.

XII. Coding for the BOTTOMSIDE data type has been removed since it is no longer considered in PRISM.

XIII. INCLUDE file *dlta.inc* has been removed since it is not used.

XIV. A number of unused PARAMETERs and variables have been removed.

The performance gain due to these changes is hard to predict since it depends on the amount and character of the real-time data. For many of the standard test cases provided with delivery, run-time has been decreased by about 15%. The memory requirement has been reduced by about 0.5 MB, a 7% decrease.

The table below describes the changes that I made to PRISM 1.7 to produce PRISM 1.7a.

Module	Program Unit	Description of Changes
ALPHAN.INC	n/a	Removed since it is no longer used.
CHEM.INC	n/a	Removed since it is no longer used.
DLTA.INC	n/a	Removed since it is no longer used.
ESPECT.INC	n/a	Removed since it is no longer used.
CGM_UTIL.FOR	Subroutine BNDRY	Added INCLUDE statement for INCLUDE file rtdlimit.inc.
ENVIRON.FOR	Subroutine NEUATM	Removed since it is no longer used.
	Subroutine GTS5	Removed since it is no longer used.
	Function DENSS	Removed since it is no longer used.
	Function GLOBE5	Removed since it is no longer used.
	Function GLOB5L	Removed since it is no longer used.
	Function DNET	Removed since it is no longer used.
	Function CCOR	Removed since it is no longer used.
	Block Data PRMDTD	Removed since it is no longer used.
	Function SOLANG	Removed since it is no longer used.
	Subroutine SOLSUB	Removed since it is no longer used.
	Function SOLSZA	Removed since it is no longer used.
GETDAT.FOR	Subroutine GETDAT	Replaced call to routine DO_DIR with calls to routine INRTD and routine DETOSL. Removed output parameter SUSI since it is not used. Removed PARAMETERs NSTA and MAXTYPE since they are no longer used. Removed local variable NDAT since it is no longer used.
	Subroutine DO_DIR	Removed since it is no longer used (it has been replaced by routine INRTD).
	Subroutine DO_IONO	Removed since it is no longer used (it has been replaced by routines INDISS and DETOSL).
	Subroutine DO_TEC	Removed since it is no longer used (it has been replaced by routine INIMS).
	Subroutine DO_DMSP	Removed since it is no longer used (it has been replaced by routine INDMSP).
	Subroutine INRTD	New routine.
	Subroutine INDISS	New routine.
	Subroutine INIMS	New routine.
	Subroutine INDMSP	New routine.
	Subroutine DETOSL	New routine.
	Subroutine PREC_DATA	Output parameter NREC is now initialized to zero. PRECIPITATION records are now written to data file at the current file position instead of the end of the file. A PRECIPITATION data header is no longer written to the data file. Standard deviation placeholders are no longer included in the data record written to the data file. INCLUDE statements for INCLUDE files dpath.inc and direct_d.inc have been removed since they are no longer needed. Removed local variable DUMMY since it is no longer used.
	Subroutine LOADDIR	Removed since it is no longer used.
HLEMODEL.FOR	n/a	Removed since it is no longer used.
HLIM.FOR	Subroutine REGMOD	Removed coding for HLE model since it is no longer used. Removed input parameters F10ANA, RF10NA, and APNA since they are no longer used. Removed local variables SZA, HMED, and ZNEU since they are no longer used. Removed PARAMETER NZNEU since it is no longer used. Removed coding for BOTTOMSIDE data since the BOTTOMSIDE data type is no longer used. Removed INCLUDE statement for INCLUDE file phys4_co.inc since it is not needed.
HLISM.FOR	Subroutine HLISM	Removed arguments RF10P7, F10P7A, and AP from call to routine MATRIX since they are no longer used by that routine. Removed input parameters RF10P7, F10P7A, and AP since they are no longer used.
	Subroutine MATRIX	Removed arguments F10P7A, RF10P7, and AP from calls to routine REGMOD since they are no longer used by that routine. Removed input parameters RF10P7, F10P7A, and AP since they are no longer used.
INIT.FOR	Subroutine INITPR	Added INCLUDE statement for INCLUDE file rtdlimit.inc. PARAMETER MAXORB has been renamed to MORBIT.
INT.INC	n/a	Removed since it is no longer used.
LOGICUNI.INC	n/a	Removed PARAMETERs LUIDL, LUNATM, LUNUMB, LURATE, LURI, LURO, LUSGP, and LUTEMP since they are not used. Removed PARAMETERs LUCHEM, LUSOLR, and LUTIME since they are no longer used.
LT.INC	n/a	Removed since it is no longer used.

Module	Program Unit	Description of Changes (*continued*)
MATH_UTI.FOR	Subroutine RTBIS	Removed since it is no longer used.
	Subroutine INTRP	Removed since it is no longer used.
	Subroutine CHMRRC	Removed since it is no longer used.
MATH4_CO.INC	n/a	Removed PARAMETERs DPH, PIO2, and TWOPI since they are not used.
MIDLAT.FOR	Subroutine MIDLAT	Rewrite for the following reasons: 1. To optimize calculation of corrections. 2. To prevent extraneous zero corrections from being included in the real-time adjustment. The extraneous corrections were not based on valid data, and although zero, did influence the correction fields, and increased run time. 3. To remove coding for BOTTOMSIDE data since that data type is no longer used. 4. To remove redundant and commented-out coding. 5. To improve readability. Removed arguments F10P7A, RF10P7, and AP from calls to routine REGMOD since they are no longer used by that routine.
	Subroutine PER_ARR	Removed since it is no longer used.
NATMOS.INC	n/a	Removed since it is no longer used.
NEUATM..INC	n/a	Removed since it is no longer used.
NEWFIT.INC	n/a	Combined common blocks INWFT and NEWFT into common block NEWFIT. Removed variables NHFM, NFFM, NHEM, NFEM, NB1M, NB1D, NB2M, NB2D, NHTM, NNTM, FFDATA, EFDATA, FHDATA, EHDATA, B1DATA, B2DATA, NTDATA, HTDATA, BT1LAT, BT1LON, BT2LAT, BT2LON, B1C, and B2C from common block NEWFIT since they are no longer used. Replaced PARAMETERs NMAX and NNMAX with PARAMETERs MFFD, MHFD, MFED, MHED, MNTD, and MHTD. The new PARAMETERs are dependent on PARAMETERs in INCLUDE file rtdlimit.inc.
OUTPUT.FOR	Subroutine GRID_OUTPUT	Removed arguments F10P7A, RF10P7, and AP from call to routine REGMOD since they are no longer used by that routine. Removed INCLUDE statement for INCLUDE file dlta.inc since it is not used.
	Subroutine STATION_OUTPUT	Removed arguments F10P7A, RF10P7, and AP from call to routine REGMOD since they are no longer used by that routine.
PHANTOM.FOR	Subroutine PHANTM	Removed arguments F10P7A, RF10P7, and AP from calls to routine REGMOD since they are no longer used by that routine. Removed INCLUDE statement for INCLUDE file indirect.inc since it is no longer needed.
PHYS4_CO.INC	n/a	Removed since it is no longer used.
PRECIP.FOR	Subroutine PRECIP	Added INCLUDE statement for INCLUDE file rtdlimit.inc.
PRECIP.INC	n/a	PARAMETER MAXORB has been moved to INCLUDE file rtdlimit.inc and renamed to MORBIT.
PRISM.FOR	Block Data PREC	Added INCLUDE statement for INCLUDE file rtdlimit.inc. PARAMETER MAXORB has been renamed to MORBIT.
	Program PRISM	Removed argument SUSI from call to routine GETDAT since it is not used. Removed arguments RF10P7, F10P7A, and AP from calls to routine HLISM since they are no longer used by that routine. Removed INCLUDE statement for INCLUDE file dlta.inc since it is not used. Updated the version number and version date.
PSPECT.INC	n/a	Removed since it is no longer used.
READ_DBA.FOR	Subroutine DBASES	Removed argument PLHE(J9:J10) from call to routine READ_DBASES since it is no longer used by that routine. Removed local variables J9 and J0 since they are no longer used.
	Subroutine READ_DBASES	Removed call to routine RDFILES since it is no longer needed. Removed input parameter HLEPATH since it is no longer used.
	Subroutine RDFILES	Removed since it is no longer used.
	Subroutine RDCHEM	Removed since it is no longer used.
	Subroutine RDTIME	Removed since it is no longer used.
	Subroutine RDSOLR	Removed since it is no longer used.

Module	Program Unit	Description of Changes (*continued*)
RTA.FOR	Subroutine RTA	Added INCLUDE statement for INCLUDE file rtdlimit.inc. Removed arguments FFDATA, EFDATA, FHDATA, EHDATA, NTDATA, and HTDATA from calls to routine CORRECT1 since they are no longer used by that routine. Removed arguments NMAX and NNMAX from calls to routine CORRECT1 since they are no longer used by that routine. Removed coding for BOTTOMSIDE data since the BOTTOMSIDE data type is no longer used. Removed INCLUDE statement for INCLUDE file dlta.inc since it is not used.
	Subroutine CORRECT1	Validity checking is no longer needed since all data points reaching this routine are to be used. Removed input argument MDAT since it is no longer used. Removed input argument LDAT since it is no longer used.
RTDLIMIT.INC	n/a	New file.
SOLAR.INC	n/a	Removed since it is no longer used.
SPECIE.INC	n/a	Removed since it is no longer used.
STRINGS.FOR	Subroutine STRTRM	New routine.
TIME.INC	n/a	Removed since it is no longer used.

M·E·M·O·R·A·N·D·U·M

DATE: *14-February-1997*

TO: *Rob Daniell*

FROM: *Lincoln Brown*

RE: *Changes to PRISM 1.7a for PRISM 1.7b*

The changes to PRISM 1.7a for PRISM 1.7b focus on miscellaneous bug fixes. The changes are summarized as follows:

1. **BUG FIX**: The maximum allowed number of real-time IMS data points that PRISM can accept has been changed from 21,600 to 40,800 in order to be consistent with the I/O Specification ("200 IMS stations reporting 12 simultaneous measurements and a time resolution of 15 minutes in a +/- 2 hour time window centered on the date and UT of the run", or 200·12·[1+4·60/15]=40,800). The previous value of 21,600 was consistent with a time resolution of 30 minutes (200·12·[1+4·60/30]=21,600).

2. **BUG FIX**: Array allocation for real-time data has been increased to allow for phantom data. Previously, the presence of the maximum allowed number of real-time data points in combination with phantom data points could cause an array-out-of-bounds error in the calculation of the low/midlatitude correction fields.

3. **BUG FIX**: In the determination of the output station list from accepted real-time DISS data, the search of the direct data file for the IONOSONDE data section has been modified to prevent a read-past-end-of-file error. In subroutine DETOSL in module GETDAT.FOR, variable NSTOUT is now reinitialized to zero after a non-IONOSONDE data section in the direct data file is skipped over during the search. Previously, if the direct data file contained one or more non-IONOSONDE data sections, but contained no IONOSONDE data section, the value of NSTOUT from the last non-IONOSONDE data section would be used to attempt to read an IONOSONDE data section past the end of the direct data file, resulting in a run-time error.

4. **BUG FIX**: In the determination of the output station list from accepted real-time DISS data, the corrected geomagnetic local times of the output stations now correspond to the day of the year and Universal Time of the run. Previously, the corrected geomagnetic local times of the DISS data records were used for the output stations, resulting in as much as a 2 hour error in corrected geomagnetic local time.

PRISM's memory requirement has been increased by about 0.25 MB, a 3% increase. Its run-time will be unaffected unless the output station list is taken from a very large set of accepted DISS data.

The table below describes the changes that I made to PRISM 1.7a to produce PRISM 1.7b.

Module	Program Unit	Description of Changes
GETDAT.FOR	Subroutine INDISS	A maximum of MDISS-MPIONO DISS data records are now accepted instead of a maximum of MDISS DISS data records in order to leave room for phantom DISS data.
	Subroutine INDMSP	A maximum of MISP-MPINSI SSIES IN SITU PLASMA data records are now accepted instead of a maximum of MISP SSIES IN SITU PLASMA data records in order to leave room for phantom SSIES IN SITU PLASMA data.
	Subroutine DETOSL	Variable NOUTST is now reinitialized to zero after non-IONOSONDE data sections in the direct data file are skipped over. When the output station list is taken from the DISS data list, the corrected geomagnetic local time of an output station list record is now calculated from the nominal day of the year and Universal Time instead of being taken from the corresponding DISS data record.
PHANTOM.FOR	Subroutine PHANTM	Moved PARAMETERs NZMLAI, NZMLAP, NZMLOI and NZMLOP to INCLUDE file rtdlimit.inc. Added INCLUDE statement for INCLUDE file rtdlimit.inc.
PRISM.FOR	Program PRISM	Updated the version number and version date.
RTDLIMIT.INC	n/a	Moved PARAMETERs NZMLAI, NZMLAP, NZMLOI, and NZMLOP from subroutine PHANTM. Added PARAMETERs MPIONO and MPINSI. Changed value of PARAMETER MDISS from 850 to 850+MPIONO. Changed value of PARAMETER MIMS from 21600 to 40800. Changed value of PARAMETER MISP from 3848 to 3848+MPINSI.

M·E·M·O·R·A·N·D·U·M

DATE: *13-January-1998*

TO: *Rob Daniell*

FROM: *Lincoln Brown*

RE: *Changes to PRISM 1.7b for PRISM 1.7c*

The changes to PRISM 1.7b for PRISM 1.7c focus improving the midlatitude real-time adjustment algorithm and on replacing the LLF and MLF parameterized models. The changes are summarized as follows:

5. **BUG FIX**: The calculation of the topside half-width of the O^+ density has been corrected. Previously, due to a sign convention error, the topside half-width was calculated as a negative value. It is now correctly calculated as a positive value. Because the minimum of the bottomside and topside half-widths is used by PRISM, and the bottomside O^+ density probably always falls off more rapidly than the topside O^+ density, this bug has probably never influenced the results of PRISM.

6. **BUG FIX**: A minor bug in the selection of magnetic latitudes for interpolation in the MLF parameterized model has been fixed. This bug should not have affected past results.

7. The algorithm for scaling the molecular ion and O^+ model density profiles using simultaneous E-layer and F-layer real-time data corrections has been redesigned. Previously, in the presence of disparate E-layer and F-layer corrections, discontinuities could be introduced into the density profiles, resulting in unintentional changes in peak heights as well as scaled peak densities inconsistent with the real-time data corrections. The new scaling algorithm preserves the heights of the peaks and smoothly transitions the density profile scaling from a pure E-layer correction at the molecular ion density peak height to a pure F-layer correction at the O^+ density peak height.

8. The conversion of TEC real-time data to critical frequency corrections is now based simply on the ratio of data TEC to model TEC, and both f_oF_2 and f_oE corrections are now provided from the conversion. Previously, a more complicated algorithm based on the topside model TEC was used, and only f_oF_2 corrections were provided.

9. Phantom data now no longer influences the sunspot number iteration. Previously, due to the placement of the call to routine PHANTM in the main program, phantom data was generated and included in the real-time data set prior to the sunspot number iteration. Since the sunspot number iteration fits an optimum sunspot number to the real-time data, the phantom data erroneously influenced the outcome of the sunspot number iteration. The call to routine PHANTM has been moved so that the phantom data influences only the midlatitude real-time adjustment.

10. In order to eliminate problems in merging the LLF and MLF parameterized models due to differences between the two theoretical models (LOWLAT and MIDLAT) previously used as their basis, the LLF and MLF parameterized models have been regenerated from a single theoretical model (LOWLAT). In addition, the following improvements have been made to LOWLAT:

    a. The equatorial vertical E×B drift and its radial derivative now vary smoothly to zero in the drift transition region. Previously, a simple linear fall-off was used, resulting in discontinuities in the radial derivative at the drift transition region endpoints.

    b. The radial derivative of the equatorial vertical E×B drift is now zero above the drift transition region. Previously, it was never set to zero above the transition region.

c. The dayside and nightside electron temperatures now merge at 0600 and 1800 solar local time. Previously, the electron temperature was discontinuous at 0600 and 1800 solar local time.

d. The neutral wind is now calculated for the correct geographic longitude at all points along a field line. Previously, a fixed geographic longitude was used, resulting in an error in the neutral wind due to the magnetic declination of the field line.

11. The LLF parameterized model has been extended to 44° in absolute latitude, in order to broaden the merge region between the LLF and MLF parameterized models. Previously, the LLF parameterized model only went up to 34° in absolute latitude.

12. The lower absolute latitude boundary of the MLF parameterized model is now 34°, in order to reduce the error due to the assumption of verticality of the midlatitude field lines and to make sure that the midlatitude field lines are outside the region of vertical E×B drift. Previously, the lower absolute latitude boundary of the MLF parameterized model was 30°.

13. The merge region for the LLF and MLF parameterized models has been broadened to the absolute latitude range 34°-44°, in order to improve the quality of the merge. Previously, the range was 30°-34°, too narrow to effectively merge the two parameterized models.

14. Some header comments have been corrected.

The plots of f_0F_2 and TEC vs. magnetic latitude below illustrate the improvement in PRISM 1.7c regarding the agreement and merging of the LLF and MLF parameterized models. Notice the discontinuities in f_0F_2 and TEC at the LLF/MLF merge region of PRISM 1.7b (±30°-34° magnetic latitude), and their absence in PRISM 1.7c. The plots were generated by PRISM for the following conditions: year 1981, day of the year 173, Universal Time 0000, $F_{10.7}$ 210, K_p 3.5, IMF B_y positive, IMF B_z negative, 270°E magnetic longitude, no URSI f_0F_2 normalization, and no real-time data.

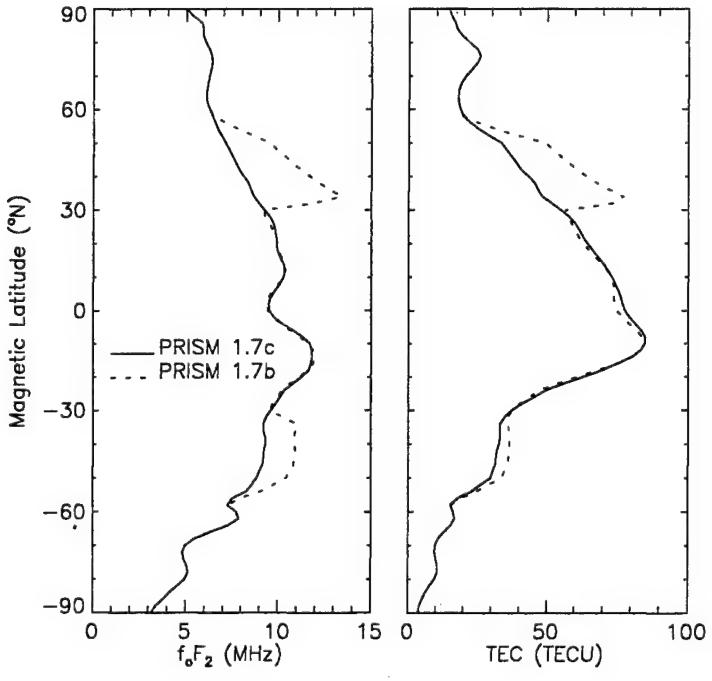

The table below describes the changes that I made to PRISM 1.7b to produce PRISM 1.7c.

Module	Program Unit	Description of Changes
GEN.FOR	Subroutine GENEC	Changed PARAMETER MAXMX from 40 to 50 to accommodate new LLF parameterization.
HLIM.FOR	Subroutine REGMOD	Removed calculations of topside ion column density and critical height difference for TEC data type since they are no longer needed. Removed output parameters TC1 and TC2 since they are no longer used. Removed calculation of n_mF_2 since it is no longer needed. Removed local variable NMF2 since it is no longer needed.
HLISM.FOR	Subroutine MATRIX	Removed arguments TC1 and TC2 from calls to routine REGMOD since they are no longer used by that routine. Removed local variables TC1 and TC2 since they are no longer used.
LOWER.INC	n/a	Changed PARAMETER MOPM1 from 11 to 14 for new LLF parameterization. Changed PARAMETER MX from 35 to 45 for new LLF parameterization.
MID_PARA.FOR	Subroutine MID_F	Corrected test for magnetic latitude above the magnetic latitude grid by changing "(AMLAT .GT. ASMLAT+FLOAT(NMLAT(I,1))*ADMLAT)" to "(AMLAT .GT. ASMLAT+FLOAT(NMLAT(I,1)-1)*ADMLAT)".
MIDLAT.FOR	Subroutine MIDLAT	The conversion of TEC data to critical frequency corrections is now based solely on the ratio of the data TEC to the model TEC, and both f_0F_2 and f_0E corrections are now provided from the conversion process. Removed arguments TC1 and TC2 from calls to routine REGMOD since they are no longer used by that routine. Removed local variables TC1, TC2, W, WFACT, WB, DTEC, TFACT, and NMF2N since they are no longer used. Removed INCLUDE statement for INCLUDE file tomid.inc since it is no longer needed.
MIDLAT.INC	n/a	Changed PARAMETER MX from 12 to 11 for new MLF parameterization.
NEWFIT.INC	n/a	Changed value of PARAMETER MFED from MDISS to MDISS+MIMS to accommodate additional midlatitude f_0E corrections from converted TEC data.
OUTPUT.FOR	Subroutine GRID_OUTPUT	Removed arguments TC1 and TC2 from call to routine REGMOD since they are no longer used by that routine. Removed local variables TC1 and TC2 since they are no longer used.
	Subroutine STATION_OUTPUT	Removed arguments TC1 and TC2 from call to routine REGMOD since they are no longer used by that routine. Removed local variables TC1 and TC2 since they are no longer used.
PARAM.FOR	Subroutine PARAM	Changed lower absolute latitude boundary of pure mid-latitude region from 34. degrees to 44. degrees. Changed upper absolute latitude boundary of low/mid-latitude transition region from 34. degrees to 44. degrees. Changed lower absolute latitude boundary of low/mid-latitude transition region from 30. degrees to 34. degrees. Changed upper absolute latitude boundary of pure low-latitude region from 30. degrees to 34. degrees. Removed comments regarding f_0E normalization from METHOD comment section since no f_0E normalization is done.
PHANTOM.FOR	Subroutine PHANTM	Removed arguments TC1 and TC2 from calls to routine REGMOD since they are no longer used by that routine. Removed local variables TC1 and TC2 since they are no longer used.
PRISM.FOR	Program PRISM	Moved the call to routine PHANTM from after the conversion of the nominal UT from hours to seconds to before the call to routine MIDLAT so that phantom data does not influence the sunspot number iteration. Removed the call to routine INIT that accompanied the call to routine PHANTM since it is no longer needed. Updated the version number and version date.
READ_DBA.FOR	Subroutine LRDOPCF	Changed PARAMETER MOPM1 from 11 to 14 for new LLF parameterization.
RTA.FOR	Subroutine RTA	Removed INCLUDE statement for INCLUDE file tomid.inc since it is not needed.
	Subroutine COR_MAX	Removed arguments EE, EF, FE, FF from the call to routine DO_ADJ since they are no longer needed by that routine.
	Subroutine DO_ADJ	Modified adjustment algorithm to use a unified multiplicative scaling that varies smoothly across altitude boundaries. Removed input parameters NMHME, NMHMF2, NOHME, and NOHMF2 since they are no longer used.
	Subroutine GETHW	Corrected calculation of topside half-width by changing difference HMH-ALTF(J) to ALTF(J)-HMH.

M·E·M·O·R·A·N·D·U·M

DATE: *29-March-2001*

TO: *Files*

FROM: *Rob Daniell*

RE: *Changes to PRISM 1.7c for PRISM 1.7d*

The changes to PRISM 1.7c for PRISM 1.7d focus on correcting problems in both the high latitude and midlatitude real-time adjustment algorithms, bringing the use of TEC data in line with PRISM 1.5 documentation, and providing a logical switch to control whether or not "phantom stations" are used. The changes are summarized as follows:

1. **BUG FIX**: Dwight Decker discovered that when PRISM was driven with TEC data *alone*, no phantom stations were assigned even though there were large regions with no data. This problem has been corrected so that phantom stations are correctly assigned regardless of what combination of ionosonde and TEC data are ingested. The changes were made in file "phantom.for". (However, note item 2 below.)

2. A compile time logical parameter PHANTOM has been added to PRISM to control whether "phantom stations" are generated to force the model to relax to climatology in regions where data is absent. For operational use, this parameter should be set to .FALSE. to suppress the generation of phantom stations. This change was made in the file "prism.for".

3. **BUG FIX**: An error in the call to SUBROUTINE OVAL from SUBROUTINE FMODEL was corrected. In addition a programming error in SUBROUTINE OVAL itself was also corrected. These errors were identified by Dwight Decker and caused problems under certain conditions in the auroral oval corrections. The changes were made in file "fmodel.for".

4. **BUG FIX**: Several lines of code used to adjust the high latitude E-layer was "commented out" in Version 1.7c without any accompanying documentation. This caused errors in the high latitude adjustments under some circumstances. The lines were "uncommented" in Version 1.7d, and this seems to have corrected these errors. This change was made in the file "init.for".

5. The time limits on DMSP data were changed to conform to PRISM documentation. PRISM now accepts DMSP data for all times within ±2 hours of the nominal time of the run. This change was made in file "rtdlimit.inc".

6. **BUG FIX:** An error in the interpolation of EOF coefficients in UT was corrected. The error caused incorrect calculation of the interpolated coefficients when data from more than one time are ingested. This change was made in the file "gen.for".

7. The coding that sets a floor for the electron density was corrected to ensure that the floor is always enforced. This change was made in the file "gen.for".

8. **BUG FIX:** The threshold electron flux and proton flux for identification of the auroral oval boundaries was corrected to conform to PRISM documentation. This problem was discovered by Dwight Decker. This change was made in the file "getdat.for".

9. The transition altitude between the E-layer and F-layer in the EDP adjustment algorithm has been lowered. This should prevent the formation of false F-layer peaks between the true F-peak and the E-peak when the E-layer adjustment is much larger than the F-layer adjustment. This change was made in the file "rta.for".

10. The algorithm for the usage of TEC data has been modified to bring it into conformance with PRISM 1.5 documentation (PL-TR-95-2061). When the DISS site (with valid f_oF_2 data) nearest to a particular TEC datum is within the "decorrelation distance" DCL (defined as a PARAMETER in "prism.for"), then the TEC data is used to calculate a pseudo-SSIES record *unless* at least one real SSIES datum is also present within a distance DCL of the TEC datum, in which case the TEC data is discarded. Otherwise, the TEC data is used to calculate a pseudo-DISS record. Although derived from the SEND version of PRISM, the implementation differs somewhat. The EDP parameter corrections fields are calculated with five consecutive passes through the real-time data. (1) The first pass uses DISS data to calculate *E*- and *F*-layer height corrections. (2) The second pass uses DISS data to calculate *E*- and *F*-layer peak density corrections. (3) The third pass simply locates DMSP SSIES data for later comparisons with the locations of DISS and IMS data. (4) The fourth pass uses TEC data to calculate pseudo-DISS corrections (if the nearest DISS site is beyond the "decorrelation length") or pseudo-SSIES corrections (if the nearest DISS site is within the "decorrelation length" and there is no SSIES data also within the "decorrelation length"). (5) Finally, the fifth pass uses the DMSP SSIES data to calculate topside corrections for the EDP. While not completely self consistent, this should cause the correction fields to more closely reproduce the TEC data at the TEC data locations. These changes were made in the files "hlim.for", "midlat.for", and "newfit.inc" as well as several other subroutines that call SUBROUTINE REGMOD.

11. The parameter limiting the amount of high latitude data that can be ingested by PRISM was increased from 8000 to 20000 by Dwight Decker. This change was made in the file "hlism.for".

12. **BUG FIX:** When B_y vanishes exactly, PRISM would halt. This has been changed so that B_y=0 is treated as B_y>0. This problem was identified by SMC Det 11 personnel during testing of PRISM with actual data. This change was made in the file "io_util.for".

13. A compile time logical parameter DIAGNOS has been added to PRISM 1.7d to control certain diagnostic output that is useful for debugging and code development. While this diagnostic output has been designed not to interfere with operational use of PRISM, it does alter the standard output. Therefore, we strongly recommend that for normal operations, DIAGNOS should be set to .FALSE. in the file "prism.for". When DIAGNOS is TRUE, there are two separate kinds of diagnostic output that are produced:

    a. The region code (CAP, OVAL, TROUGH, MIDLAT) is included in the standard output. In gridded output, it is added to the end of the line containing the geographic and geomagnetic coordinates of each grid point. In station output, its location depends on the user's choice of output. If the user has selected EDP data only, the region code appears immediately after the magnetic local time (as for gridded output). If the user has selected profile parameter data only or both EDP and profile parameters, the region code appears immediately after the profile parameters.

    b. PRISM writes a file named "boundary.txt" containing the parameters that determine the boundaries between the trough, the auroral oval, and the polar cap. An example file is shown below. The printed parameters correspond to the parameters described in PL-TR-95-2061 (PRISM: A PARAMETERIZED REAL-TIME IONOSPHERIC SPECIFICATION MODEL, VERSION 1.5) on pages 25-26 and in Appendix D. The first line of the file includes the name of the gridded output file *if it exits*. (If there is no gridded output, then the first line simple reads "Boundary Parameters". The second line is the actual K_p as provided in the user input. The third line gives the effective K_p for the auroral *E*-layer. The remainder of the file gives the

```
Boundary Parameters for "prism_21.out"
   3.0000 = actual Kp
   3.0000 = "effective" Kp for auroral E-layer
   3.0000    3.0000    3.0000 = "effective" Kp for F-layer boundaries
   0.0000    0.0000    0.0000 = THETA0(0:2)
 -10.5000    0.0000    0.0000 = AB(0:2)
  11.5000    0.0000    0.0000 = BB(0:2)
   3.8800    0.0000    3.0000 = CB(0:2)
   2.7300    0.0000    0.0000 = PB(0:2)
 -10.5000    2.7000    0.8000 = CAB(0:2)
   0.0000    0.2670   -0.2670 = VAB(0:2)
  24.4000   20.9000   13.4000 = CTH(0:2)
   2.1200    1.7000    1.7000 = VTH(0:2)
  11.5000    2.6333 = CBB(0:1)
   0.0000   -0.0833 = VBB(0:1)
   0.0000    0.0051 = QBB(0:1)  ,
```

parameters that define the *F*-layer boundaries as used in SUBROUTINE FMODEL. They are described in the header to the file "region_b.inc" which defines the boundary parameters contained in the block common BNDS. This header is displayed below.

```
C  Declarations for high latitude region boundaries
C     As of 6 April 1990 the trough equatorward boundary is a distorted circle
C  of the form
C
C     THETA(PHI) = THETA0(Kp) + AB*EXP(-(ABS((PHI-BB)/CB)^PB))
C
C  where THETA is magnetic co-latitude (degrees), PHI is magnetic local time
C  (hours).  THETA0 definitely depends on Kp; AB, BB, CB, and PB may or may
C  not.  The equatorward auroral oval boundary is an undistorted circle whose
C  center is displaced from the magnetic pole.  The polar cap boundary is also
C  a displaced circle.  For these THETA0 is the radius (degrees), AB is the CGM
C  co-latitude of the center, BB is the MLT of the center.
C
C     At low magnetic activity, the precipitation oval and the trough overlap
C  during midmorning (0800-1000) magnetic local times.  This may (or may not)
C  be an indication of the absence of a morning trough at low activity
C  levels.  CB(1) is a minimum displacement of the oval boundary from the
C  trough boundary, i.e., a minimum width of the trough.  Likewise, CB(2) is a
C  minimum width of the oval.  PB(1) and PB(2) are currently unused.
C
C       CB (0) = the local time scale size of the distortion:
C
C       CB(1:2) are the minimum trough and oval widths
C       PB(0) is the exponent:
C       PB(1:2)  are currently unused
C
C        THETA0(0) = 24.4 + 2.12*KP(0)
C        THETA0(1) = 20.9 + 1.7*KP(1)
C        THETA0(2) = 13.4 + 1.7*KP(2)
C
C       And fix the amplitude and local time of the distortion of the trough
C         boundary:
C        AB(0) = -10.5
C        AB(1) = 2.7 + 0.267*KP(1)
C        AB(2) = 0.8 - 0.267*KP(2)
C
C
      REAL THETA0(0:2),AB(0:2),BB(0:2),CB(0:2),PB(0:2),CAB(0:2),
     1 VAB(0:2),CTH(0:2),VTH(0:2),CBB(0:1),VBB(0:1),QBB(0:1)
C
      COMMON/BNDS/THETA0,AB,BB,CB,PB,CAB,VAB,CTH,VTH,CBB,VBB,QBB
```

14. A number of mainly cosmetic changes were made to improve readability and internal documentation of the code, to provide diagnostic output to the log file, to improve portability, and to simplify test runs during code development. These changes are transparent to the user.

15. **BUG FIX:** A logic error in the DMSP data ingestion routine INDMSP (in file "getdat.for") was corrected. If there was a blank line or an erroneous section label line, the routine would loop through the data file indefinitely. Now, if a line cannot be identified as belonging to one of the three data types (drift, in situ plasma, or precipitating particles) the line is skipped, and the next line is read. Note that this bug would have no effect on properly formatted DMSP data files.

16. The parameter MDISS, defined in the file "rtdlimit.inc," was changed to MDISS = 41000+MPIONO to accommodate the potentially large number of pseudo-DISS sites to be generated from SSUSI disk images.

The table on the next page describes the changes that I made to PRISM 1.7c to produce PRISM 1.7d.

Module	Program Unit	Description of Changes
prism.for	PROGRAM PRISM	(1) Modified the way SUBROUTINE PHANTM write phantom ionosonde data to the scratch files that PRISM uses to organize the real-time data it has ingested. This corrected a problem the failure of PRISM to store phantom station data when IMS data was ingested in the absence of DISS data. (2) Added the logical parameter PHANTOM to control whether phantom station data is generated (PHANTOM = .TRUE.) or whether phantom stations are suppressed (PHANTOM = .FALSE.). The value of PHANTOM is printed at the beginning of the log file. (3) Added the logical parameter DIAGNOS to controls whether or not RCODE is appended to the standard output and whether or not SUBROUTINE WRTBND is called to produce the file "boundary.txt" containing the boundary parameters for the trough, auroral oval, and polar cap boundaries. The value of DIAGNOS is printed in the log file immediately below PHANTOM. (4) Added the logical parameter LTECTOP to control whether or not IMS data that is "near" DISS data is used to generate pseudo-SSIES data or pseudo-DISS data. The real parameter DCL specifies the "TEC decorrelation length" that is used to determine whether IMS data is "near" DISS data. The values of these parameters are now printed at the beginning of the log file immediately after PHANTOM and DIAGNOS.
phantom.for	SUBROUTINE PHANTOM	Modified the way phantom stations are assigned so that it is done correction regardless of the combination of DISS and IMS data.
fmodel.for	SUBROUTINE FMODEL	Corrected out of order variables in the call to OVAL
fmodel.for	SUBROUTINE OVAL	Corrected error in linear formula. (Note: cubic formula should be reinstated and tested when time permits.)
getdat.for	SUBROUTINE INDMSP	Changed PARAMETER CRTEF from 2.5 to 0.25 to conform to documentation. Changed PARAMETER CRTPF from 1.0 to 0.1 to conform to documentation. Corrected logic error in SUBROUTINE INDMSP which could potentially cause the routine to enter an indefinite loop condition in the case of certain errors in the format of the DMSP data files.
output.for	SUBROUTINE OUTPUT	Added DIAGNOS to the argument list and to the calls to GRID_OUTPUT and STATION_OUTPUT. Changed STATUS parameter from 'NEW' to 'UNKNOWN' in OPEN statements for output files. This allows PRISM to overwrite old output files rather than crashing.
output.for	SUBROUTINE GRID_OUTPUT	(1) Added latitude region code (CHARACTER*8 RCODE) to standard output. (2) Added DIAGNOS to argument list to detemine whether or not RCODE is appended to standard output. (3) Added TECTOP to call to REGMOD. (4) Added diagnostic print statements to permit the observation of the profile adjustment process at a specific grid point. (See also SUBROUTINE DO_ADJ in "rta.for".) These print statements are set off by lines of "#####" symbols.
output.for	SUBROUTINE STATION_OUTPUT	Added TECTOP to call to REGMOD. Added DIAGNOS to argument list and to call to W_ST_DATA.
output.for	SUBROUTINE WRITE_DATA	Added RCODE and DIAGNOS to argument list. Added logic to determine whether or not to append RCODE to the write statement that writes GLAT, GLON, etc. depending on the value of DIAGNOS.
output.for	SUBROUTINE W_ST_DATA	Added RCODE and DIAGNOS to argument list. Added logic to determine whether or not to append RCODE to write statements. The location of RCODE in the station output depends on the type of output selected by the user.
output.for	SUBROUTINE WRTBND	Created this subroutine (called from PROGRAM PRISM) to write latitude boundary parameters to file "boundary.txt".
rta.for	SUBROUTINE DO_ADJ	(1) Modified the way the transition height between the E- and F-layers is calculated to prevent (or reduce the chances of) the formation of false F1-layers below the true F2-layer peak. (2) Added diagnostic write statements (controlled by a logical variable set in GRID_OUTPUT and passed in common block RTAFL) to allow the profile adjustment process to be monitored.
gen.for	SUBROUTINE GEN_E	Modified final test on DEN to insure that densities are no smaller than DENMIN
gen.for	SUBROUTINE GTCFF	Corrected error in logic that caused incorrect interpolation in UT when near a midnight crossing and data from more than one UT has been ingested.
hlim.for	SUBROUTINE REGMOD	Modified argument list and code to allow for a calculation of the "topside TEC" (the TEC above the peak density) needed for the corrected TEC ingestion algorithm.
midlat.for	SUBROUTINE MIDLAT	Modified code to allow for the corrected TEC ingestion algorithm.
hlism.for	SUBROUTINE HLISM	Increased MMODEL from 8000 to 20000.
init.for	SUBROUTINE INIT	Restored call to LDITER for E-layer height adjustment (lines 296-299)
io_util.for	SUBROUTINE UDETID	Corrected handling of By = 0 case so that it is treated as By = 1.
rtdlimit.inc	N/A	Modified limits on DMSP data so that PRISM accepts DEMSP data for all times within ±2 hours of the nominal time of the run. Modified the limits on DISS data to accommodate the potentially large number of pseudo-DISS sites to be generated from SSUSI image data.
newfit.inc	N/A	Changed the parameters MNTD and MHTD to equal MISP+MIMS to reflect the possible addition of pseudo-SSIES records from TEC data collocated with DISS data.

M·E·M·O·R·A·N·D·U·M

DATE: *9-January-2002*

TO: *Files*

FROM: *Rob Daniell*

RE: *Changes to PRISM 1.7d for PRISM 1.7e*

The changes to PRISM 1.7d for PRISM 1.7e are principally designed to correct a problem with the assimilation of TEC data in the presence of SSIES data. However, other changes were intended to bring PRISM 1.7 into compliance with PRISM 1.5 documentation, particularly with regard to the assimilation of TEC data, and the remaining changes were designed to make the coding easier to follow.

1. The data ingestion algorithm in SUBROUTINE MIDLAT was modified. It still makes four passes through the data, and the first two passes continue to search for h_mF_2 data and f_oF_2 data, respectively. Pass 3 now searches for TEC data that is farther than the "decorrelation length" (DCL, a PARAMETER in the main program) from the nearest DISS site and uses it to calculate a pseudo-DISS data record. Pass 4 now searches for both SSIES and TEC data. TEC data that is farther than DCL from the nearest SSIES datum is used to calculate a pseudo-SSIES record. TEC data that lies closer than DCL to an SSIES datum is ignored. In connection with this change, SUBROUTINE PRO_COR and SUBROUTINE COR_PRO were completely rewritten to conform to Version 1.5 documentation regarding the topside profile correction algorithm. These changes were made in the file "midlat.for" and "rta.for".

2. The variable TOPHT has been added to the calls to SUBROUTINE PARAM and SUBROUTINE FMODEL in SUBROUTINE REGMOD and SUBROUTINE RTA. Previously, the variable HTOP did double duty as TOPHT (the altitude of the topside density correction) on input and HTOP (the topside scale height) on output. Now the variables are separate entities, resulting in cleaner, easier to understand code. These changes were made in the files "hlim.for", "fmodel.for", "param.for", and "rta.for".

3. **BUG FIX**: Dwight Decker modified the loop over DMSP data types in SUBROUTINE INDMSP to correct a problem reading data from multiple satellites. He also added some information messages to the log file from this subroutine. The changes were made in file "getdat.for".

The table on the next page describes the changes made to PRISM 1.7d to produce PRISM 1.7e.

Module	Program Unit	Description of Changes
midlat.for	SUBROUTINE MIDLAT	Modified the data ingestion algorithm. The revised algorithm makes four passes through the DMSP data. The first pass searches for h_mF_2 data from DISS sites and calculates height corrections. The second pass searches for f_oF_2 data from DISS sites and calculates peak density corrections. The third pass searches for TEC data that are farther than the "decorrelation length" (PARAMETER DCL specified in PROGRAM PRISM) from the nearest f_oF_2 datum and calculates a peak density correction. The fourth pass searches for both SSIES and TEC data. Topside density and scale height (where applicable) corrections are calculated from the SSIES data and from TEC data that are farther than DCL. TEC data that are closer than DCL to at least one SSIES datum are ignored.
midlat.for	SUBROUTINE PRO_COR	Rewrote subroutine to conform to Version 1.5 documentation regarding topside corrections.
hlim.for	SUBROUTINE REGMOD	Added TOPHT to argument list so that HTOP would not change meaning between input and output
fmodel.for	SUBROUTINE FMODEL	Added ZTOP to argument list and changed HTSAV to HTOP
param.for	SUBROUTINE PARAM	Added ZTOP to argument list so that HTOP would not change meaning between input and output
rta.for	SUBROUTINE RTA	(1) Added ZTOP to argument list so that HTOP would not change meaning between input and output. Added ZTOP to call to SUBROUTINE COR_PRO. (2) Changed topside correction algorithm so that it is invoked only if DNTP or DHTP is nonzero.
rta.for	SUBROUTINE COR_PRO	Rewrote subroutine to conform to Version 1.5 documentation
getdat.for	SUBROUTINE INDMSP	Modified loop over data types (SSIES ION DRIFT, SSIES IN SITU PLASMA, and SSJ/4 DATA) according to recommendation of Dwight Decker to correct problems reading data from multiple satellites.

References

Anderson, D. N., A theoretical study of the ionospheric *F*-region equatorial anomaly, II, Results in the American and Asian sectors, *Planet. Space. Sci.*, **21**, 421-442, 1973.

Bailey, G. J., and R. Sellek, A mathematical model of the Earth's plasmasphere and its application in a study of He^+ at L = 3, *Ann. Geophys.*, *8*, 171, 1990.

Beckmann, P., *Orthogonal Polynomials for Engineers and Physicists*, The Golem Press, Boulder, pp. 91-92, 1973.

Brace, L. H., and R. F. Theis, Global empirical models of ionospheric electron temperature in the upper F-region and plasmasphere based on in situ measurements from the Atmosphere Explorer-C, ISIS 1, and ISIS 2 satellites, *J. Atmos. Terr. Phys.*, *43*, 1317, 1981.

Daniell, R. E., W. G. Whartenby, and L. D. Brown, *PRISM Validation*, PL-TR-94-2198, Phillips Laboratory, Hanscom AFB, Massachusetts, 1994, ATA288476.

Davis, R. E., Predictability of Sea Surface Temperature and Sea Level Pressure Anomalies Over the North Pacific Ocean, *J. Phys. Oceanogr.*, 6, 249, 1976.

Decker, D. T., C. E. Valladares, R. Sheehan, Su. Basu, D. N. Anderson, and R. A. Heelis, Modeling daytime *F* layer patches over Sondrestrom, *Radio Sci.*, *29*, 249-268, 1994.

Fejer, B. G., The equatorial ionospheric electric fields, A review, *J. Atmos. Terr. Phys.*, *43*, 377-386, 1981.

Fejer, B. G., E. R. de Paula, I. S. Batista, E. Bonelli, and R. F. Woodman, Equatorial *F* region vertical plasma drifts during solar maxima, *J. Geophys. Res.*, *94*, 12049-12054, 1989.

Fejer, B. G., E. R. de Paula, R. A. Heelis, and W. B. Hanson, Global equatorial ionospheric vertical plasma drifts measured by the AE-E satellite, *J. Geophys. Res.*, *100*, 5769-5776, 1995.

Gussenhoven, M. S., D. A. Hardy, and N. Heinemann, Systematics of the equatorward diffuse auroral boundary, *J. Geophys. Res.*, *88*, 5692-5708, 1983.

Hardy, D. A., M. S. Gussenhoven, R. R. Raistrick, and W. J. McNeil, Statistical and functional representations of the pattern of auroral energy flux, number flux, and conductivity, *J. Geophys. Res.*, **92**, 12275-12294, 1987.

Hedin, A. E., MSIS-86 Thermospheric Model, *J. Geophys. Res.*, **92**, 4649-4662, 1987.

Hedin, A. E., Empirical global model of upper thermosphere winds based on Atmospheric and Dynamics Explorer satellite data, *J. Geophys. Res.*, *93*, 9959-9978, 1988.

Heppner, J. P., and N. C. Maynard, Empirical high-latitude electric field models, *J. Geophys. Res.*, *92*, 4467-4489, 1987.

Hildebrand, F. B., *Methods of Applied Mathematics*, Prentice-Hall, Englewood Cliffs, pp. 30-34, 1965.

Jasperse, J. R., The photoelectron distribution function in the terrestrial ionosphere, in *Physics of Space Plasmas*, ed. by T. S. Chang, B. Coppi, and J. R. Jasperse, Scientific Publishers, Cambridge, MA, pp. 53-84, 1982.

Kutzbach, J. E., Empirical Eigenvectors of Sea-Level Pressure, Surface Temperature, and Precipitation Complexes over North America, *J. Appl. Meteor.*, 6, 791, 1967.

Lorenz, E. N., *Empirical Orthogonal Functions and Statistical Weather Prediction*, Sci. Rep. No. 1, Contract AF19(604)1566, AFCRC-TN-57-256, Dept. Meteor., MIT, 1956.

Moffett, R. J., The equatorial anomaly in the electron distribution of the terrestrial F-region, *Fundamentals of Cosmic Phys.*, **4**, 313-391, 1979.

Peixota, J. P., and A. H. Oort, *Physics of Climate*, Appendix B, American Institute of Physics, New York, 1991.

Schunk, R. W., A Mathematical Model of the Middle and High Latitude Ionosphere, *Pageoph*, **127**, 255-303, 1988.

Secan, J. A., and T. F. Tascione, The 4D Ionospheric Objective Analysis Model, in *Proceedings of the 1984 Ionospheric Effects Symposium*, ed. by Goodman, Klobuchar, and Soicher, 336-345, 1984.

Strickland, D. J., D. L. Book, T. P. Coffey, and J. A. Fedder, Transport equation techniques for the deposition of auroral electrons, *J. Geophys. Res.*, **81**, 2755-2764, 1976.

Strickland, D. J., R. E. Daniell, J. R. Jasperse, and B. Basu, Transport-theoretic model for the electron-proton-hydrogen atom aurora: 2. Model results, in press, *J. Geophys. Res.*, 1994.

Tascione, T. F., H. W. Kroehl, R. Creiger, J. W. Freeman, R. A. Wolf, R. W. Spiro, R. V. Hilmer, J. W. Shade, and B. W. Hausman, New ionospheric and magnetospheric specification models, *Radio Science*, *23*, 211-222, 1988.